STRUCTURAL STUDIES OF THE CATALYTIC AND REGULATORY MECHANISMS OF PHENYLALANINE HYDROXYLASE

A Dissertation

by

JUN LI

Submitted to the Office of Graduate Studies of
Texas A&M University
in partial fulfillment of the requirements for the degree of

DOCTOR OF PHILOSOPHY

August 2010

Major Subject: Biochemistry

STRUCTURAL STUDIES OF THE CATALYTIC AND REGULATORY MECHANISMS OF PHENYLALANINE HYDROXYLASE

A Dissertation

by

JUN LI

Submitted to the Office of Graduate Studies of
Texas A&M University
in partial fulfillment of the requirements for the degree of

DOCTOR OF PHILOSOPHY

Approved by:

Co-Chairs of Committee,	Paul Fitzpatrick
	Gregory Reinhart
Committee Members,	Gary Kunkel
	Frank Raushel
Head of Department,	Gregory Reinhart

August 2010

Major Subject: Biochemistry

ABSTRACT

Structural Studies of the Catalytic and Regulatory Mechanisms of Phenylalanine Hydroxylase. (August 2010)

Jun Li, B.S., Peking University Health Science Center

Co-Chairs of Advisory Committee: Dr. Paul F. Fitzpatrick
Dr. Gregory Reinhart

The catalytic and regulatory mechanisms of phenylalanine hydroxylase were investigated by structural studies of in this research. Phenylalanine hydroxylase (PheH) hydroxylates phenylalanine to produce tyrosine using tetrahydrobiopterin (BH_4) and oxygen. The three ligands to the iron, His285, His290, and Glu330, were mutated to glutamine, glutamate, and histidine. All the mutants had low but measurable activity. Mutation of Glu330 had the greatest effect on activity and mutation of His290 the least. All the mutations resulted in an excess of tetrahydropterin oxidized relative to tyrosine formation, with mutation of His285 having the greatest effect on the coupling of the two partial reactions. All the mutants greatly decreased the affinity for iron, with mutation of Glu330 the most deleterious. The results complement previous results with tyrosine hydroxylase in establishing the plasticity of the individual iron ligands in this enzyme family.

Hydrogen/deuterium exchange and mass spectrometry showed that peptides lying in the interface between the regulatory and catalytic domains display large increases of deuterium incorporation in the presence of phenylalanine. However, the effects of

phenylalanine on a mutant enzyme lacking the regulatory domain are limited to peptides surrounding the binding site of phenylalanine. These results support the autoinhibitory function of the N-terminus of PheH. No peptides show a changed deuterium incorporation pattern in the presence of BH_4, suggesting that BH_4 binding does not change the structure significantly from the resting form. In phosphorylated PheH, three peptides show a deuterium incorporation pattern similar to that of unphosphorylated PheH plus phenylalanine, while the other peptides sensitive to phenylalanine binding in unphosphorylated PheH show the same pattern as that of unphosphorylated PheH without phenylalanine. Therefore, the conformational changes induced by phosphorylation are similar to but not identical to those associated with phenylalanine activation.

The isolated regulatory domain ($PheH_{1-117}$) was expressed and purified using a Q-Sepharose column followed by a gel filtration column. Analytical gel filtration shows that $PheH_{1-117}$ exists as a dimer in solution. In the presence of phenylalanine, the retention time of $PheH_{1-117}$ is significantly changed. The ^{1}H-^{15}N NMR spectra of $PheH_{1-117}$ show that the cross-peaks of several residues are altered in the presence of phenylalanine. These results support the existence of a regulatory binding site for phenylalanine in the regulatory domain of PheH.

ACKNOWLEDGMENTS

I would like to thank my committee co-chairs, Dr. Fitzpatrick and Dr. Reinhart, and my committee members, Dr. Kunkel and Dr. Raushel, for their guidance and support throughout the course of this research. I also extend gratitude to my friends, colleagues, the department faculty and staff for making my time at Texas A&M University a great experience. Deep thanks go to my mother, father, and sister for their encouragement and love.

TABLE OF CONTENTS

LIST OF FIGURES

Page

LIST OF TABLES

LIST OF SCHEMES

CHAPTER I

GENERAL INTRODUCTION

Phenylalanine Hydroxylase

Overview of phenylalanine hydroxylase

Human phenylalanine hydroxylase (hPheH) converts the essential amino acid L-phenylalanine into L-tyrosine using (6R)-l-erythro-5,6,7,8-tetrahydrobiopterin (BH_4) and molecular oxygen. The catalysis by this iron dependent non-heme monooxygenase is the major pathway for catabolic degradation of dietary phenylalanine and accounts for 75% of the disposal of phenylalanine. Mutations in the hPheH gene lead to altered kinetic properties and/or reduced in vivo stability of the enzyme associated with the autosomal recessive metabolic disorder phenylketonuria (PKU). Phenylalanine hydroxylase (PheH) is coded for by the *PAH* gene, found on human chromosome 12 (*1*). So far, over 400 mutations in PheH gene have been associated with PKU or a milder form of hyperphenylalaninemia (HPA) (*2*).

Human PheH mostly exists in the liver as a pH-dependent equilibrium of homodimer and homotetramer (*3-5*). PheH belongs to the aromatic amino acid hydroxylase family along with tyrosine hydroxylase (TyrH) and tryptophan hydroxylase (TrpH). Like TyrH and TrpH, each monomer of PheH is composed of three domains: an N-terminal regulatory domain, a catalytic domain and a C-terminal tetramerization domain. Each subunit of PheH is near 52 kD. PheH requires ferrous iron atom for

---

This dissertation follows the style of *Biochemistry*.

reaction, while the enzyme is purified with ferric iron bound in the active site (*3*).

The earliest report of PheH was in 1913, when the conversion of phenylalanine to tyrosine was demonstrated through in vitro experiments (*4*). About forty years later, scientists began to actually characterize the enzyme (*4*). The early work provided evidence that rat liver contains a hydroxylation system that was later identified as PheH (*4*). PheH is widely distributed in animal tissues such as heart, spleen, brain, thyroid, kidney, rabbit muscle, and pancreas.

Structure of phenylalanine hydroxylase

Overall structure of phenylalanine hydroxylase

Because of the difficulty of crystallizing full-length PheH, there are no full-length tetrameric structures for PheH. The crystal structure of the hPheH catalytic domain with no ligand has been determined (PDB 1PAH) (*5*). An N-terminal truncated form of PAH including the catalytic and tetramerization domains (residues 118–452) was crystallized as a dimer (PDB 2PAH) (*6*). The structures of the catalytic domain of hPheH (residues 102-427) were also determined in the presence of ferric iron and cofactor or the inhibitors L-epinephrine (PDB 3PAH), L-norepinephrine (PDB 4PAH), dopamine (PDB 5PAH) and L-DOPA (PDB 6PAH) (*7*). Two important crystal structures of rat PheH including the regulatory and catalytic domains (ΔCOOH430) were determined in the phosphorylated and non-phosphorylated states with ferric iron (PDB 1PHZ and 2PHM) (*8*). They provided the structure of the regulatory domain for the first time, although the N-terminal first 18 residues were missing. The structure of the catalytic domain of hPheH (residues 118-424) in complex with ferric iron and the oxidized form of cofactor

7, 8-dihydro-L-biopterin, BH_2 has also been determined (PDB 1DMW) (*9*). The structures of the catalytic domain of hPheH in the presence of ferrous iron atom alone (PDB 1J8T) (*10*), in the binary complex with BH_4 (PDB 1J8U)(*10*), and in ternary complex with BH_4 and 3-(2-thienyl)-l-alanine (THA) (PDB 1KW0) or L-norleucine (NLE) (PDB 1MMT) were also solved (*11*). Although there is no full length crystal structure, a composite full-length structural model can be constructed by superimposing the catalytic domains of a dimeric form containing the regulatory and catalytic domains and a tetrameric form containing the catalytic and tetramerization domains (Figure 1.1) (*12*).

Regulatory domain

The regulatory domain of PheH is an α-β sandwich, forming an interlocking double βαβ motif (βαββαβ) motif. This domain is composed of a four-stranded antiparallel β-sheet flanked on one side by two short α-helices and on the other side by the segments of 118-131 and 409-422 of the catalytic domain. The N-terminal sequence (residues 19-33) extends over the active site in the catalytic domain, contacting residues 130-136, 249-252, 315-326 and 376-379 (*8*). Bacterial PheHs do not have a regulatory domain. Eukaryotic PheH regulatory domains share low similarities with those of TyrH and TrpH. The best match instead is the regulatory domain of phosphoglycerate dehydrogenase (PGDH). The regulatory domain of PheH also resembles the regulatory domains of two other enzymes: threonine deaminase (TD) and aspartate carbamoyltransferase (ATCase) (*8*). All three enzymes sharing structural similarity with the regulatory domain of PheH

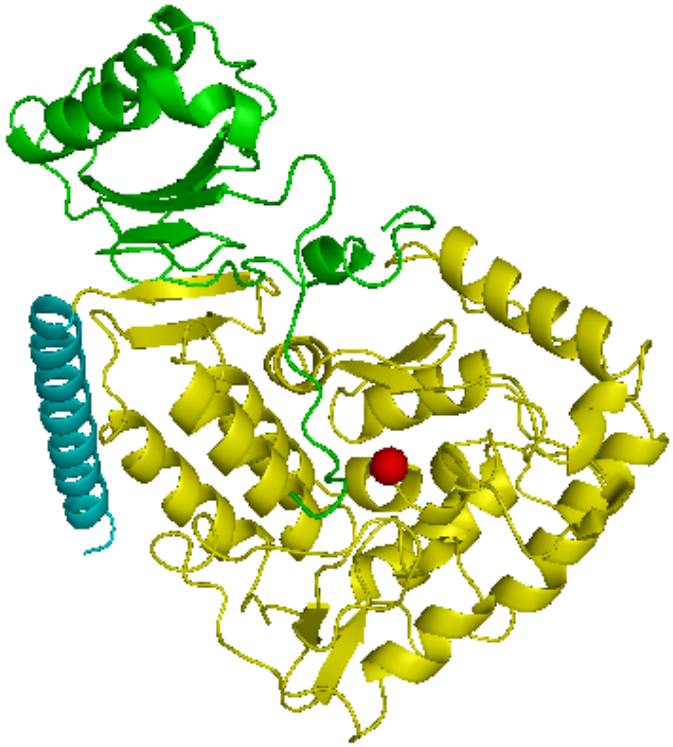

Figure 1.1. The crystal structure of full-length phenylalanine hydroxylase (Protein Data Bank codes 2PAH and 2PHM). The iron atom is shown as a red sphere. The regulatory domain (1-142), catalytic domain (142-427) and tetramerization domain (428-453) are indicated in green, yellow and cyan.

are feedback allosteric enzymes. The core of the regulatory domain of PheH is far from the active site, but the N-terminus extends from the core of the regulatory domain to the active site pocket (Figure 1.2). The N-terminal 18 residues including the phosphorylation site Ser16 are missing from the structure of the regulatory domain of both dephosphorylated and phosphorylated ΔCOOH24 PheH, suggesting that this region is highly mobile. No structural difference is observed between dephosphorylated and phosphorylated ΔCOOH24 PheH.

Catalytic domain: the active site and binding sites for iron and substrates

The PheH monomer is composed of 13 α-helices and 8 β-strands, with approximate dimensions of 50 Å × 45 Å × 45 Å. The catalytic domain is a novel basket-like arrangement of helices and loops with an open active-site that is approximately 13 Å × 13 Å wide 10 Å deep. The majority of the residues lining the active site are hydrophobic residues except for three charged glutamates, two histidines, and a tyrosine. Covering the entrance of the active site from the channel direction is a short loop (residues 378−381) (*5*).

The Fe(III) atom is located at the bottom of the active site pocket, 10 Ǻ below the surface of protein (*5*). The iron atom is coordinated to His285 (N···Fe, 2.2 Å), His290 (N···Fe, 2.2 Å) and one oxygen atom in Glu330 (O···Fe, 2.2 Å). Three water molecules are also coordinated to the iron (H2O(1)···Fe, 2.3 Å; H2O(2)···Fe, 2.1 Å; H2O(3)···Fe, 2.3 Å). In the absence of phenylalanine, the iron ligands are arranged in an octahedral geometry (Figure 1.3). In the presence of phenylalanine, the iron is 5-coordinate, with Glu330 binding the iron atom in a bidentate fashion (*13*).

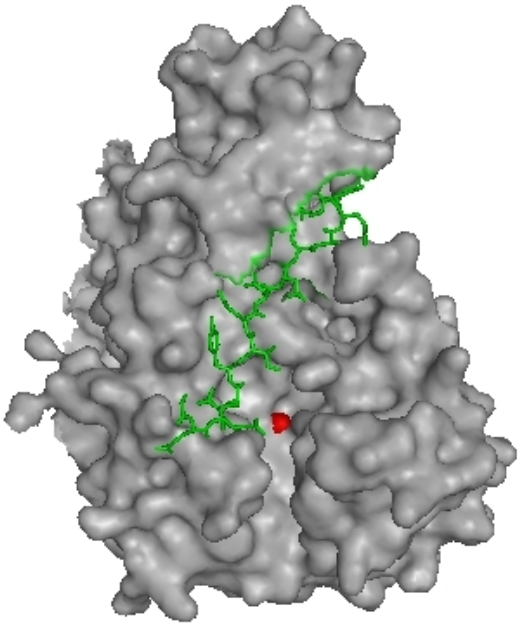

Figure 1.2. The position of the N-terminal sequence (residues 19-33) in PheH. The structure of PheH, constructed as in Figure 1.1, is shown in surface format except that residues 19−33 are shown as green sticks. The iron atom is displayed as a red sphere.

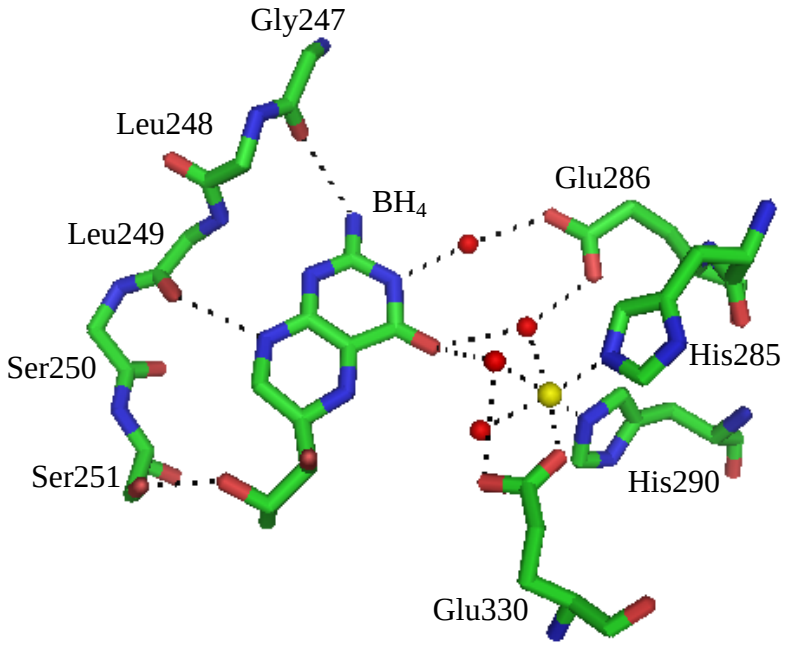

Figure 1.3. The iron and tetrahydrobiopterin binding sites of PheH. The structures are from the PDB files 1J8U. The iron atom is shown as a yellow sphere, and the three water molecules involved in coordination are shown as red spheres.

The loop residues 247-251 form direct hydrogen bonds to the BH_4. In the structure of the ternary complex, the BH_4 C3′ forms hydrophobic contacts with Leu255 $C^{\delta 1}$ (3.6 Å), Ser 251 C^{α} (3.8 Å) and Phe254 $C^{\delta 2}$ (3.8 Å), while the BH_4 C8a and C7 form contacts with Leu248 $C^{\delta 1}$ (Figure 1.3) (*13*). Glu286 forms hydrogen bonds directly to N3 and O4 of BH_4; in the structure of binary complex this residue forms two similar but water-mediated hydrogen bonds to BH_4 and a 2.7 Å hydrogen bond to one of the water molecules coordinated with the iron atom (*10*). Phe254 is close to the iron, at the edge of the proposed BH_4 binding site. The aromatic ring of Phe254 may form a π-stacking interaction with the pterin ring (*5*).

There is no crystal structure of PheH in complex with L-phenylalanine, but there is one of the ternary complex of the catalytic domain of PheH with BH_4 and 3-(2-thienyl)-l-alanine (THA), an analogue of phenylalanine. Because THA binds competitively with L-phe (*14*), the current structure with THA can help model the binding site for phenylalanine. A modeled phenylalanine is directly hydrogen-bonded to Arg270, Thr278 and Ser349. It forms water-mediated hydrogen bonds to Tyr277, Gly346, Ser350 and Glu353. In addition, it forms hydrophobic contacts with His285 and Phe331 (Figure 1.4) (*13*).

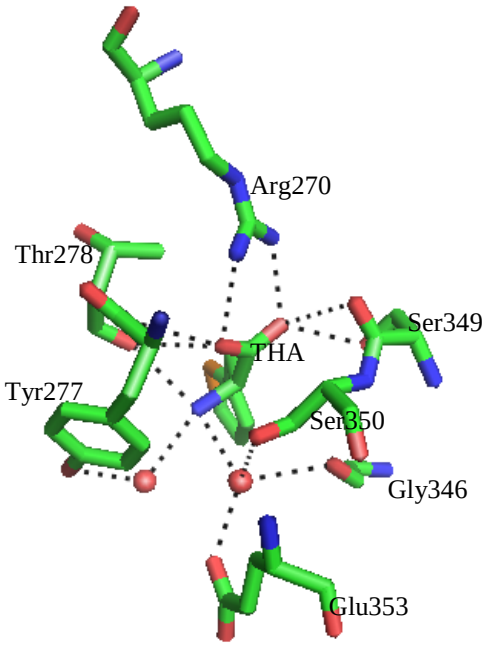

Figure 1.4. THA-binding ligands in the ternary complex of PheH (PDB file 1MMK). Arg270, Thr278 and Ser349 are directly hydrogen-bonded to THA. Tyr277, Gly346, Ser350 and Glu353 form water-mediated hydrogen bonds to THA. Two water molecules are shown as red spheres. His285 and Phe331 form hydrophobic contacts with THA that are not shown here.

Catecholamine inhibitors directly coordinate to the metal center, forming blue-green ligand-to-metal charge-transfer complexes for hTyrH (*15, 16*). Competitive inhibition by catecholamines versus BH_4 was observed for PheH (*17, 18*). The overall structures of hPheH in complex with L-DOPA, dopamine, noradrenaline, and adrenaline are very similar to each other and to the uncomplexed enzyme. These structures clearly show that the inhibitors bind to the iron atom in a bidentate coordination of the two hydroxyl groups by replacing two iron-bound water molecules (distances of 2.0−2.1 Å). In addition to the bidentate coordination to the iron center, the catecholamines form hydrogen bonds with Glu330 and Tyr325 at the active site (distances of 2.6 Å between O2 and Tyr325 OH and Glu330 Oε2). These two residues may be involved in the stabilization of the relatively high-affinity binding ($[S]_{0.5} < 1$ μM) of the amines at neutral pH. The residues are highly conserved in the aromatic amino acid hydroxylases (*7*).

Tetramerization domain

Full-length PheH has been described as existing as both a tetramer and dimer in a pH-dependent equilibrium, and possibly as some monomer (*16*). Lowering the pH or binding of phenylalanine shifts the equilibrium toward the tetrameric form of PheH (*17*). The tetramerization domain is composed of a C-terminal “arm” containing two anti-parallel β-strands, forming a β-ribbon, and a 40 Å long α-helix. The C-terminal arm extends over a neighboring monomer bringing the four helices (one from each monomer) into a tightly packed anti-parallel coiled-coil motif in the center of the structure. The tetramer is formed by two conformationally different dimers resulting in a distortion of

the 222 symmetry, caused by the occurrence of two alternate conformations of the hinge region leading to the coiled-coil helix (*6*).

Regulation

Given the fact that there is enough PheH in liver to remove phenylalanine rapidly and completely if the enzyme is fully activated, it is important that PheH be tightly controlled by a variety of mechanisms. The major mechanisms are activation by phenylalanine, inhibition by BH_4, and additional activation by phosphorylation (*18*). There are other regulatory mechanisms, including transcriptional regulation, chymotrypsin proteolysis and other activators such as lysolecithin.

Substrate-induced activation

Activation by the substrate phenylalanine is considered the key regulatory event. If the enzymatic reaction is started by adding enzyme, a lag in the rate of tyrosine formation is observed. Pretreatment with phenylalanine or lysolecithin can remove the lag, but treatment with BH_4 or 6-methyl-tetrahydropterin ($6MePH_4$) increases it (*19*). Activation of full-length PheH by phenylalanine is a reversible allosteric regulation with positive cooperativity. The activity of PheH manifests a sigmoidal dependence on the phenylalanine concentration (*19*). It has been postulated that there exist two phenylalanine-binding sites: a regulatory site and a catalytic site (*19, 20*). The regulatory binding site is responsible for the allosteric cooperativity. There is no crystal structure of PheH with phenylalanine that can directly support this two binding site model. However, there is some indirect evidence. The native PheH binds 1.5 equivalents of phenylalanine

per subunit with strong positive cooperativity but the thiol-modified enzyme can only bind one equivalent without cooperativity (*20*).

Activation of PheH by phenylalanine can directly induce conformational changes detectable by UV spectroscopy (*21*) and by an increase of the surface hydrophobicity of PheH in the presence of phenylalanine (*22*). The binding of phenylalanine induces both local and global conformational changes, based on the comparison of crystal structures of PheH. The structure of the ternary enzyme complex is slightly smaller than the binary or ligand-free PheH structure because of more compact packing. A prominent local structural change in the presence of phenylalanine is the manner in which the iron atom binds at the center of active site. As mentioned above, in the absence of phenylalanine, the iron atom is coordinated by six ligands: three amino acid residues and three water molecules. Glu330 has a monodentate interaction with iron atom. In the presence of phenylalanine, the iron atom ligands are three amino acid ligands and a water molecule, and Glu330 has a bidentate interaction. Part of loop 131-155 is refolded in the presence of phenylalanine, resulting in substantial displacement of Tyr138. The hydroxyl of this residue moves from an exposed position on the surface to the active site, where the phenol ring packs between Leu248 and Val379 forming a hydrophobic pocket (Figure 1.5). In addition to the large motion of loop 131-155, loop 247-252 moves 2.6 Å closer to the iron atom in the presence of phenylalanine.

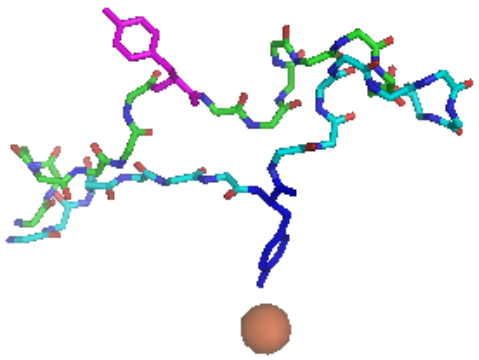

Figure 1.5. Movement of the 131-146 loop in PheH upon binding of β-thienylalanine to the tetrahydrobiopterin-bound enzyme. The loop in green with Tyr138 in magenta is from the binary complex (PDB file 1J8U); the loop in cyan with Tyr138 in dark blue is from the ternary complex (PDB file 1KWO). The iron atom is shown as a brown sphere.

The structures of phosphorylated and dephosphorylated PheH provide more information about the mechanism of phenylalanine-induced activation (*8*). The N-terminal sequence 19-33, the so-called N-terminal autoregulatory sequence (NARS), extends across the active site, contacting residues 130-136, 249-252, 315-326 and 376-379. The NARS is proposed to cover the entrance of the active site, leaving a narrow access for substrates. Later research showed that a mutant PheH lacking the NARS does not require activation by phenylalanine and is not inhibited by BH_4, supporting the proposed function of the NARS (*23*). A similar activation can be achieved by the modification of Cys237, which is located on the surface, near the interface of the regulatory and catalytic domains. It is possible that phenylalanine binding induces conformational changes that alter the relative orientation of the regulatory and catalytic domains, exposing the interface region including Cys237 (*8*).

Activation by phosphorylation

PheH can be phosphorylated at Ser16, a physiologically relevant post-translational modification (*24*). Phosphorylation of PheH is by cyclic AMP-dependent protein kinase (PKA) (*25*). A calmodulin-dependent protein kinase (CaM-PK) can phosphorylate PheH at the same site as PKA (*26*). There is controversy about the effect of phosphorylation on the kinetic characteristics of PheH. The phosphorylated PheH is reported to be two to four fold more active than the dephosphorylated enzyme in the presence of BH_4, with little or no change in the K_m for BH_4 or phenylalanine (*25*). It also has been reported that phosphorylation does not affect the V_{max} but merely decreases the concentration of phenylalanine needed to activate PheH (*27, 28*). The concentration of phenylalanine

required for the half-maximal activation of the phosphorylated enzyme is 30 to 40% less compared to the dephosphorylated protein (*28*). Phenylalanine makes PheH more readily phosphorylated by PKA (*28*). The combined effects of these two regulatory mechanisms in vivo could increase the efficiency of the regulation of PheH by phenylalanine. Comparison between the crystal structures of phosphorylated and dephosphorylated PheH indicates that phosphorylation has no major structural effects in the absence of phenylalanine, consistent with the proposal that phenylalanine and phosphorylation act in concert to activate the enzyme through a combination of intrasteric and possibly allosteric mechanisms (*8*).

The phosphorylation site, Ser16, located in the N-terminal region beyond the NARS (residues 19-33), is missing in the crystal structures of phosphorylated and dephosphorylated PheH. Mutation of Ser16 to glutamate has the same effect on activity as phosphorylation (*29*), while mutation of Ser16 to alanine results in a mutant protein with the same characteristics as the dephosphorylated PheH. These results indicate that activation of PheH by phosphorylation is due to the introduction of a negative charge, suggesting the involvement of electrostatic interactions (*30*). The negative charge on Ser16 allows the NARS (residues 19-33) to make electrostatic interactions with the catalytic domain. In the absence of phenylalanine, the NARS covers the entrance into the active site leaving a narrow access for substrate. Incubation with phenylalanine causes a relative rotation of the regulatory and catalytic domains, which could be stabilized by phosphorylation on Ser 16, resulting in the displacement of the NARS from the entrance of the active site (*8*).

Inhibitors

PheH is inhibited by catecholamines, similarly to the other aromatic amino acid hydroxylases (*18*). The physiological cofactor of PheH, BH_4, is reported to inhibit the activation by phenylalanine. The lag observed when starting the reaction by adding enzyme is increased if the enzyme is treated with BH_4 (*19*). BH_4 is also reported to inhibit activation by lysolecithin (*31*). BH_4 protects native PheH from cleavage between the regulatory and catalytic domains by chymotrypsin, while the regulatory domain is cleaved from the catalytic domain in the absence of BH_4 (*32*). Phosphorylation of PheH by PKA is inhibited by BH_4, in contrast to the effect of phenylalanine (*28*).

Other activation

Proteolysis of PheH by chymotrypsin increases the measured V_{max} value. Chymotrypsin reduces the size of PheH from 52 kDa to 36 kDa in the presence of BH_4 by removing an N-terminal 11 kDa fragment, and a C-terminal 5 kDa fragment. The 36 kDa domain that remains is 30-fold more active than native PheH when assayed in the presence of BH_4, suggesting that the N-terminal 11 kDa region may mediate PheH inhibition (*32*).

Treatment of rat PheH with lysolecithin or a thiol-modifying reagent such as N-ethylmaleimide has a similar activation effect and exposes a single thiol group (*20, 33*). These results suggest the two treatments may result in similar conformational changes. Activation of PheH by thiol-modification results in up to 82% of the activity found with phenylalanine-activated enzyme. The modified cysteine was identified as Cys237 (*34*). Cys237, localized on the surface of the catalytic domain, is conserved in rat, human,

mouse and *Drosophila melanogaster* PheHs. The mutant C237D-hPAH has higher basal activity than phenylalanine-activated hPAH (*35*). Cys237 is spatially close to residues in the oligomerization and regulatory domains of an adjacent subunit in the dimer, notably Arg68. Arg68 is in loop 68-75 in the regulatory domain and also has contacts with residues from the same subunit. The mutations C237D, R68A, and C237A result in increases in the basal activity and affinity for phenylalanine, while the mutant C237R PheH shows a reduced affinity for the substrate and elimination of positive cooperativity. These activating mutations induce a series of conformational changes, including the displacement of the NARS from the active site, the domain movements around the hinge region Arg111−Thr117, and the rearrangement of loop 68−75 (*36*). These conformational changes seem to also occur during activation of PheH by phenylalanine, supporting the proposal that phenylalanine-induced activation also occurs through a combination of sequential conformational changes.

The activity of PheH is also under transcriptional regulation, though little is known about this. The 5’ region of gene for mammalian PheH lacks a proximal TATA box but contains various sequences that can interact with multiple transcriptional factors (*37*). The level of PheH in the liver is controlled at the transcriptional level by glucocorticoids, which interact with a partial glucocorticoid response element (*37*).

Model of regulation mechanism

Based on the regulatory characteristics of phenylalanine and BH_4, Shiman and his colleagues proposed a model for the mechanism of regulation of PheH (Scheme 1.1) (*38, 39*). Purified PheH is proposed to be in an inactive form, Ei; binding of phenylalanine,

converts the enzyme into an active form, Ea; binding of cofactor BH_4, traps the enzyme in the inactive BH_4·enzyme complex and blocks phenylalanine activation. This model predicts that conformational changes accompany binding of both amino acid and cofactor, in agreement with the crystal structures.

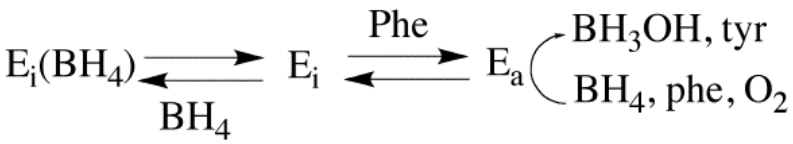

Scheme 1.1. Model for regulation of PheH.

PKU and PKU therapy

Phenylalanine is an essential amino acid in the diet. PheH catalyzes the hydroxylation of phenylalanine and produces tyrosine. As an aromatic amino acid, phenylalanine, tyrosine and tryptophan are not only constituents of proteins, but also the precursors of monoamine neurotransmitters, serotonin and the catecholamines (dopamine, norepinephrine and epinephrine). Most dietary phenylalanine is hydroxylated to tyrosine. Defects in the function of PheH result in high-level accumulation of phenylalanine in blood. The high concentration of phenylalanine in blood has a toxic effect on cognitive development (*40*). Excess phenylalanine is excreted through the urinary system as intact phenylalanine or as phenylpyruvic acid (*41*).

A deficiency of phenylalanine hydroxylase due to mutations in the PheH gene is the most common cause of the human disease phenylketonuria (PKU). PKU is an autosomal recessive disease; the most common symptoms are high blood serum levels of phenylalanine, lighter skin and hair pigmentation, a 'mousy' odor and mental retardation (*42*). Ledley et al. (*43*) found no detectable phenylalanine hydroxylase enzymatic

activity or immunoreactive protein in the liver of a fetus aborted after prenatal DNA diagnosis of PKU, while both were found in control specimens of similar gestational age. The size and the amount of the PheH mRNA were normal, suggesting that the mutations affected the translation or stability of the protein (*43*).

The most important thing learned from the study of PKU pathogenesis is that the treatment of PKU must reduce the phenylalanine content in blood. Traditional treatment of PKU includes restriction of dietary phenylalanine and adequate intake of tyrosine (*44*). Injection of phenylalanine ammonia-lyase (PAL), a recombinantly produced phenylalanine metabolizing enzyme, can help clear the excess phenylalanine from the circulation (*45*). For a subset of PKU patients, oral administration of sapropterin dihydrochloride, a synthetic form of BH_4, can reduce blood phenylalanine levels (*46*). Patients with mutations in the regulatory domain often respond to BH_4 (*47*). PheH is a liver enzyme; therefore liver transplant is another potential treatment of PKU. However, the life-long need for immunosupression due to transplantation reduces the quality of life. Liver repopulation is an alternative method that might avoid the suffering of long-term immunosupression. This method attempts to replace PheH-deficient hepatocytes with healthy cells with PheH activity. These cells could be fully differentiated hepatocytes from a healthy donor or embryonic stem cells. Like liver transplantation, this treatment method is also limited by the scarcity of donors. Although still under research in the laboratory, gene therapy is a promising strategy for PKU. This method attempts to recover PheH activity by transferring PheH cDNA into the livers of a PKU patient. Most published experiments of gene therapy for PKU use recombinant viral vectors (*48, 49*).

This method avoids an immune response but is limited by the low rate of cell transduction and inefficient expression. Much work remains before gene therapy can be applied in the clinic safely.

C. violaceum *PheH*

PheH is also present in bacteria. Only the PheH from *Chromabacterium violaceum* has been characterized. *C. violaceum* PheH has many characteristics similar to mammalian liver PheH. This bacterial enzyme is a monomeric enzyme (33 kD) (*50*), while mammalian PheH is a mixture of dimer and tetramer. The primary structure of *C. violaceum* PheH is 24% identical to rat and human PheH and 11% identical to eukaryotic TyrH and TrpH (*50*). In contrast to the complex composition of three domains in mammalian PheH, *C. violaceum* PheH has only one domain, corresponding to the catalytic domain of mammalian PheH. The complex regulatory behaviors found with the mammalian PheH have not been reported, making *C. violaceum* PheH a model to study the activity without inference from regulation.

There are conflicting evidences reported in literatures on the metal requirement of *C. violaceum* PheH. It was first described as a Cu^{2+}-dependent enzyme (*51*). It was subsequently reported to be a metal-independent enzyme (*52*). Finally, biochemical studies showed that the Fe^{2+}-dependent enzyme was the active form, and copper-substituted *C. violaceum* PheH has no L-phenylalanine hydroxylation activity (*53*).

The kinetic mechanism of recombinant *C. violaceum* PheH was reported as a sequentially ordered mechanism. The enzyme binds pterin first reversibly, followed by reversible binding of amino acid and finally oxygen. No product is released before all

three reactants bind (*54*). This mechanism is different from that of TyrH (*55, 56*). For rat TyrH, the amino acid is believed to bind last.

The activity of *C. violaceum* PheH is the highest among all forms of PheH known. *C. violaceum* PheH is ten-fold as active as the regulatory and tetramerization domain-truncated human PheH (*57*). The isotope effects on the initial hydroxylation, subsequent tautomerization step and benzylic hydroxylation for *C. violaceum* PheH are close to those of the catalytic domain of eukaryotic PheH, suggesting the reactivities of the prokaryotic and eukaryotic hydroxylases are similar (*58*).

Various crystal structures of Fe^{2+}-dependent *C. violaceum* PheH including the Fe-free, Fe(III)-bound and Fe(III) plus 7,8-BH_2-bound have been determined (*59*). The structure of *C. violaceum* PheH resembles the catalytic domains of human PheH and rat TyrH. However, the N-terminal and C-terminal residues of *C. violaceum* PheH adopt different folds from those of human PheH and rat TyrH. The active sites of *C. violaceum* PheH and human PheH are similar. As in human PheH, the iron atom in the structure of *C. violaceum* PheH coordinates with two histidine residues (His138 and His143) and one glutamate residue (Glu184), forming an approximate octahedral coordination geometry together with two water molecules. Glu184 coordinates with the iron atom in a bidentate fashion in both the Fe(III)-bound and Fe(III) plus 7,8-BH_2 structures, whereas it is monodetate in the human PheH Fe(III) plus 7,8-BH_2 form structure. The pterin-binding loop 245-250 in human PheH moves toward the iron atom upon pterin binding. However, the corresponding loop 98-103 in *C. violaceum* PheH only shows a minor conformational change. The N-terminal regions of the three forms of *C. violaceum* PheH

are completely different from those of hPheH and rat TyrH. The lack of the NARS and other residues interacting with the active site makes the active site of *C. violaceum* PheH more accessible to solvent. The C-terminus of *C. violaceum* PheH adopts a different secondary structure from the C-termini of hPheH and rat PheH that form long alpha helices for dimer or tetramer formation. The ten-fold higher specific activity of *C. violaceum* PheH, compared to hPheH, may result from its more solvent accessible active site, differential placement of the pterin binding loop, or the lack of the NARS. *C. violaceum* PheH lacks many of mobility-restricting interactions that are seen in hPheH; hence, the flexibility of the structure of *C. violaceum* PheH increases, resulting in more catalytic efficiency.

Aromatic amino acid hydroxylase family

PheH belongs to the small enzyme family of aromatic amino acid hydroxylases that includes two other members: tyrosine hydroxylase (TyrH) and tryptophan hydroxylase (TrpH). The three enzymes are all homotetramers, and each monomer is composed of an N-terminal regulatory domain (PheH 1-117; TyrH 1-164; TrpH 1-105), a catalytic domain (PheH 118-410; TyrH 165-455; TrpH 105-401) and a C-terminal tetramerization domain (PheH 411-453; TyrH 456-498; TrpH 402-444). Each monomer binds an iron atom at the center of the catalytic domain. The catalytic domains of the three rat enzymes are 52% identical, while the identity of the regulatory domains is less than 14% (*60*).

Phenylalanine catabolism is a necessary metabolic pathway for emerging life forms before neurotransmitter synthesis. Phenylalanine hydroxylation is ancestral

phylogenetically, and PheH is close to the precursor of the aromatic amino acid hydroxylase family (*61*). It is estimated that the gene for TyrH deviated from the ancestral PheH about 750 million years ago and the gene for TrpH 600 million years ago, explaining why TyrH alone acquired the ability to hydroxylate tyrosine (*62*).

Tyrosine Hydroxylase

Overview of tyrosine hydroxylase

Tyrosine hydroxylase (TyrH) is another well-studied member of aromatic amino acid hydroxylase family. This enzyme was discovered by Nagatsu *et al*. in the laboratory of Sidney Udenfriend at National Institute of Health in 1964 (*63*). TyrH hydroxylates tyrosine forming L-3, 4-dihydroxyphenylalanine (DOPA); this is the rate-limiting step in production of the catecholamines dopamine, norepinephrine and epinephrine.

TyrH is found in the central nervous system, adrenal gland, gut and retina. It forms a homotetramer in solution with a mass close to 240 kD. It is predominantly found in the cytoplasm (*64*). Rat TyrH has 498 residues forming three domains. There are four different isoforms of human TryH, two in anthropoids and one in rat and cow (*65*). TyrH is coded by a single gene in all species. Multiple isoforms are due to alternative splicing of mRNA (*66*). All the sequence differences lie in the N-termini (*67, 68*). The C-terminal region (156-498) of TyrH possesses the same catalytic activity as the whole enzyme (*69*). The crystal structure of the C-terminal region of rat TyrH has been determined (*70*).

Structure and active site

The active site of TyrH is a 17 Å deep cleft at the center of the catalytic domain basket. The entrance into the active site is guarded by two loops: residues 423−428 and 290−296, which are within 12 Å of each other across the top of the 30 Å long and 15 Å wide active site. The N-terminus of the C-terminal region, located near this entrance in a reasonable position for placement of the regulatory region, has been postulated to function by directly controlling the accessibility of substrate or cofactor to the active site (*18, 32*). The iron atom is 10 Å below the enzyme surface within the active site cleft; the coordinating residues are His331, His336 and Glu376. These three residues are conserved in all three aromatic amino acid hydroxylases. The iron atom is in a square pyramidal geometry with His331 as the axial ligand and two water molecules joining the iron ligands in the equatorial positions. The region opposite His331 is distinctly void of density where a possible sixth ligand would be located (*70*). This iron coordination is similar to that seen in the crystal structures of both the ferric and ferrous forms of an iron-utilizing bacterial extradiol dioxygenase and is referred to as a 2-His-1-carboxylate facial triad (*71*). Surrounding the iron binding site there are many conserved residues that may play roles in catalysis. Phe300 and Phe309 are completely conserved in the 16 known mammalian gene sequences in this family. In the crystal structure of rTyrH, these two residues are exposed on the surface of the active site and point toward the iron. These residues may help to attract the hydrophobic portions of the substrate and cofactor (*70*). Pro327 is another highly conserved residue. In the structure, Pro327 noticeably protrudes into the active site. The proline C^{β} and C^{γ} are 4.8 and 5 Å, respectively, from

the active site iron atom. The mutant P327L TyrH shows reduced activity and a 20-fold increased K_m for BH_4 (*72*). Another mutation, P327A, does not substantially affect the K_m value for the cofactor, but it does eliminate substrate inhibition. These data are consistent with enzyme kinetic studies in which tyrosine is a competitive inhibitor versus $6MePH_4$ at concentrations above 150 μM (*56*).

The loop 131-150 in PheH takes on a dramatically different conformation in the presence of amino acid, especially residue Tyr138, moving from an exposed position on the surface to being buried in the active site (*13*). An alanine substitution scanning mutagenesis study on the homologous polypeptide 177-191 in TyrH showed alterations in the K_m values for substrates, the V_{max} value, and the coupling of BH_4 oxidation to tyrosine hydroxylation (*73*). TyrH mutants with alanine substituted for residues Lys183 to Pro186 had the greatest alteration on K_{tyr} values and V_{max} values, consistent with the central region of the loop being most critical for binding and catalysis. The homologous residue of Tyr138 of PheH in TyrH is Phe184. Mutants of F184Y TyrH and of Y138F PheH did show modest changes in the relative preferences of the two enzymes for tyrosine versus phenylalanine, but the effects are better described as a loss of specificity rather than a reverse of specificity. These results suggest that Phe184 of TyrH and Tyr138 of PheH do not play dominant roles in determining amino acid substrate specificity (*73*).

Several conserved residues in the active site have been studied by site-directed mutagenesis. The charged residues Arg316, Glu326, Asp328 and Glu332 in the active site of TyrH are conserved among all three hydroxylases. Mutagenesis has shown that

Arg316 and Asp328 are important in tyrosine binding, presumably by interacting with the carboxylate and amino moieties. Glu326 is not directly involved in catalysis. Glu332 is required for productive tetrahydropterin binding (*74*). Characterization of mutations of the conserved residues Phe309 and Phe300 of TyrH showed that Phe309 plays an indirect role in catalysis by maintaining the proper overall structure of the active site and Phe300 plays a role in maintaining the strength of the interaction of the pterin with TyrH (*75*). The conserved residue Asp425 of TyrH plays an important role in determining the amino acid specificity. A possible reason is that carboxyl oxygen of Asp425 is necessary to hydrogen bond to the hydroxyl group of tyrosine in order to properly orient that substrate in the active site (*62*). Ser395 in the active site of rat TyrH is conserved in all three members of the family of pterin-dependent hydroxylases. The hydroxyl oxygen of Ser395 is located 2.78 Å from the imidazole N-1 of the iron ligand His331, an appropriate distance for a hydrogen bond. A mutagenesis study suggests that Ser395 is required for amino acid hydroxylation but not for cleavage of the oxygen−oxygen bond (*76*).

Regulation

Inhibition by catecholamines

Catecholamines are competitive inhibitors versus the BH_4, the first substrate to bind in the TyrH kinetic mechanism (*56, 77*). A commonly accepted explanation of inactivation of TyrH by binding with dopamine is that dopamine binds tightly to the ferric iron atom to produce an inactive complex (*78*). TyrH has a single iron atom per subunit that must be in the ferrous form for catalysis (*79*). The iron is readily oxidized to

the ferric form during catalytic turnover resulting in inactive enzyme; the ferric iron can be reduced by a tetrahydropterin (*80*). The oxidized enzyme can be trapped by the product dihydroxyphenylalanine or DOPA.

Activation by phosphorylation

TyrH can be phosphorylated at Ser8, Ser19, Ser31 and Ser40 by different protein kinases (*81*). Ser19 can be phosphorylated by CaM-PKII, and Ser31 can be phosphorylated by the MAP kinases ERK1 and ERK2 (*82*). Ser8 is phosphorylated by a novel proline-directed serine/threonine kinase (*83*). Among the four serines, phosphorylation on Ser40 causes the most dramatic activation (*66*). Ser40 can be phosphorylated by PKC, CaM-PKII, cGMP-dependent protein kinase, and cyclic AMP-dependent protein kinase (PKA) (*84, 85*). CaM-PKII phosphorylates TyrH at Ser19 without any activation. However, this phosphorylated enzyme can be activated by addition of 14-3-3 protein (*86, 87*). Unlike the strong activating effect of PKA phosphorylation, phosphorylation by CaM-PKII and protein 14-3-3 can only moderately increase activity at acidic pH.

The activation effects of phosphorylation on TyrH without any other ligands are small (*77, 82*). The effects of most of these phosphorylations have not been established. The effect of phosphorylation of Ser 40 is best understood. The primary effect of phosphorylation at Ser40 is to decrease the enzyme's affinity for catecholamines (*77, 78, 88*). Phosphorylation of the ferric TyrH results in a 17-fold decrease in affinity for DOPA and a 300-fold decrease in the affinity for dopamine (*88*). The reason for this activation by phosphorylation is that TyrH requires ferrous iron atom for activity (*79*)

and phosphorylation of Ser40 releases catecholamines tightly bound to the ferric form iron, allowing tetrahydrobiopterin to reduce the iron for activity.

Phosphorylation of TyrH and catecholamine binding result in opposite changes in the structure of TyrH. TyrH phosphorylated at Ser40 has a shorter retention time on gel filtration chromatography compared to TyrH alone, while dopamine-bound TyrH has a slightly longer retention time (*86*). Binding of dopamine greatly decreases the sensitivity of residues 33 and 50 in the regulatory domain to proteolysis, while phosphorylation of Ser40 increases the sensitivity by a comparable amount (*87*). Truncated TyrH lacking the first 39 residues is not inhibited by preincubation with dopamine (*89*). The interaction between the regulatory domain and the amino moiety of the catecholamine is critical to determine the affinity for a catecholamine (*90*). These results support a model in which there is direct interaction between the regulatory domain and the amino group of a catecholamine bound in the active site, preventing substrate access; phosphorylation triggers a conformational change, weakening this interaction (*90*).

Allosteric regulation

Heparin, phospholipids, and polyanions have all been shown to increase the activity of TyrH by interaction with the enzyme in a reversible manner (*91-93*). Polyanions bind the regulatory domain of TyrH, specifically the N-terminal residues between 76 and 90 (*69, 94*). Therefore, affinity columns such as heparin-Sepharose (*95*) can be used to purify TyrH. Nucleic acids are also reported to nonspecifically activate TyrH (*96*).

Kinetic and chemical mechanism of TyrH

TyrH reacts through a fully sequential mechanism in which all the substrates bind to the enzyme in the order of BH_4 first, then oxygen, and finally tyrosine (*56*) . In addition to the three substrates, TyrH also requires ferrous iron atom for its reaction(*79*). TyrH is purified with ferric iron, and reaction requires pre-reduction of the metal atom. BH_4 or 6-methyltetrahydropterin ($6MePH_4$) can rapidly reduce the iron atom (*97*). TyrH can use tyrosine, phenylalanine or tryptophan as the amino acid substrate (*62, 98*). The products of hydroxylation of phenylalanine by TyrH are mostly tyrosine and a small amount of 3-hydroxyphenylalanine, with the V_{max} value one fourth of that with tyrosine and the K_m value about 6-fold higher (*95, 96*). Tryptophan is a poor substrate for TyrH, with a significantly lower V_{max} value and higher K_m value (*56*). Chimeric TyrH containing the regulatory domain of PheH and catalytic domain of TyrH has similar substrate specificity to TyrH, establishing that it is the catalytic domain that determines substrate specificity (*99*).

The chemical mechanism of TyrH is the most-studied among all three members of aromatic amino acid hydroxylase family. In this mechanism, oxygen reacts with BH_4 to form a Fe(II)-μ-peroxypterin, a precursor of the hydroxylating intermediate. The peroxy OO bond of this precursor is cleaved to form the actual hydroxylating intermediate, Fe(IV)O, and 4a-hydroxypterin (Scheme 1.2) (*76, 100, 101*). In a recent study, this high spin Fe(IV)O intermediate was directly detected by rapid-freeze quench Mössbauer spectroscopy (*102*). The Fe(IV)O intermediate reacts with the aromatic side chain of the tyrosine through an electrophilic aromatic substitution to form the product

dihydroxyphenylalanine (DOPA) (*103*). The rate-limiting step in TyrH turnover is release of DOPA and/or 4a-hydroxypterin (*104*).

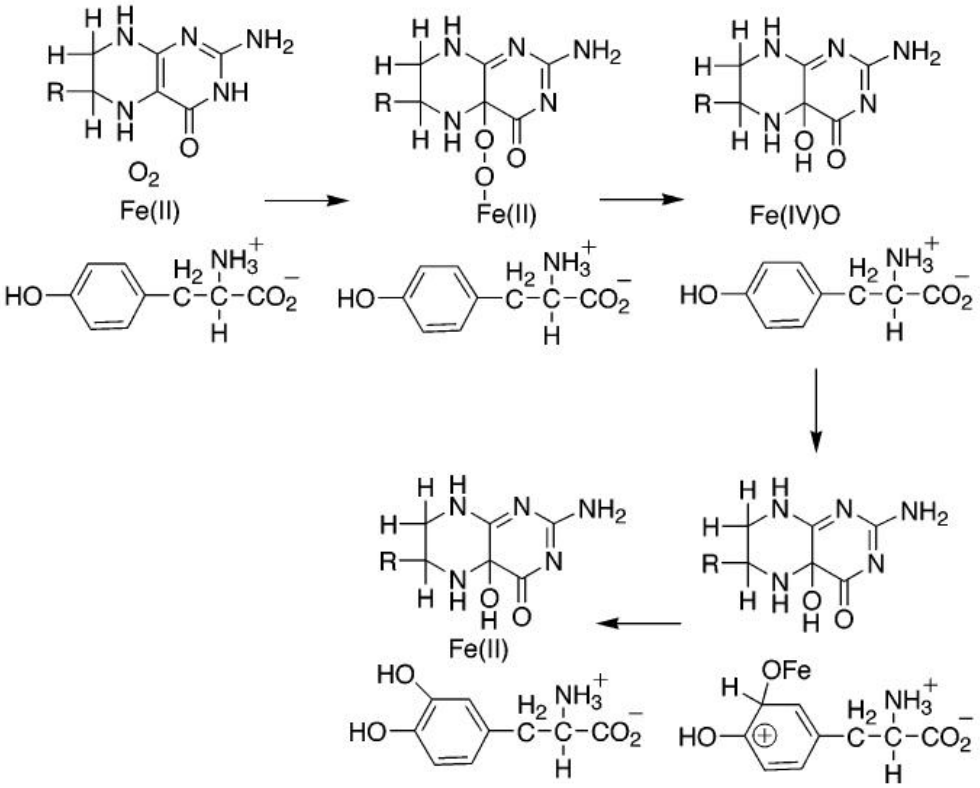

Scheme 1.2. Chemical mechanism of TyrH.

Related diseases

The characteristics of TyrH deficiency include broad phenotypes ranging from tyrosine-deficient DOPA-responsive dystonia to DOPA-unresponsive infantile Parkinsonism and progressive infantile encephalopathy. Parkinson's disease (PD) is a common neurodegenerative disorder with symptoms of tremor, bradykinesia and rigidity, which has been associated with the degeneration of dopamine biosynthesis in the central nervous system (*105*). A logical and efficient treatment for PD is to correct or bypass the enzyme deficiency by treatment with L-DOPA, DA agonists, inhibitors of DA

metabolism, or brain grafts with cells expressing TH (*106*). Surgical treatment and gene therapy are novel treatments for PD, though extensive work still remains to be done before clinical application. In addition, TyrH is also suspected to have a direct pathogenetic role because the enzyme is a source of reactive oxygen species (ROS) in vitro and a target for radical-mediated oxidative injury (*107*). However, this hypothesis is difficult to test because it is hard to separate the possible pathogenetic effects from the effects of catecholamines and other components of catecholaminergic neurons.

Tryptophan Hydroxylase

Overview of tryptophan hydroxylase

Tryptophan hydroxylase (TrpH) catalyzes the hydroxylation of tryptophan using oxygen and BH_4 as the other substrates. This enzyme produces 5-hydroxy-L-tryptophan in the rate-limiting step of serotonin (5-hydroxytryptamine) synthesis. Serotonin is a neurotransmitter that has been implicated in numerous physiological functions and pathological disorders. Serotonergic dysfunctions are involved in psychiatric diseases such as depression, anxiety, drug abuse, eating disorder and schizophrenia (*108*). Serotonin is the precursor for melatonin. Melatonin regulates the behavioral and physiological circadian rhythms, and may be involved in the sleep pathway (*109*). TrpH has two isoforms (*110*). Isoform 1 (TPH1) is expressed mainly in the peripheral parts of the body (*111*) and in the pineal gland (*112*). In the periphery, it is found in mast cells, stem cells, and enterochromaffin cells in the pancreas, intestine and gastric system (*113, 114*). Isoform 2 (TPH2) is responsible for tryptophan hydroxylation in the brain (*115*).

Overall structure

TrpH is a homotetramer with a mass of 51 kD for each subunit (*116*). As with PheH and TyrH, TrpH is composed of three domains. Sequence alignments reveal 48% sequence identity between rabbit TrpH and rat TyrH, and 53% identity between rabbit TrpH and human PheH (*117*). The sequence identity of the catalytic domains of rabbit TrpH and rat TyrH is 60%, whereas the identity of the regulatory domains is only 11% (*118*).

A structure of doubly truncated (ΔNH102-ΔCOOH402) human TrpH has been determined with 7, 8-dihydro-L-biopterin (BH_2) bound and ferric iron (1MLW) (*115*). The catalytic core of TrpH is a mixed α and β structure, similar to those of hPheH and rTyrH, as well as *C. violaceum* PheH. The hTrpH active site consists of an approximately 9 Å deep and 10 Å wide cavity. Lining the active site channel are two loops, 263-269 and 363-372. This structure also shows that hTrpOH binds a catalytic Fe(III) atom ~13 Å below the surface and at the intersection of the channel and the opening to the active site. As in PheH, the iron in TrpH is octahedrally coordinated to three residues, His272 (N-Fe distance of 2.1 Å), His277 (N-Fe distance of 2.0 Å), and one carboxyl oxygen atom of Glu317 (O-Fe distance of 2.4 Å), together with three water molecules: Wat1 (axial to His272, 2.2 Å to Fe), Wat2 (axial to His277, 2.3 Å to Fe), and Wat3 (axial to Glu317, 2.2 Å to Fe. The oxidized cofactor BH_2 π-stacks on Phe241 and Tyr235, forming hydrogen bonds to Gly234 and Leu236. The pterin O4 atom is also hydrogen bonded to two of the three water molecules coordinated to the iron, with distances of 2.4 and 2.8 Å. Glu273 also forms two water-mediated hydrogen bonds to

the pterin. The octahedral coordination of iron is approximately similar to what is seen in the ferric doubly truncated hPheOH structure (*5*), in contrast to the five coordination observed in ferric rTyrH (*70*).

The only crystal structure of TrpH with bound amino acid is for the catalytic domain (Δ1-100/Δ415-445) of chicken TrpH isoform 1 (TrpH1) in complex with tryptophan and an iron-bound imidazole (*119*). Tryptophan directly interacts with residues Thr266, Ile367, Arg258, Ser337 and two water molecules. The tryptophan stacks against Pro269 with a distance of 3.9 Å between the iron and the tryptophan, yielding an angle of 141° between them. The iron binds His273, His278, and Glu318 (partially bidentate) and one imidazole in a distorted trigonal bipyramidal coordination.

As seen in PheH, binding of amino acid substrate triggers conformational changes. Compared to the structure of the human TrpH1 without tryptophan, the structure of chicken TrpH 1 is more compact, and the loops of residues Leu124-Asp139 and Ile367-Thr369 close around the active site. Tyr126 corresponds to Tyr138 in PheH, and Phe184 in TyrH. Crystal structures of PheH have shown that this tyrosine changes from a position on the surface to a buried position close to the active site upon binding of the substrate analogue THA or NLE. In chicken cTrpH1, Tyr126 has not moved to a buried position, but the loop has made an extra turn, still keeping Tyr126 on the surface where it is packed against Phe137, with a triethylene glycol molecule nearby (4 Å). The chicken TrpH1·Trp·imidazole structure is more like the PheH·BH_4·thienylalanine structure than the human TrpH1 structure (*119*).

Regulation

TrpH is phosphorylated by CaM-PKII and PKA (*120, 121*). Ser58 is the phosphorylation site for PKA (*122*). The phosphorylation site for CaM-PKII has not been determined. However, Ser58 cannot be ruled out. Phosphorylation-dependent activation of TrpH by both PKA and CaM-PKII requires the presence of an activator protein that has been identified as a 14-3-3 protein (*88, 89*). Direct binding of 14-3-3 to phosphorylated TrpH has been observed, with a K_d value of 30 nM (*123*). The binding of 14-3-3 is hypothesized to stabilize TrpH through an interaction with the regulatory domain (*123, 124*). Another possible effect is that binding of 14-3-3 prevents dephosphorylation of TrpH (*123*).

TrpH is subject to significant substrate inhibition when tryptophan is varied at a fixed concentration of either BH_4 or $6MePH_4$, and vice versa (*123, 125*). Unlike TyrH, TrpH is not subject to feedback inhibition by its product 5-hydroxy-L-tryptophan (*126*). L-DOPA has been reported to inhibit TrpH activity (*127*). Many Parkinson's disease patients undergoing L-DOPA treatment have the side effect of depression, which may be explained by the reduced production of serotonin. Nitric oxide (NO) is another compound found to modulate the TrpH activity. NO irreversibly inactivates TrpH (*119, 125*). The inactivation may occur through modification of sulfhydryls. TrpH is also inhibited by thiol-binding compounds (N-ethylmaleimide and mercurials) (*128*) or other agents that form disulfides in protein (DNTB and dithiodiglycolic acid) (*122*).

The substrate inhibition at high concentrations of tryptophan reported for TrpH suggests an ordered kinetic mechanism (*129*). The binding order of amino acid and

tetrahydropterin is likely random for TrpH (*60*). TrpH shares the same catalytic mechanism as TyrH, forming an electrophilic Fe(IV)O hydroxylating intermediate (*60*). The rate-limiting step in the reaction catalyzed by TrpH is oxygen addition to the aromatic ring of the amino acid (*130*).

Substrate specificity

TrpH can also hydroxylate tyrosine and phenylalanine. Tyrosine is a very poor substrate (*125*). Tyr236 is involved in BH_2 binding and tryptophan binding. Two positions of TrpH are believed to be involved in determining substrate specificity, Phe314 (*131, 132*) and Ile367 (*133*). Trp372 is conserved in all TyrH sequences. The residue at this position in TrpH is Phe314. Phe314 is conserved in all known tryptophan hydroxylases. F314W TrpH no longer shows a preference for tryptophan over phenylalanine as substrate, consistent with a role of this position in substrate specificity (*132*). The residues corresponding to Ile367 are Val379 in PheH and Asp425 in TyrH. Asp425 in TyrH is involved in determining the substrate specificity of TyrH.

CHAPTER II

CHARACTERIZATION OF METAL LIGAND MUTANTS OF PHENYLALANINE HYDROXYLASE: INSIGHTS INTO THE PLASTICITY OF A 2-HISTIDINE-1-CARBOXYLATE TRIAD

Phenylalanine hydroxylase (PheH) is a tetrahydropterin-dependent nonheme enzyme that catalyzes the hydroxylation of phenylalanine to tyrosine, an important pathway for phenylalanine catabolism (Scheme 2.1) (*81*). As a liver enzyme, PheH is critical for catabolizing excess phenylalanine in the diet. Consequently, a deficiency in PheH results in the debilitating disease phenylketonuria (*134*). PheH belongs to the small family of aromatic amino acid hydroxylases, all of which use tetrahydrobiopterin as the source of electrons to hydroxylate the aromatic ring of an aromatic amino acid. Tyrosine hydroxylase (TyrH) and tryptophan hydroxylase (TrpH) are the other two members; these are the rate-limiting catalysts for catecholamine and serotonin biosynthesis, respectively. The three eukaryotic enzymes form homotetramers in solution (*135-137*). Each monomer consists of three domains: a regulatory domain at the amino terminus, a catalytic domain and a tetramerization domain at the carboxyl terminus (*117, 129*). The catalytic domains are homologous and contain all the residues required for catalysis and the determination of substrate specificity (*99*), while the regulatory domains show low levels of sequence identity, consistent with their diverse regulatory mechanisms (*129*).

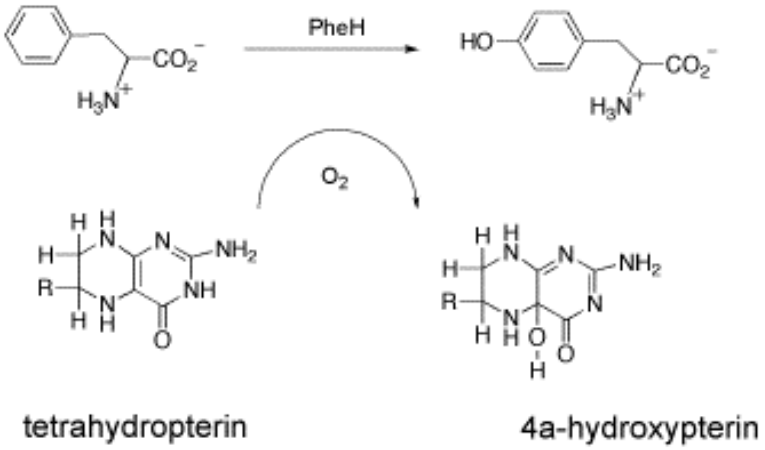

Scheme 2.1. The phenylalanine hydroxylase reaction.

The similar structures of the catalytic domains (*138*) and a variety of mechanistic studies suggest that the three aromatic amino acid hydroxylases share a common catalytic mechanism (*60*). For all three enzymes, hydroxylation of the physiological substrate occurs via an electrophilic aromatic substitution reaction with an activated oxygen species (*101, 103, 139*). In the case of TyrH the latter has been shown to be an Fe(IV) species (*102*), consistent with the proposed involvement of an Fe(IV)O as the hydroxylating intermediate in all three enzymes (*60*). The reactivities of the hydroxylating intermediates in all three enzymes are similar (*140*), and they have overlapping substrate specificities (*125, 140, 141*), supporting the proposal for a common Fe(IV)O intermediate. The iron atom in each is coordinated by two histidines and a glutamate (*70*). This metal-binding arrangement has been named a "2-His-1-carboxylate facial triad" and is also found in a variety of nonheme iron enzymes with different three-dimensional structures, including the extradiol and Rieske dioxygenases, the α-ketoglutarate-dependent hydroxylases, and isopenicillin N synthase (*142*). The

ubiquity of the 2-His-1-carboxylate facial triad suggests that it is ideally suited for formation of a high-valent iron-oxo hydroxylating intermediate (*142*).

The extent to which the 2-His-1-carboxylate facial triad is optimal for specific reactions should in principle be reflected in the tolerance to substitution of the three amino acid residues in the triad in the different families of enzymes containing this motif. The metal sites of TyrH and PheH are shown in Figure 2.1. Mutagenesis of either histidine in TyrH to alanine (*143*) or in PheH to serine (*144*) is reported to give inactive enzyme. However, in the case of TyrH, less drastic mutations give more interesting results (*145*). Both the H336E and H336Q enzymes retain significant activity at tyrosine hydroxylation. H331E TyrH is unable to hydroxylate tyrosine, but is able to catalyze tetrahydropterin oxidation in the absence of tyrosine. Finally, both E376Q and E376H TyrH retain low activity for tyrosine hydroxylation. This very limited series of results suggests that the different ligands in the 2-His-1-carboxylate triad differ in their plasticity. As a test of this hypothesis for the aromatic amino acid hydroxylases in general, the effects of mutating the iron ligands in PheH to histidine, glutamate or glutamine have now been determined.

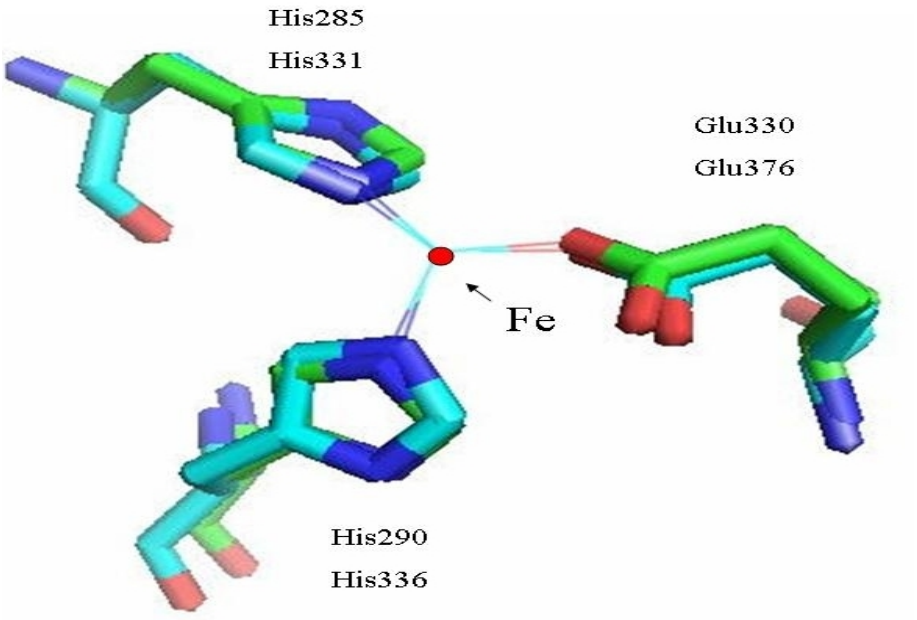

Figure 2.1. Iron ligands in TyrH (green) and PheH (cyan). The structures are from PDB files 1TOH and 2PHM.

Materials and Experimental Procedures

Materials

Leupeptin and pepstatin A were from Peptides Institute, Inc. (Osaka, Japan). Glycerol was from EM Science. Hepes was purchased from USB (Cleveland, Ohio). Tetrahydrofuran, 2, 3-naphthalene dicarboxaldehyde and dihydropteridine reductase (DHPR) were from Sigma. Restriction and DNA modification enzymes were purchased from New England Biolabs (Ipswich, MA) and Promega (Madison, WI). Tween-80 and 6-methyltetrahydropterin ($6MePH_4$) were from Calbiochem (San Diego, California). Phenyl-Sepharose CL-4B was purchased from Amersham Biosciences (Sweden). Catalase was from Roche Pharmaceuticals (Nutley, NJ).

Mutagenesis

The wild-type rat phenylalanine hydroxylase cDNA-containing plasmid pERPH5 was described previously (*99*). This plasmid was used as a template to construct plasmids for expression of PheH mutants. Site-directed mutagenesis was carried out with the Stratagene QuikChange Kit using pfu DNA polymerase. The mutagenic oligonucleotides were from Integrated DNA Technologies, Inc. The sequences of the oligonucleotides and the corresponding new restriction cleavage sites created are given in Table 2.1. QIAfilter plasmid midi prep kits and QIAprep Spin miniprep kits were used for purifying plasmids, which were used to transfect OmniMax competent cells from Invitrogen (Carlsbad, California). Mutant plasmids were sent to the Gene Technology Laboratory of Texas A&M University for DNA sequencing to confirm the mutations.

Table 2.1. Oligonucleotides used to perform site-directed mutagenesis [a]

mutation	Oligonucleotides sequence	New digest site
H285E	5’- gaa cct gac ATA tgg GAG ctc ttg gg – 3’	NdeI
H285Q	5’-cct gac ata tgc CAG gaa ctc ttg gga cat– 3’	NdeI
H290E	5’-gc cat gaa ctc ttg gga GAG GTA cct ttg ttt tca g– 3’	Acc651
H290Q	5’-gaa cct GAT atc tgg cat gaa ctc ttc gga CAG gtg cct– 3’	EcoRV
E330H	5’-c tgg ttt act gtg CAC ttt ggg ctt tgc– 3’	ApalI
E330Q	5’-tgg ttt act gtg CAG ttt GGT CTC tgc aag gaa gga– 3’	BsaI

[a] The changes from the wild-type sequence are capitalized.

Bacterial cell growth and protein purification

Mutant and wild-type PheH were expressed in C41(DE3) *E. coli* and purified on a Phenyl-Sepharose CL-4B column according to the protocol of Daubner et al. (*99*), except for the use of 50 mM Hepes and 15% glycerol instead of 50 mM Tris–HCl and 10% glycerol in the elution buffer. In addition, 50 μM EDTA was added to the elution buffer. Cells expressing wild-type PheH were grown at 37 °C, while cells expressing the mutant enzymes were grown at 22 °C after induction. The purified proteins were concentrated and stored in 50 mM Hepes, 15% glycerol, 1 μM leupeptin and 1 μM pepstatin A, pH 7.0, at −80 °C.

Assays

For wild-type PheH, the formation of tyrosine from phenylalanine was determined by monitoring the absorbance increase at 275 nm (*146*). For the mutant enzymes, a more sensitive HPLC assay (*147, 148*) was used. The standard conditions were 5 mM dithiothreitol, 50 mM Hepes, pH 7.0, at 25 °C, and varied amounts of ferrous ammonium sulfate, phenylalanine and $6MePH_4$ as indicated in figure and table legends. The total volume of each assay was 100 μl. The assays were quenched after 1 min and derivatized with 2, 3-naphthalene dicarboxaldehyde before being injected onto a 2.1 × 150 mm Waters Nova-Pak C18 column with fluorescence detection.

A coupled assay with dihydropteridine reductase and NADH was used to measure tetrahydropterin oxidation (*99*). The standard condition was 30 mM Hepes, pH 7.0, 250 μM NADH, 200 μM $6MePH_4$, 4 mM phenylalanine, 0.2 mM ferrous ammonium sulfate, 0.1 mg/ml catalase, and 0.1 U/ml dihydropteridine reductase at 25 °C. The total

volume was 1 ml. The amount of $6MePH_4$ oxidation was determined by monitoring the decrease of absorbance at 340 nm and correcting for autoxidation of $6MePH_4$. In order to determine the ratio of phenylalanine hydroxylation to $6MePH_4$ oxidation, a 100 µl aliquot was removed from the cuvette after 1 min and quenched with 100 µl 10 mM NaCN, pH 9, 100 µl 10 mM 2, 3-naphthalene dicarboxaldehyde in methanol, and 0.34 ml 10 mM sodium borate buffer, pH 9, and then analyzed by HPLC to measure tyrosine. Steady-state kinetic data were fit to the Michaelis–Menten equation using the program KaleidaGraph (Synergy Software, PA).

Results

Expression and purification of PheH mutant proteins

The three iron ligands of PheH, His285, His290 and Glu330, were each replaced with glutamate, histidine or glutamine using site-directed mutagenesis. All the mutant enzymes were expressed at significantly higher levels in C41(DE3) *E. coli* than in BL21(DE3). A significant amount of protein was found in insoluble inclusion bodies for all of the mutant proteins; this could be minimized by growth at 22 °C. The yield of the mutant enzymes was about 1 mg of purified protein per liter of bacterial culture, significantly less than the typical 20 mg/l of the wild-type enzyme.

Kinetic characterization of PheH mutant proteins

The activities of all of the mutant proteins were significantly less than that of the wild-type enzyme. Still, by using a sensitive HPLC-based assay it was possible to determine the kinetic parameters of most of the mutant proteins. While PheH requires Fe(II) for activity, the affinity of the wild-type enzyme for iron is high enough that the

enzyme is fully active even in the absence of added iron. However, the activities of all the mutant proteins are clearly iron-dependent (Figure 2.2). Mutation of Glu330 has the greatest effect on the value of K_{Fe}, the concentration of ferrous ion required for half-maximal activity, while the magnitude of the effects of mutating the two histidines differ with the individual mutation (Table 2.2). Even in the presence of saturating concentrations of Fe(II), the apparent V_{max} values for the H285E and E330Q enzymes decrease by 105-fold from the wild-type value. Because of these very low activities, further kinetic characterization of these two enzymes was not attempted. The K_m values for phenylalanine and $6MePH_4$ for the remaining mutant enzymes are given in Table 2.2. Mutation of any of the iron ligands increases the K_{6MePH4} value about one order of magnitude. The K_{phe} values of mutants similarly increase 3- to16-fold. The K_{phe} value of H285Q PheH is the largest at about 15-fold the wild-type value. H290E and E330H PheH display more modest increases.

Hydroxylation stoichiometry of PheH mutant proteins

The activity of PheH can be determined by following the formation of tyrosine or of dihydropterin. For the wild-type enzyme these yield the same result, since phenylalanine hydroxylation is tightly coupled to tetrahydropterin oxidation. This need not be the case for mutant proteins, where unproductive breakdown of an iron–oxygen intermediate to release hydrogen peroxide can occur without hydroxylation of the amino acid. The relative stoichiometries of tyrosine formation and $6MePH_4$ oxidation for each of the enzymes were determined using a coupled assay with NADH-dependent

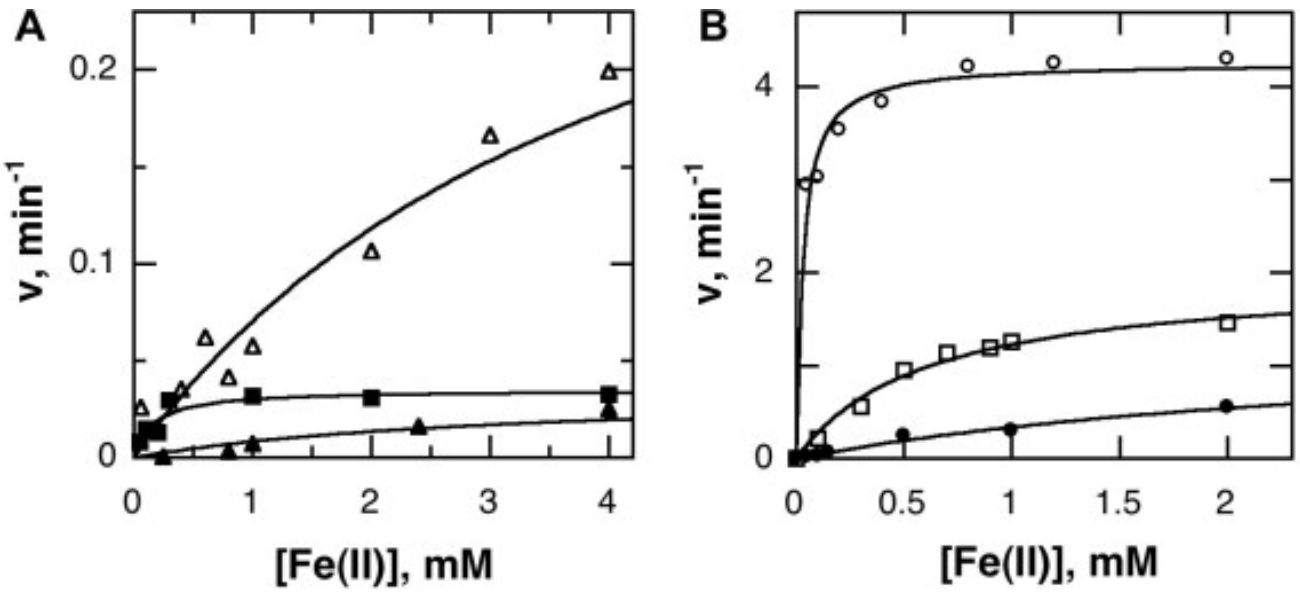

Figure 2.2. Iron dependence of tyrosine formation by PheH mutant enzymes. (A) E330H (open triangles), E330Q (filled triangles), and H285E (filled squares); (B) H290Q (open circles), H285Q (open squares), and H290E (filled circles).

Table 2.2. Steady-state kinetic parameters for phenylalanine hydroxylation by PheH mutant enzymes[*]

kinetic parameter	wt PheH[a]	H285E[b]	H285Q[c]	H290E[d]	H290Q[b]	E330H[b]	E330Q[b]
V_{max} (min^{-1})	399±14	0.035±0.003	2.0±0.15	1.3±0.4	4.3±0.1	0.35±0.07	0.035±0.009
K_{Fe} (mM)	NA	0.16±0.06	0.60±0.11	3.00±1.4	0.03±0.01	3.9±1.5	3.2±1.9
K_{6MePH4} (mM)	0.05±0.01	ND[e]	0.82±0.40	0.23±0.04	0.38±0.11	0.25±0.074	ND
K_{phe} (mM)	0.43±0.04	ND	6.9±3.1	3.4±2.1	1.2±0.4	1.6±0.4	ND

[*] Commonly used conditions: 5 mM dithiothreitol, 50 mM Hepes, pH 7, at 25°C.
[a] 0.2 mM ferrous ammonium sulfate, 2 mM phenylalanine, 0.2 mM $6MePH_4$.
[b] 4 mM ferrous ammonium sulfate, 5 mM L-phenylalanine, 2 mM $6MePH_4$.
[c] 2 mM ferrous ammonium sulfate, 12 mM L-phenylalanine, 2 mM $6MePH_4$.
[d] 6 mM ferrous ammonium sulfate, 8 mM L-phenylalanine, 2 mM $6MePH_4$.
[e] ND, not determined.

dihydropteridine reductase to measure $6MePH_4$ oxidation and an HPLC assay to determine the amount of tyrosine formed in the same reaction mixture. All of the enzymes oxidized an excess of $6MePH_4$ relative to the amount of tyrosine formed (Table 2.3). The His285 mutant enzymes exhibited the greatest uncoupling of $6MePH_4$ oxidation and phenylalanine hydroxylation, while the two partial reactions were most tightly coupled with the His290 mutant enzymes. Knowledge of these stoichiometries made it possible to calculate the V_{max} value for $6MePH_4$ oxidation by each of the mutant enzymes by dividing the V_{max} value for tyrosine formation by the stoichiometry (Table 2.3). Based on the ability to catalyze $6MePH_4$ oxidation, the H285Q enzyme is only 5-fold less active than the wild-type enzyme, while the H285E enzyme is another 100-fold less active. In contrast, the $6MePH_4$ oxidation activities of the other four mutant enzymes are comparable at two orders of magnitude less than the wild-type value.

Discussion

The conservative mutations of the iron ligands in PheH described here affect virtually all aspects of catalysis. Mutagenesis of the metal ligands appears to have effects on protein stability in addition to the effects on catalysis. All of the mutant proteins described here readily form inclusion bodies when expressed at 37 °C, in contrast to the wild-type enzyme, and yield lower amounts of active protein even when grown at lower temperatures. Moreover, attempts to obtain enzymes containing multiple mutations were not successful (results not shown). The lower yields of the mutant proteins are probably not due to the loss of a stabilizing effect of bound iron, since wild-type versions of the aromatic amino acid hydroxylases can readily be isolated in large amounts even when

Table 2.3. Coupling of phenylalanine hydroxylation to $6MePH_4$ oxidation for the wild-type and mutant PheH enzymes*

Enzyme	Phenylalanine hydroxylation /$6MePH_4$ oxidation [a]	$6MePH_4$ oxidation V_{max} (min^{-1}) [b]
Wild-type PheH	0.99 ± 0.05	403 ± 24
H285E	0.062 ± 0.009	0.68 ± 0.11
H285Q	0.031 ± 0.008	67 ± 16
H290E	0.15 ± 0.03	8.7 ± 2.6
H290Q	0.42 ± 0.06	10 ± 1.4
E330H	0.12 ± 0.03	1.8 ± 0.48
E330Q	0.079 ± 0.017	0.44 ± 0.15

* 30 mM Hepes (pH 7.0), 250 µM NADH, 200 µM $6MePH_4$, 4 mM L-phenylalanine, 0.2 mM ferrous ammonium sulfate, 0.1 mg/ml catalase, 0.1 unit/ml dihydropteridine reductase.

[a] Determined from the amount of $6MePH_4$ oxidation in 1 min as measured using an NADH-linked assay and the amount of tyrosine produced in the same sample in 1 min as measured by HPLC.

[b] Calculated from the value for phenylalanine hydroxylation / $6MePH_4$ oxidation and the V_{max} for phenylalanine hydroxylation.

containing substoichiometric iron or in the apo form (*69, 125, 149, 150*). Instead it suggests that interactions of the side chains of the metal ligands with other residues in the protein are important for structural integrity. A corollary of this is that other residues in the protein play a significant role in properly positioning the metal ligands for metal binding and reactivity.

Still, the results do allow some general distinctions to be drawn about the plasticity of the individual residues, especially when combined with the results of similar mutations in TyrH (*145*). The results also show that there are significant differences in the plasticity of these residues in the two enzymes. In combination, the two mutations of Glu330 in PheH have the greatest effects on the V_{max} value for $6MePH_4$ oxidation and tyrosine hydroxylation and intermediate effects on the coupling of these two partial reactions. These two mutations also have the greatest effects on iron affinity as measured by the dependence of activity on the iron concentration. A qualitatively similar result was obtained with TyrH, in that the Glu376 mutant enzymes were on average the least active. Both structural (*11*) and spectroscopic (*151*) studies of the iron site in PheH show that Glu330 is a monodentate ligand to the metal in the resting enzyme, but binds in bidentate fashion once both amino acid and tetrahydropterin are bound. However, the structure of TyrH with an amino acid bound has not been determined, so there is no direct evidence to date that the glutamate in that enzyme must be able to bind the iron with both carboxylate oxygens. The present results with PheH are consistent with the need for a negative charge at this position for iron binding and for the ability to act as a bidentate ligand for efficient formation of the Fe(IV)O intermediate and its reaction with

the amino acid substrate in that enzyme. The similarities in the effects of mutating this residue in TyrH and PheH support a similar requirement for bidentate binding in TyrH.

Mutations of His290 yield the highest V_{max} values for tyrosine formation, with mutation to glutamate resulting in greater uncoupling of the two reactions. A similar result was found for TyrH, in that the H336Q enzyme was the most active mutant protein of those examined, although the activity in that case was much higher at one-third the activity of the wild-type enzyme. In general, mutation of His290 in PheH to glutamate has a much more deleterious effect than mutation to glutamine. The K_{Fe} value for the H290E enzyme is two orders of magnitude greater than that of H290Q PheH. This likely reflects the need for conservation of charge for iron binding. The greater effect of the H290E mutation on the K_m value for phenylalanine also likely reflects the detrimental introduction of a negative charge into the hydrophobic active site. In contrast, the coupling of $6MePH_4$ oxidation and phenylalanine hydroxylation is disrupted the least in these two mutant proteins, although substitution with glutamate again is more detrimental. This is consistent with proper positioning of the amino acid in the active site once it binds, despite the lower affinity.

The two mutations of His285 also have disparate effects. His285 plays two roles in the active site of PheH. In addition to being a metal ligand, the imidazole ring of His285 stacks on the side chain of the amino acid substrate. When the homologous residue in TyrH, His331, is mutated to glutamate, binding of the amino acid substrate is eliminated and the enzyme becomes a tetrahydropterin oxidase (*145*). In that case it was not possible to characterize the effect of a mutation to glutamine. With PheH, the activity of

the H285E enzyme at tyrosine formation is too low to measure a K_{phe} value, but the tetrahydropterin oxidation activity does require the amino acid substrate. Thus, the dramatic loss of the need for binding of an amino acid substrate to activate the iron for reaction with oxygen is not seen when this residue is mutated in PheH. H285Q PheH enzyme has the highest K_{phe} value of the four mutant proteins with enough activity to measure this value, consistent with disrupted phenylalanine binding. Both of these mutant proteins exhibit very low coupling of $6MePH_4$ oxidation to tyrosine formation, again consistent with altered positioning of the amino acid substrate in the active site. The H285Q enzyme is quite active as a phenylalanine-dependent tetrahydropterin oxidase, while the H285E enzyme has activity comparable to that of the two His290 mutant proteins. Overall, mutation of either histidine residue is less disruptive of tetrahydropterin oxidation than is mutation of the glutamate, consistent with the critical importance of the change to bidentate binding of this residue for subsequent reactions.

The plasticity in the metal ligands in PheH is much less than is the case for TyrH (*145*). In both enzymes, mutagenesis of the glutamate residue is generally more disruptive of catalysis than is mutation of either histidine. Replacement of either histidine with glutamate is more disruptive than replacement with glutamine, consistent with the more conservative nature of the latter change. Of the two histidines, His290 of PheH is less sensitive to mutagenesis than is His285; a similar situation was found for the homologous residue in TyrH. However, mutating His285 in PheH does not have the same effect on the need for an amino acid substrate that mutation of the analogous mutation has in TyrH, establishing this effect as specific to TyrH instead of a reflection

of the general plasticity of the iron ligands in this enzyme family. The iron ligands of TyrH and PheH are virtually superimposable on one another (Figure 2.1) and the two enzyme share overlapping substrate specificities (*62, 99*). Indeed, mutating Asp425 in TyrH to valine converts it to an enzyme which is a better catalyst for converting phenylalanine to tyrosine than is wild-type PheH (*62*). Asp425 does not interact directly with either substrate or with the iron in TyrH, so that the ability to convert the enzyme to PheH establishes that there is no difference in the reactivities of the iron site in the two enzymes. PheH has a much more restricted substrate range than does TyrH (*74, 99*) and binds iron more tightly. These properties may reflect an active site that is optimized for iron binding and amino acid hydroxylation to a greater extent in PheH than in TyrH and that is consequently less tolerant of any disruption.

The α-ketoglutarate-dependent family of nonheme monooxygenases also contains a 2-His-1-carboxylate metal site, although the acidic residue is aspartate. The effects of mutating the metal ligands in a number of these enzymes have been determined, as summarized in Grzyska et al. (*152*). In many cases residual activities of <1% were not measurable, limiting the conclusions one can draw. However, even with this caveat there are discernable differences in the sensitivities to substitution of the three metal ligands in this enzyme family. Using the numbering of TauD, mutation of His99 to other residues generally yields enzyme with no detectable activity. In TauD the H99E and H99Q enzymes have V_{max} values of about 0.5% the wild-type enzyme. His99 is coplanar with the α-ketoglutarate substrate in the active site, so that mutation of this residue would also be expected to disrupt substrate binding analogously to the effects of mutating His285 in

PheH. In contrast, mutation of His255 in TauD and related enzymes yields enzyme with significant activity in a number of cases. For example, H255Q and H255E TauD have V_{max} values that are 89 and 36% the wild-type values. Finally, mutation of the aspartate residue to anything but glutamate generally yields enzyme with no reported activity. Thus, the general pattern for the α-ketoglutarate-dependent family of hydroxylases is similar to that with the pterin-dependent enzymes. The acidic residue in the 2-His-1-carboxylate facial triad is very sensitive to mutagenesis. Of the two histidine residues, the residue interacting directly with a substrate, either α-ketoglutarate or the aromatic amino acid, is also not tolerant to replacement with other amino acids, while the other, His285 here and His255 in TauD, is quite plastic, tolerating replacement with glutamine or glutamate.

CHAPTER III

REGULATION OF PHENYLALANINE HYDROXYLASE: CONFORMATIONAL CHANGES DETECTED BY H/D EXCHANGE AND MASS SPECTROMETRY

Phenylalanine hydroxylase (PheH) is a mononuclear non-heme iron containing monooxygenase (*129*). This enzyme is a liver enzyme catalyzing the hydroxylation of phenylalanine to form tyrosine using molecular oxygen and tetrahydrobiopterin (BH_4), the rate limiting step in the catabolic degradation of phenylalanine (*60*), (*134*). A deficiency or defect in PheH causes the genetic disease phenylketonuria (PKU), a common metabolic disorder resulting in mental retardation (*153*). PheH belongs to the aromatic amino acid hydroxylase family that has two other members, tyrosine hydroxylase (TyrH) and tryptophan hydroxylase (TrpH). TyrH and TrpH hydroxylate tyrosine and tryptophan forming the neurotransmitters L-DOPA and serotonin, respectively (*81*). The three enzymes have similar chemical mechanisms, forming Fe(IV)O intermediate to hydroxylate an amino acid. Each enzyme is a homotetramer with subunits consisting of three domains, a regulatory domain, a catalytic domain and a tetramerization domain, proceeding from the N-terminus to the C-terminus. The iron atom lies at the center of the hydrophobic active site in the catalytic domain. The three enzymes have high identity in the catalytic domains and low identity in the regulatory domains (*99, 117*).

PheH is strictly regulated to control the metabolism of phenylalanine. Activation by phenylalanine, inhibition by BH_4 and phosphorylation of Ser16 are the three main

mechanisms of regulation (*81*). Preincubation of PheH with phenylalanine can increase the activity by more than 100-fold (*19*). Several studies have suggested that the activation of PheH by phenylalanine is accompanied by conformational changes in the protein. For example, PheH can absorb to Phenyl-Sepharose only when phenylalanine is present. Phenylalanine treatment is proposed to induce a conformational change that exposes hydrophobic residues that interact with the resin (*22*). Treatment of PheH with phenylalanine also results in increased fluorescence emission, suggesting a conformational change that exposes buried tryptophan(s) (*154*). Pretreatment with phenylalanine and BH_4 have opposite effects on the susceptibility of PheH to limited proteolysis by chymotrypsin (*155*). Surface plasmon resonance has also provided evidence for a slow reversible conformational transition upon binding phenylalanine (*156*). There is a lag in the initial rate of tyrosine formation if assays are started by adding enzyme; preincubation of PheH with phenylalanine eliminates the lag while preincubation with BH_4 increases it (*19*). Based on the opposite effects of phenylalanine and pterin, Shiman proposed a model in which PheH is purified as an inactive form. Treatment with phenylalanine induces a conformational change and converts the enzyme into the active form while treatment with BH_4 traps the enzyme in a BH_4-PheH complex that is harder to activate (*39, 40, 149*).

The only available structures of PheH with an amino acid substrate are ternary complexes consisting of the catalytic domain of human PheH with Fe(II), BH_4, plus 3-(2-thienyl)-L-alanine or L-norleucine (*6*). The ternary complex has a slightly more compact structure compared to the binary complex of hPheH-Fe(II)·BH_4. Two regions

display the largest differences when an amino acid is bound: the surface loop containing residues 131-155, in which Tyr138 is 9.6 Å closer to the iron atom, and the iron ligand residue Glu330, which binds iron in bidentate fashion in the ferrous complex. However, these structures provide no insight into the changes in the regulatory domain associated with phenylalanine or BH_4 binding. Indeed, the isolated catalytic domain does not require activation by phenylalanine (*150*). The only crystal structure containing the regulatory domain is a dimeric rat PheH lacking the C-terminal 24 residues of the tetramerization domain (*8*). This structure shows N-terminal residues 19-33 extending over the active site pocket. Based on this structure, Jennings et al. (*23*) proposed that the residues 19-33 (also called N-terminal autoregulatory sequence) obstruct the entry of the active site in the absence of phenylalanine and binding of phenylalanine activates the enzyme by displacing the sequence. NMR studies support this model, in that a number of sharp resonances attributed to the N-terminal autoregulatory sequence become weaker in the presence of phenylalanine (*157*).

Phosphorylation by PKA also activates PheH (*32*). The phosphorylation site is Ser16 (*24*). Phosphorylated PheH can be further activated by treatment with phenylalanine but lower concentrations are required for full activation (*158, 159*). Molecular dynamics simulations suggest that the conformational change induced by phosphorylation is localized to the regions around Ser16 (*160, 161*). This result is consistent with the finding that the structures of unphosphorylated and phosphorylated enzymes have no significant difference, since the first N-terminal 18 residues are not in the structures. Based on these data, Kobe et al. (*157*) proposed that phosphorylation of

PheH only causes a local change in the structure that alters the electrostatic interaction of the N-terminal autoregulatory sequence with the active site.

Hydrogen/deuterium exchange mass spectrometry (HXMS) has been proven to be a powerful tool to study the structure and dynamics of proteins in solution (*162, 163*). We have used HXMS to probe the structural changes accompanying activation by phenylalanine binding and phosphorylation and inhibition by BH_4 binding and reveal the local dynamic motions and connections between regulation and structure in PheH.

Materials and Experimental Procedures

Materials

ATP and phosphatase inhibitor cocktail 1 were purchased from Sigma-Aldrich Chemical Co. (Milwaukee, WI). Phenyl-Sepharose CL-4B was purchased from Amersham Biosciences (Sweden). Porcine stomach pepsin A was from Worthington Biochemical Co. (Lakewood, NJ). Deuterium oxide (D_2O, 99% D) was from Cambridge Isotope Laboratories (Andover, MA). Pepstatin A and leupeptin were from Peptides Institute, Inc (Osaka, Japan). The γ-^{32}P ATP (10 μCi/μl) was purchased from Perkin Elmer Life and Analytical Science (Boston, MA).

Protein purification and preparation

The purification of wild-type rat PheH and the catalytic domain (Δ117PheH) were described previously (*150, 164*). To prepare PheH containing ferrous iron, 45 ml concentrated wild-type PheH (about 2 mg/ml) in 50 mM Hepes, pH 7.0, 15% glycerol, 1 μM pepstatin A and 1 μM leupeptin was dialyzed overnight against 1 liter of the same buffer plus 50 mM EDTA and 50 mM nitrilotriacetic acid (NTA), pH 7.0, with one

buffer change. The dialysis buffer was then changed to 1 liter of the same buffer without EDTA and NTA with three changes over 12 h. After centrifuging the sample at 33,800×g for 20 min, the supernatant was stored at -80 °C. The iron content of PheH was determined as 90% apoenzyme by atomic absorption spectroscopy (*80*). To determine the amount of phenylalanine bound to PheH, an aliquot of enzyme was denatured by heating at 100 °C for 30 min, and injected onto a reverse-phase HPLC using the method as described previously (*165*). The ratio of phenylalanine to PheH was about 10%. The PheH activity was determined using a coupled assay with dihydropteridine reductase, measuring the decrease in absorbance at 340 nm upon NADH oxidation (*166*).

The PKA catalytic domain was purified from bovine heart as described by Flockhart and Corbin (*167*). Preliminary experiments used γ-^{32}P ATP to monitor the extent of phosphorylation as described before (*168*). The conditions for preparation of phosphorylated enzyme for mass spectrometry were 0.3 mM unlabeled ATP, 10 mM $MgCl_2$, 0.8 μM PKA, 12 μM PheH, and 50 mM Hepes, pH 7.0, at room temperature (about 22 °C) for 1 h. After the first 15 min, additional PKA and ATP were added for a final concentration of 1 μM PKA and 0.4 mM ATP. The total reaction volume of 65 ml contained about 40 mg PheH. The phosphorylated PheH was isolated by FPLC using a HiPrep 16/10 Q XL Column (GE Healthcare Life Science) in 50 mM Hepes, 5% glycerol, pH 7.0, with a gradient of 0-0.3 M KCl. The phosphorylated PheH solution ($\sim$ 60 ml) was then dialyzed against 1 liter of 50 mM Hepes, 15% glycerol, 50 μM EDTA, 60 μl phosphatase inhibitor cocktail 1, 1 μM pepstatin A and 1 μM leupeptin at 4 °C.

The phosphorylated PheH was then concentrated to about 200 μM using an Amicon Ultracel-30k (Millipore) ultra centrifugal filter and stored at -80 °C.

H/D exchange

The H/D exchange reactions were initiated by diluting 15 μl freshly thawed PheH (about 150 μg) into 300 μl of 50 mM Hepes, pD 7.0, in D_2O containing phenylalanine or BH_4 or no addition, at 25 °C. Before dilution, 2 μl of ferrous ammonium sulfate in 1 mM HCl was added to enzyme to achieve a subunit to iron ratio of 1:1 (mole/mole). To prevent ferrous iron oxidation, all the solutions were prepared anaerobically by applying cycles of vacuum and argon. During H/D exchange, the tube containing the enzyme in D_2O solution was sealed and filled with argon. The concentrations of phenylalanine and BH_4 were 5 mM and 400 μM, respectively. Twenty μl samples were taken out with an air-tight syringe at different time points and quenched with 20 μl ice-cold 100 mM sodium citrate buffer, pH 2.4. The mixture was immediately frozen in liquid nitrogen and stored at -80 °C.

For mass spectrometry, the 40 μl mixture was rapidly thawed, and 2 μl pepsin was added. The ratio of pepsin to PheH was about 1:1 by weight. After 5 min on ice, 20 μl of sample was injected onto a Vydac C18 HPLC column (2.1 mm × 150 mm). The HPLC buffers, column, injection loop and tubing were all immersed in an ice bath to minimize back-exchange. After desalting with 98% solvent A (0.1% formic acid in H_2O, pH 2.4) for 3 min, a 15 min linear gradient of 20-50% solvent B (0.1% formic acid in acetonitrile, pH 2.4) was used to separate the peptides. The flow rate was 200 μl / min. The outlet of the HPLC was connected to a Thermo Finnigan LCQ DECA XP ion-trap mass

spectrometer. All the peptides analyzed eluted after 6 to 12 min and with m/z values of 400 to 2000. The analysis for each condition was performed at least twice. Tandem mass spectrometry (MS/MS) under the same conditions using water instead of D_2O was used for peptide identification. The software used to process MS/MS data was TurboSEQUEST from Thermo Finnigan, version 3.1. Singly, doubly and triply charged peptides were analyzed. The mass spectrometry experiments were all conducted in the Protein Chemistry Laboratory at Texas A&M University.

To determine the back-exchange rate, 15 µl of 200 µM PheH plus 2 µl of ferrous ammonium sulfate in 1 mM HCl was diluted with 300 µl of 50 mM Hepes, pH 7.0 in H_2O followed by mixing with 315 µl of 100 mM sodium citrate buffer (pH 2.4). Pepsin was then added to give a ratio of pepsin to PheH of 1 by weight. After pepsin digestion on ice for 5 min, the mixture was immediately frozen with liquid nitrogen and lyophilized. The lyophilized powder was dissolved in 315 µl of 50 mM Hepes D_2O (pD 7.5) and heated for 30 min at 100 °C. The solution was then incubated at 25 °C for 6 hrs. For mass spectrometry, 20 µl of the solution was mixed with 20 µl of 100 mM sodium citrate buffer (pH 2.4). After 5 min on ice, 20 µl of the sample was injected onto the HPLC. The back-exchange of individual peptides was 30-35%.

Data processing

The MS data exported using Thermo Finnigan Xcalibur software were transferred into HX-Express, a Microsoft Excel-based software for generating a deuterium incorporation curve (*169*). The percent H/D exchange was calculated directly without correction for back-exchange. All of the data in figures are averages of at least two

separate runs. The kinetics of exchange were fit to equation 1 or equation 2 using KaleidaGraph (version 4.0), where N is the total percent of exchange over the observed time and A and B are the percent of amide hydrogens exchanging with rate constants k_1 and k_2, respectively.

$$Y = N - Ae^{-k1t} \qquad (1)$$

$$Y = N - Ae^{-k1t} - Be^{-k2t} \qquad (2)$$

Results

Phosphorylation of PheH

Preliminary experiments were conducted to establish the conditions for stoichiometric phosphorylation of PheH by PKA. Figure 3.1 shows the progress curve for the reactions under the conditions described in Experiment Procedures. After 30 min, the ratio of incorporated ^{32}P to PheH reached over 95%. The reaction was scaled up using unlabeled ATP together with 40 mg PheH under the same conditions. The phosphorylated PheH was purified using a Q-Sepharose column. To rule out the possibility that the phosphorylation reaction was not complete, a phosphorylation reaction was performed with the phosphorylated PheH protein after the Q-Sepharose column. No radioactivity incorporation was observed.

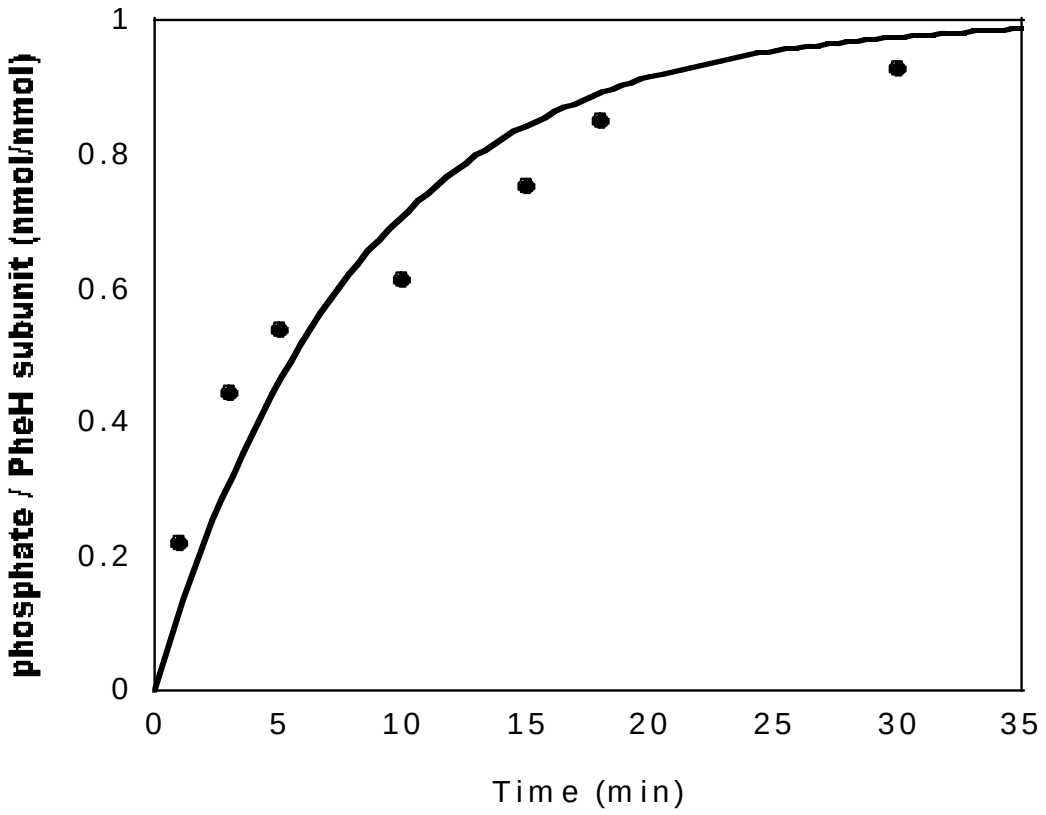

Figure 3.1. Progress curve for phosphorylation of PheH by PKA. The conditions are 0.3 mM [γ-^{32}P]-ATP, 10 mM $MgCl_2$, 0.8 μM PKA, 12 μM PheH, and 50 mM Hepes, pH 7.0, at room temperature for 1 h. After the first 15 min, additional PKA and ATP were added for a final concentration of 1 μM PKA and 0.4 mM ATP. The curve is from a single exponential fit of the data.

Peptide identification and sequence coverage

Before conducting the H/D exchange, the identities of peptides generated by pepsin digestion of wild-type PheH, the catalytic and tetramerization domains of PheH (Δ117PheH), and phosphorylated PheH were determined by tandem mass spectrometry (MS/MS). For wild-type PheH, a total of 30 peptides could be routinely identified, covering 80% of the protein sequence (Figure 3.2). For Δ117PheH, a total of 31 peptides of could be identified covering 91% of the protein sequence. A total of 28 peptides of phosphorylated PheH were identified covering 79% of the protein sequence. The back-exchange ratio in this study was determined as about 40%.

H/D exchange of wild-type PheH

To monitor the conformational change of wild-type PheH upon phenylalanine binding, 150 μg wild-type PheH was diluted with 20 volumes of 5 mM phenylalanine, 50 mM Hepes, pD 7.0, in D_2O to start the H/D exchange at 25 °C. Aliquots of 20 μl were taken at different time points from 30 s to 4 h and immediately quenched by mixing with 20 μl of ice-cold 100 mM sodium citrate buffer, pH 2.4. The 40 μl mixture was digested with pepsin (equal weight to PheH) for 5 min on ice, followed by injection onto an HPLC with a Vydac C18 HPLC column. The deuterium incorporation into wild-type PheH in the presence of phenylalanine was compared with that in the absence of phenylalanine. Most regions have similar exchange patterns under these two conditions (Figure 3.3). Eight peptides exhibit significantly different exchange patterns with an increased level of deuterium incorporation in the presence of phenylalanine (Figure 3.4).

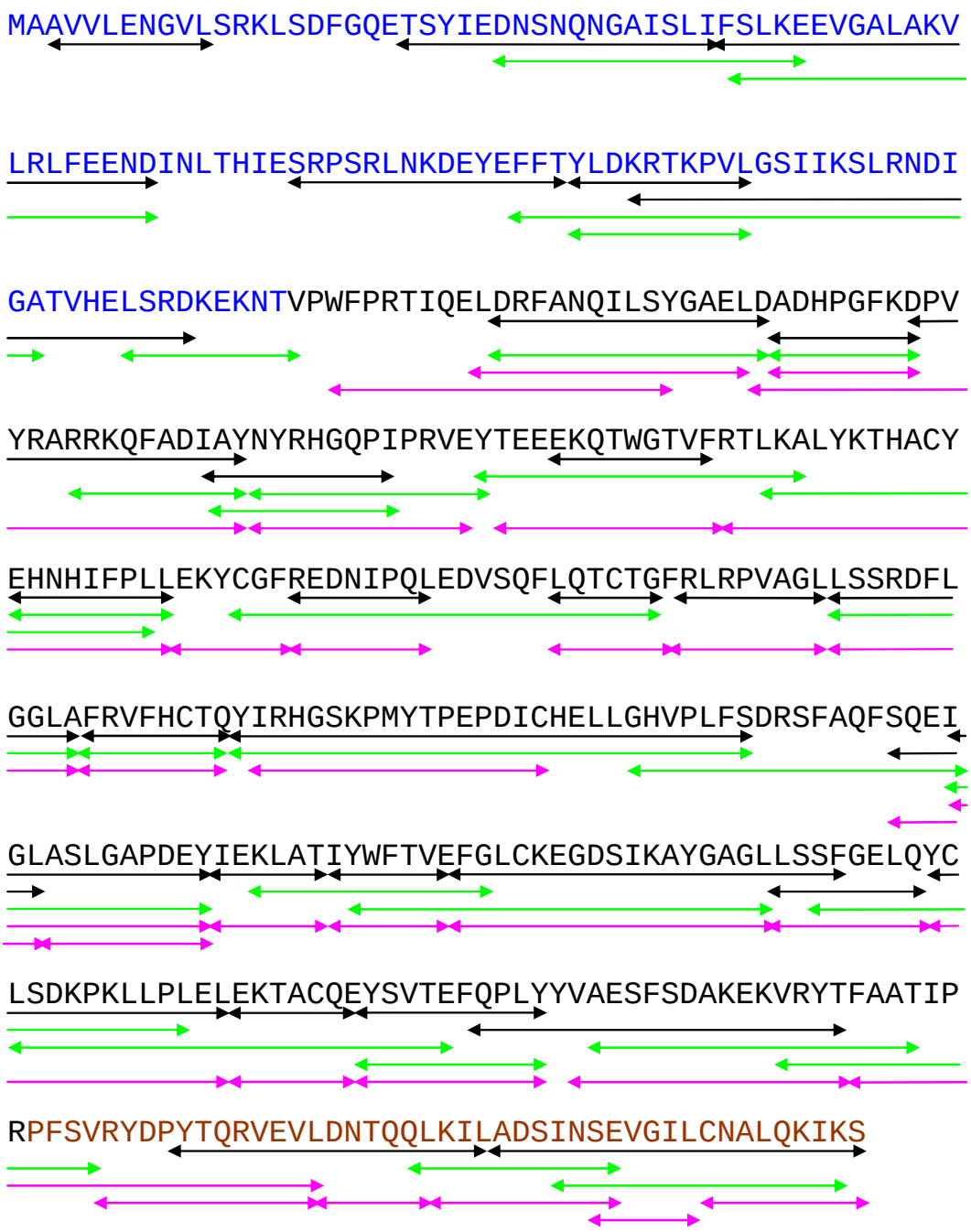

Figure 3.2. Sequence coverage of PheH. The peptides analyzed in this study are indicated by double-headed arrows. The black, green and magenta colors represent unphosphorylated PheH, phosphorylated PheH and Δ117PheH, respectively. The regulatory and tetramerization domains are in blue and brown, respectively. The catalytic domain is in black.

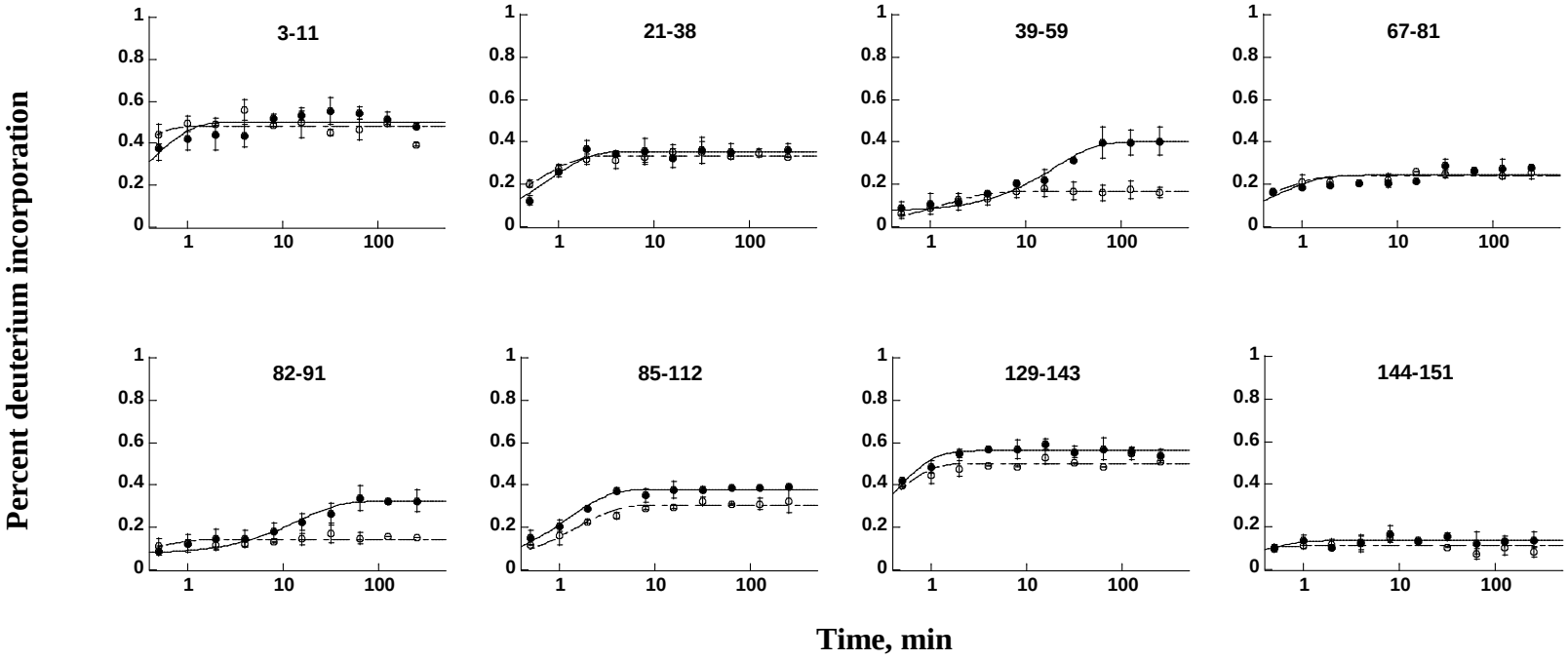

Figure 3.3. Deuterium incorporation into peptides of wild-type PheH in the absence (○, dashed line) and presence (●, solid line) of phenylalanine. Percent deuterium incorporation was calculated by dividing the observed deuterium incorporation by the number of exchangeable peptides bonds in a peptide. There is no adjustment for back-exchange. The curves were fit by equation 1, except the data for peptide 164-174 in the presence of phenylalanine were fit by equation 2.

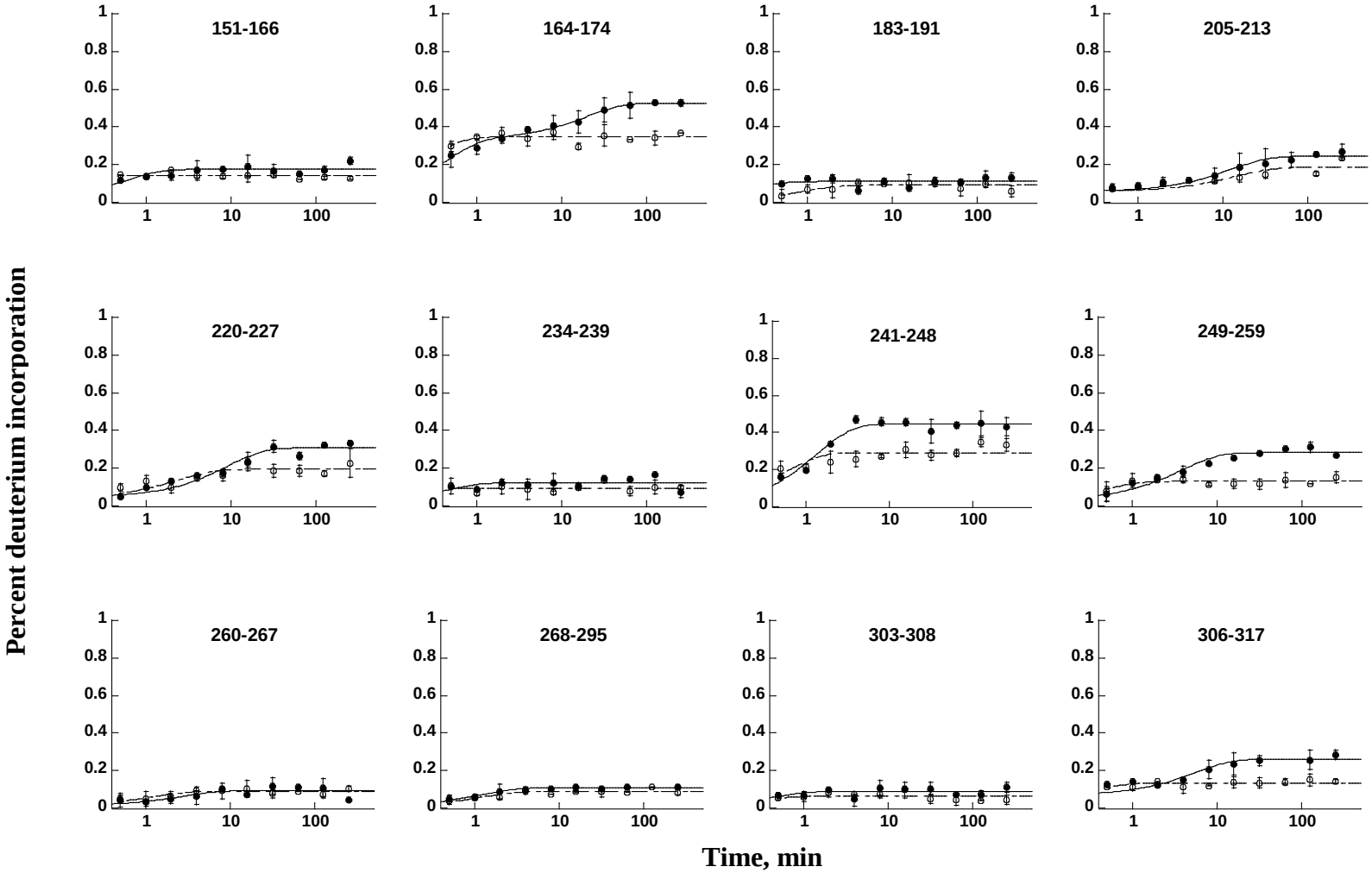

Figure 3.3 Continued.

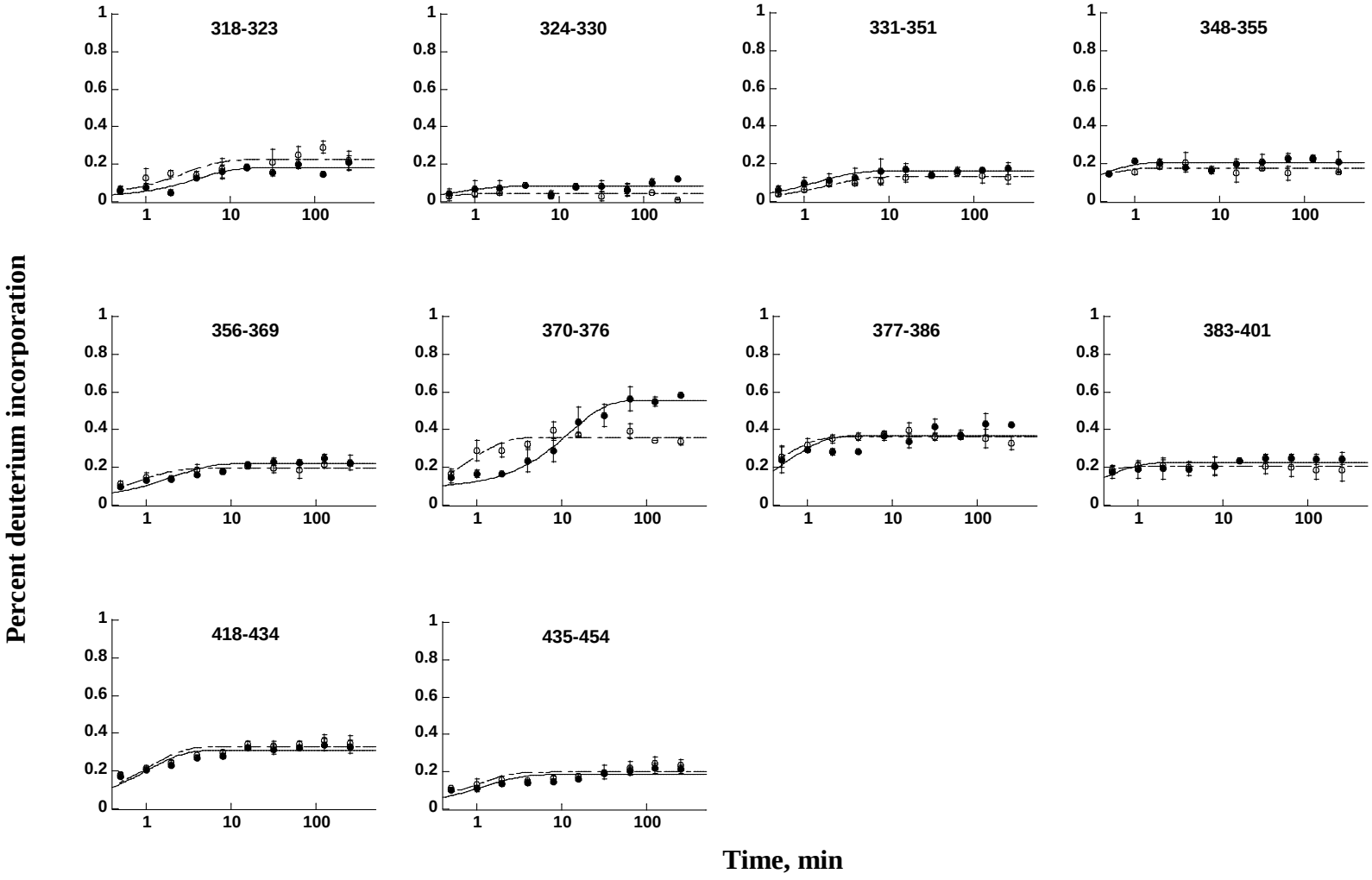

Figure 3.3 Continued.

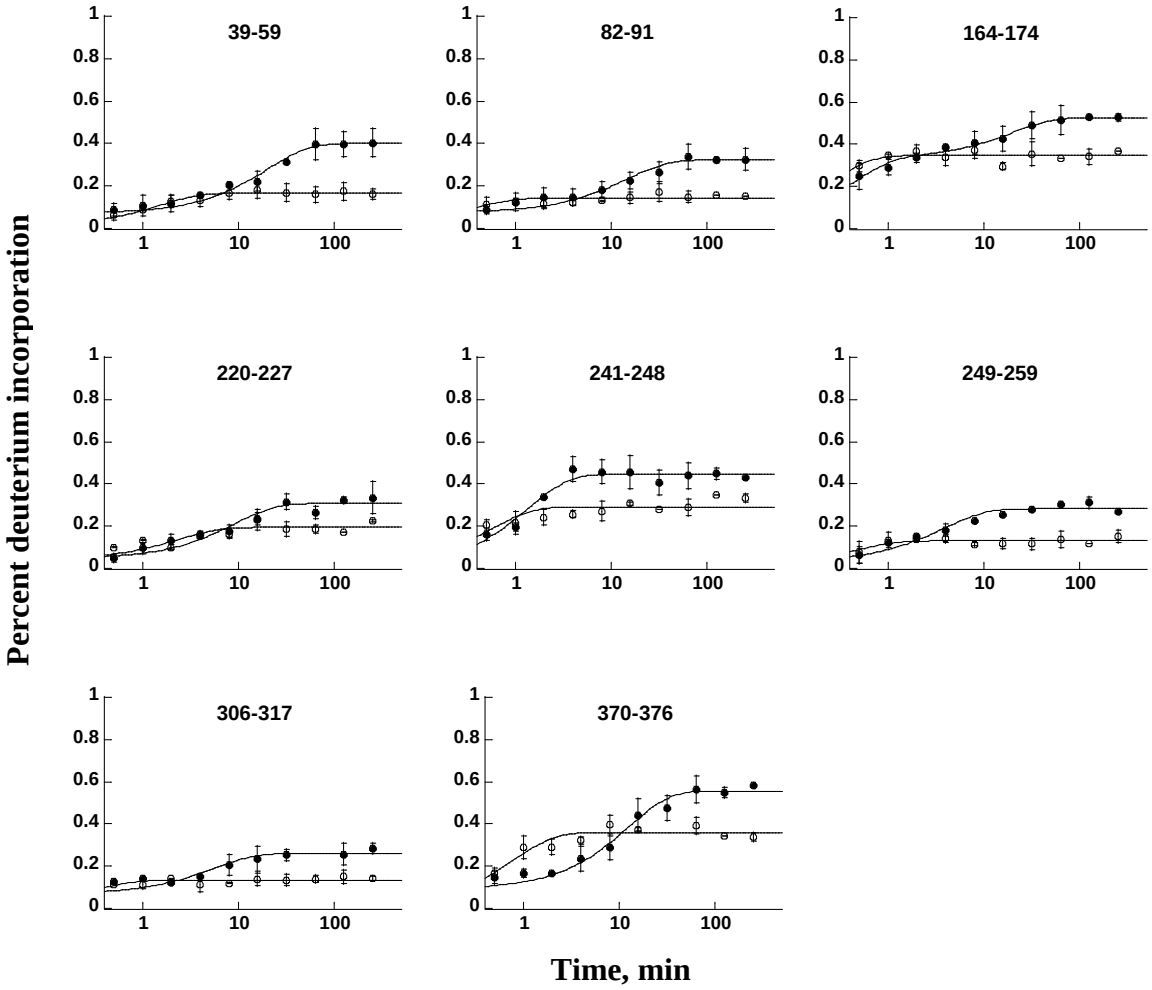

Figure 3.4. Peptides of wild-type PheH showing large differences in deuterium incorporation in the absence (○) and presence (●) of phenylalanine. Percent deuterium incorporation was calculated by dividing the observed deuterium incorporation by the number of exchangeable peptide bonds in a peptide. There is no adjustment for back-exchange. The curves were fit by equation 1, except the data for peptide 164-174 in the presence of phenylalanine were fit by equation 2.

There were no regions showing decreased deuterium incorporation after 2 h in the presence of phenylalanine. Figure 3.5 compares the deuterium incorporation of different peptides in the structure in the absence and presence of phenylalanine after 2 h. Figure 3.6 shows the locations in the structure of the peptides whose exchange was altered by phenylalanine. Two of the eight peptides are in the regulatory domain. Peptide 39-59 includes the first helix, part of the first sheet and a small loop connecting them. Peptide 82-91 includes part of the second helix and a small loop closer to the N-terminus. The increased deuterium uptake of these peptides suggests that the regulatory domain becomes more open in the presence of phenylalanine. The other six peptides lie in the catalytic domain. The residues in the peptides 249-259, 306-317 and 370-376 are in the interdomain regions between the regulatory and catalytic domains. The N-terminal autoregulatory sequence extends into the cleft between peptides 306-317 and 249-259, reaching over the loop 370-376. In addition, peptide 370-376 contacts the catalytic domain of another monomer. Peptide 241-248 is a small strand adjacent to helix 249-259. Peptide 164-174 is a loop close to residues 410-425 of the tetramerization domain. Peptide 220-227 is a short loop on the back of the active site connecting helices 205-216 and 227-237; of the eight peptides, this one showed the smallest increase in deuterium incorporation in the presence of phenylalanine. The increased deuterium incorporation in these regions establishes that phenylalanine binding results in conformational changes.

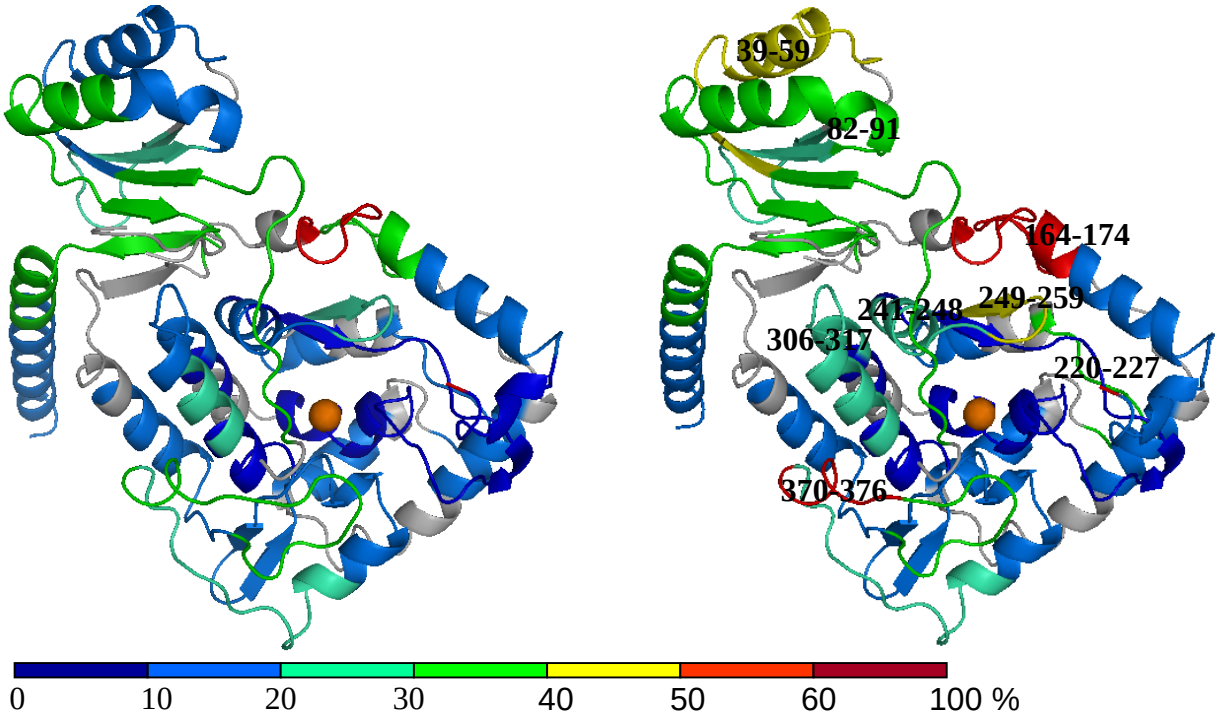

Figure 3.5. Comparison of deuterium incorporation of wild-type PheH in the absence (left) and presence of phenylalanine (right) after 2 h. Peptides are color-labeled according to the extent of deuterium uptake. The eight peptides showing dramatic difference are marked with numbers. The full length PheH structures were constructed with the pdb files of 2PHM and 2PAH. The active site is indicated by iron atom as an orange sphere. The peptides showing significantly increased deuterium incorporation are indicated in the right panel.

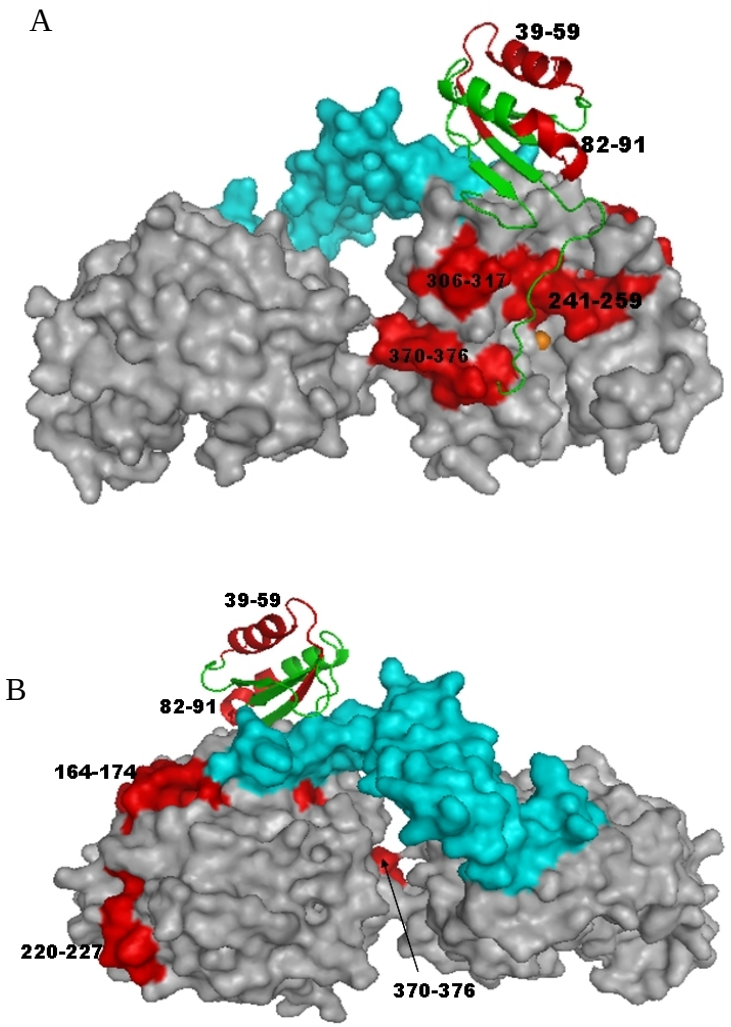

Figure 3.6. The peptides showing increased deuterium incorporation in the presence of phenylalanine. The structures in panel A and B, constructed with pdb files of 2PHM and 2PAH, represent the front and back views of PheH, respectively. The catalytic and tetramerization domains are shown in surface with grey and cyan colors, respectively. The regulatory domain is only shown in a monomer as a green cartoon. The peptides sensitive to phenylalanine are shown in red.

Similar HXMS experiments were conducted with wild-type PheH in the presence of 400 μM BH_4. 22 peptides were identified in the presence of BH_4, covering 57% of protein sequence. None of peptides showed a change as significant as was seen in the presence of phenylalanine, suggesting that BH_4 binding does not change the structure significantly from the resting form (Figure 3.7). Only three peptides of the eight showing dramatic differences in the presence of phenylalanine, 82-91, 249-259 and 306-317, were found in the presence of BH_4. Peptide 164-174 was not identified, but a similar peptide, 167-179, could be analyzed. The remaining peptides were not detected. Small differences were seen in the H/D exchange patterns of peptides 85-112, 306-317. 356-369 and 435-454.

H/D exchange of Δ117 PheH

To analyze the contribution of the regulatory domain to the effects of phenylalanine on the dynamics of the catalytic domain, similar H/D exchanges were performed with Δ117PheH in the presence and absence of 5 mM phenylalanine. Δ117PheH lacks the regulatory domain. Deuterium incorporation into the peptides of Δ117PheH was not significantly affected by phenylalanine (Figure 3.8), suggesting the treatment of Δ117PheH with phenylalanine does not result in the significant conformational changes seen in the wild-type enzyme. Peptides 192-213, 269-284, and 348-355 show small decreases in deuterium incorporation, and peptide 446-454 shows a small increase in deuterium incorporation. Peptide 167-178 displays slower exchange but reaches the same maximum exchange.

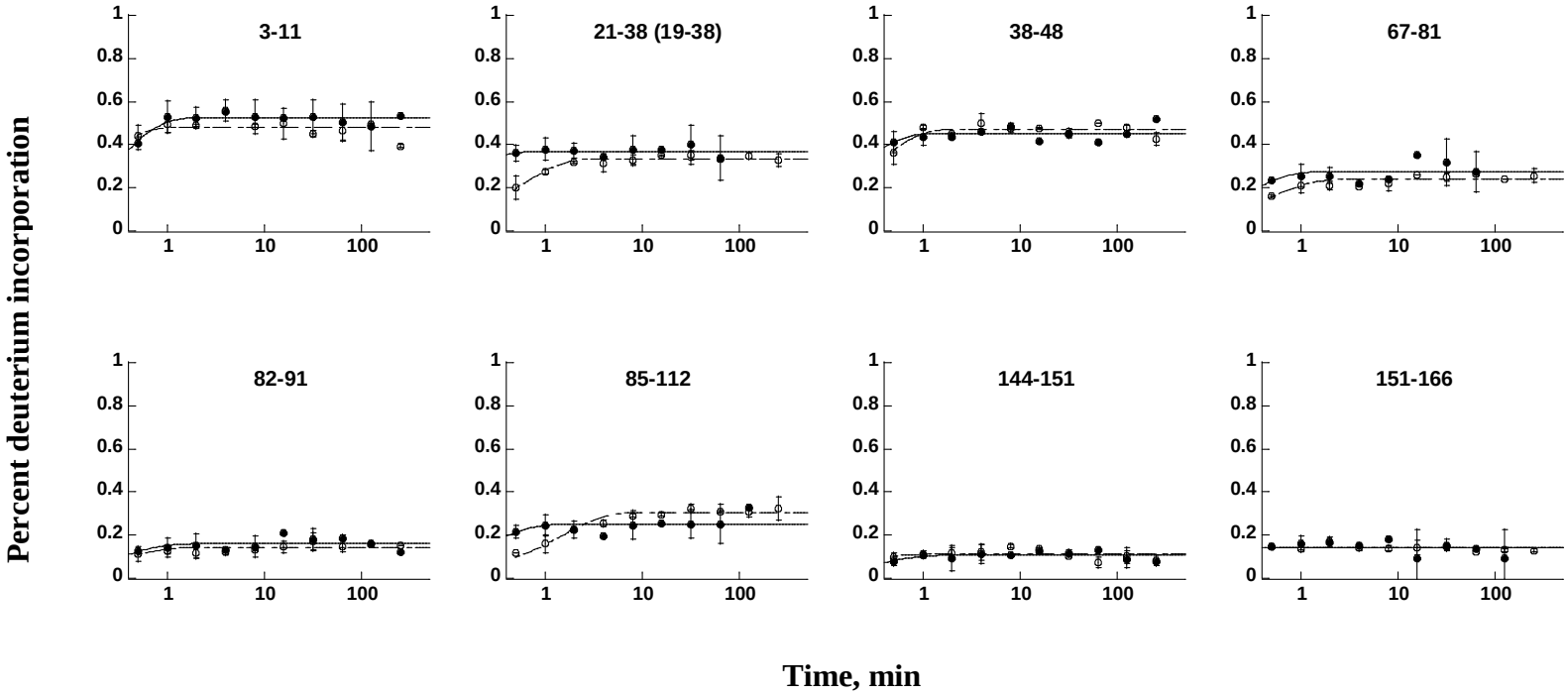

Figure 3.7. Deuterium incorporation into peptides of wild-type PheH in the absence (○, dashed line) and presence (●, solid line) of BH_4. Percent deuterium incorporation was calculated by dividing the observed deuterium incorporation by the number of exchangeable peptides bonds in a peptide. There is no adjustment for back-exchange. For peptides 21-38 and164-174, since no identical peptides identified in the presence of BH_4, two peptides 19-38 and 167-179 are compared to them.

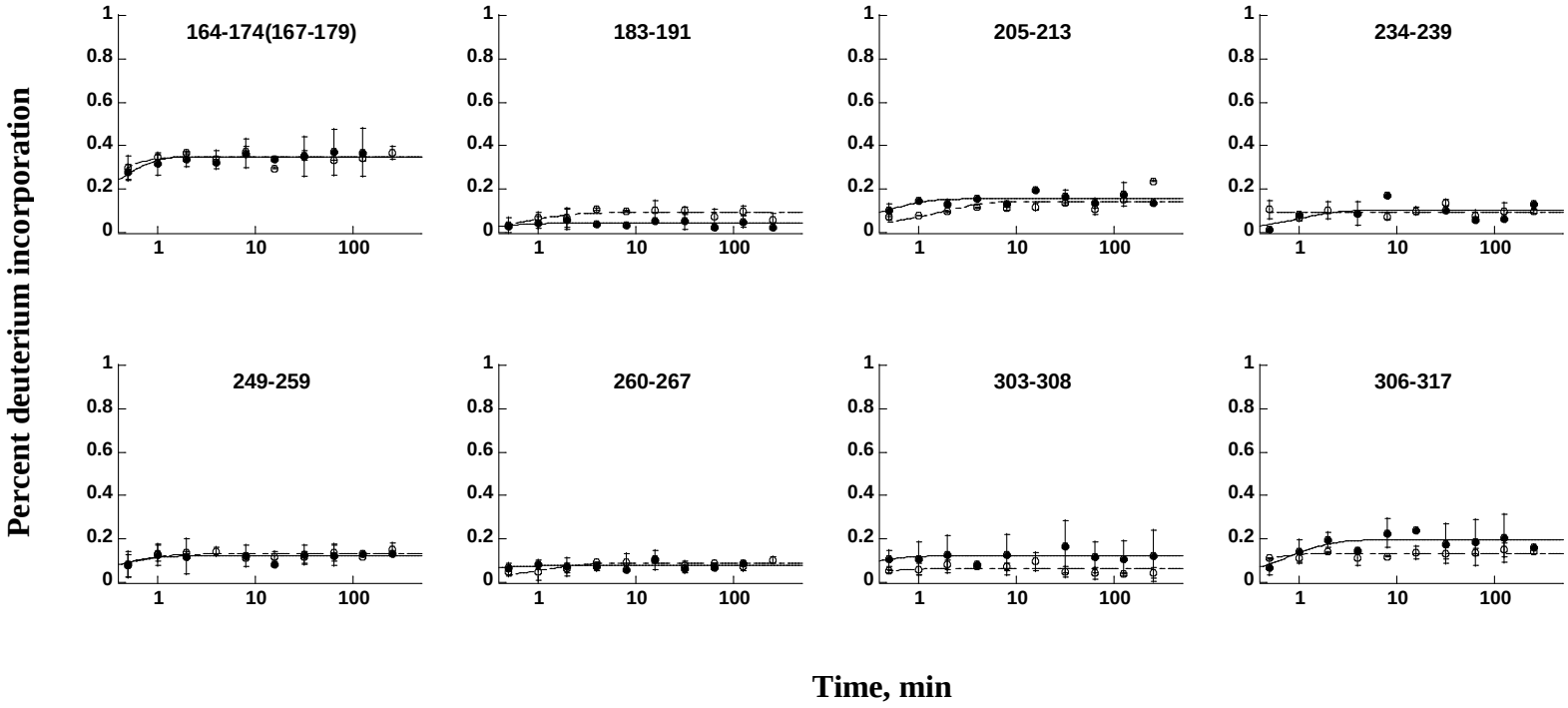

Figure 3.7 Continued.

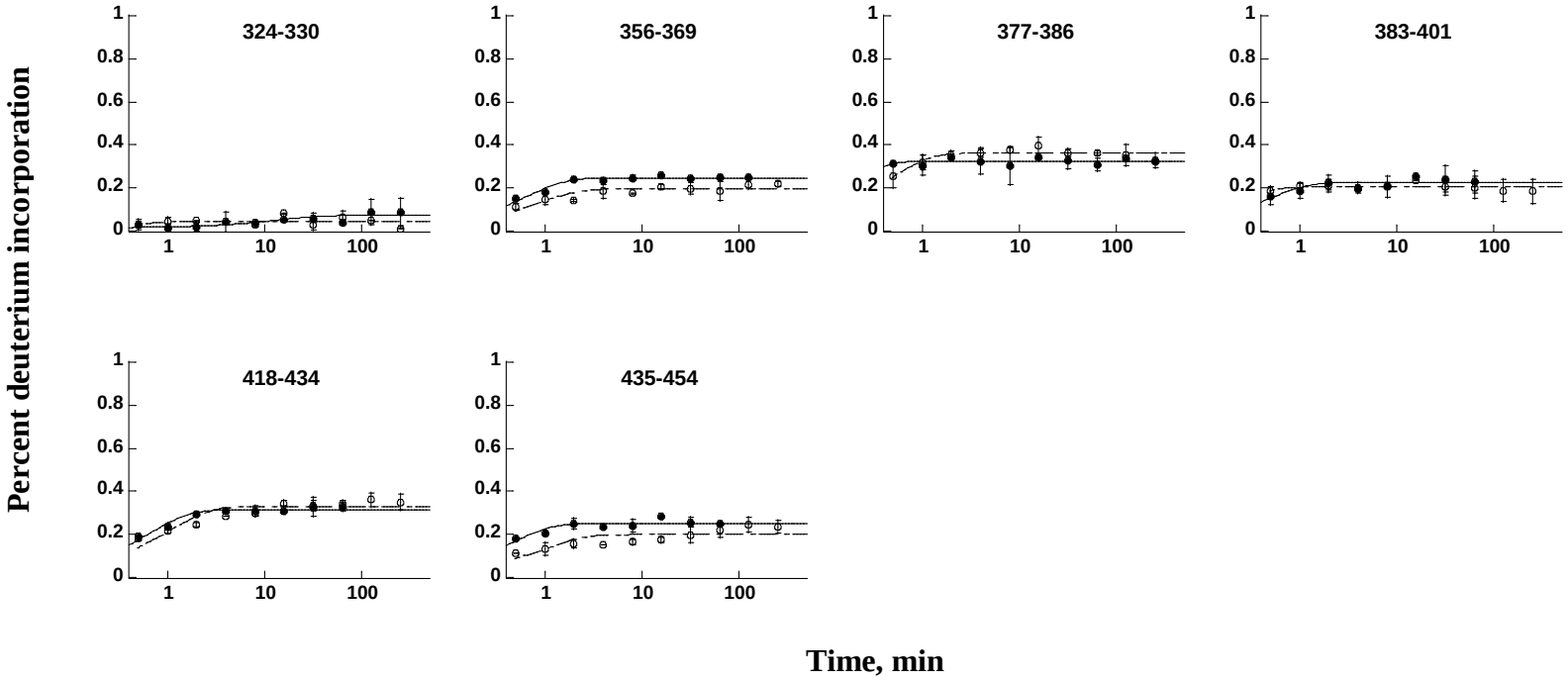

Figure 3.7 Continued.

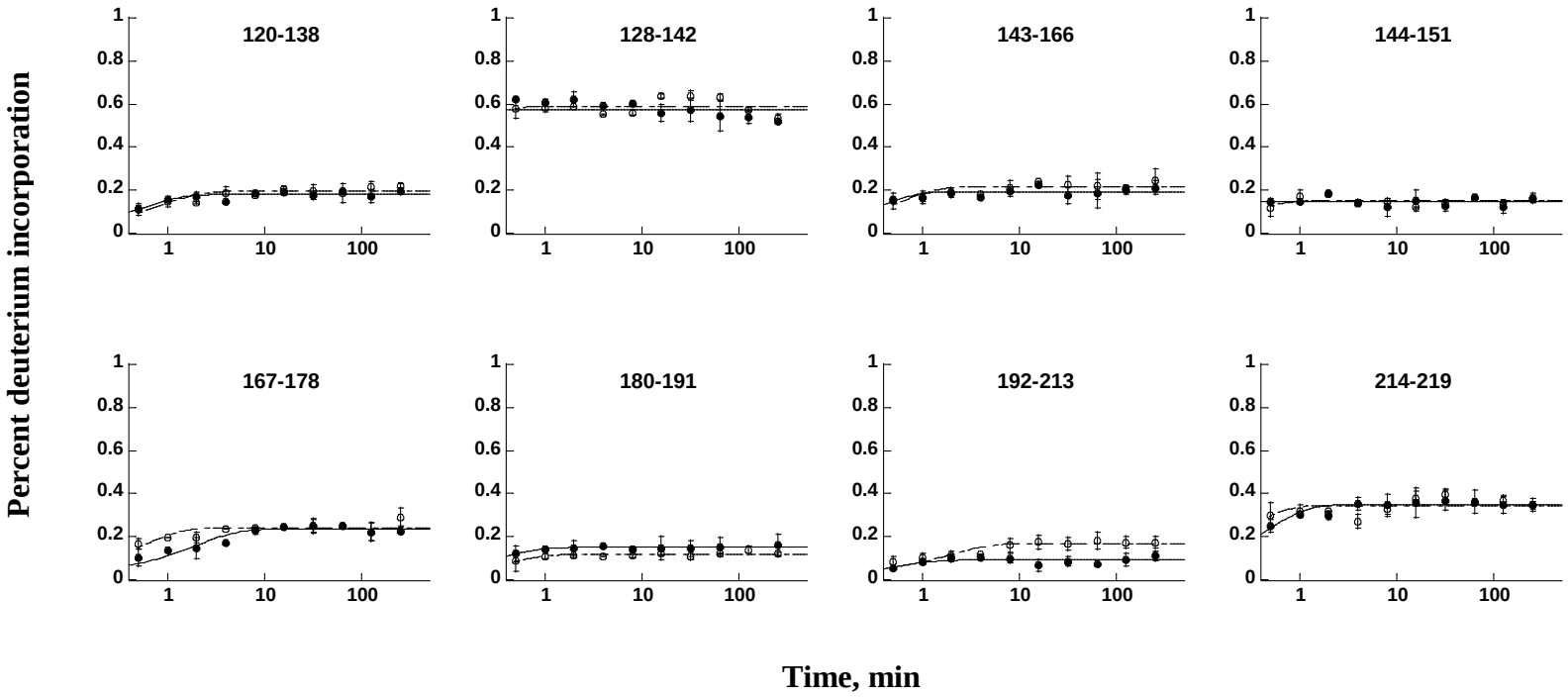

Figure 3.8. Deuterium incorporation into peptides of Δ117PheH in the absence (○, dashed line) and presence (●, solid line) of phenylalanine. Percent deuterium incorporation was calculated by dividing the observed deuterium incorporation by the number of exchangeable peptides bonds in a peptide. There is no adjustment for back-exchange.

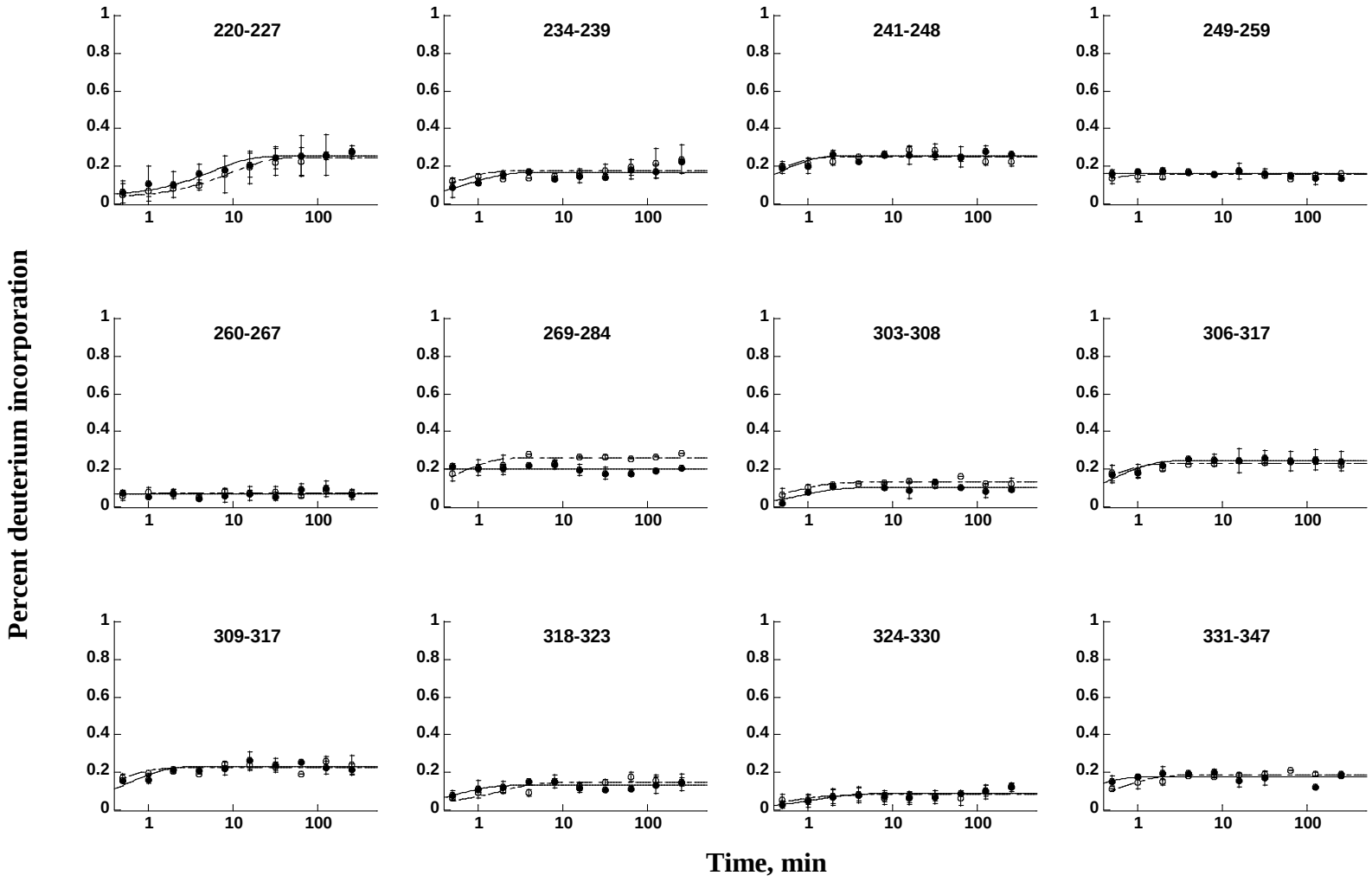

Figure 3.8 Continued.

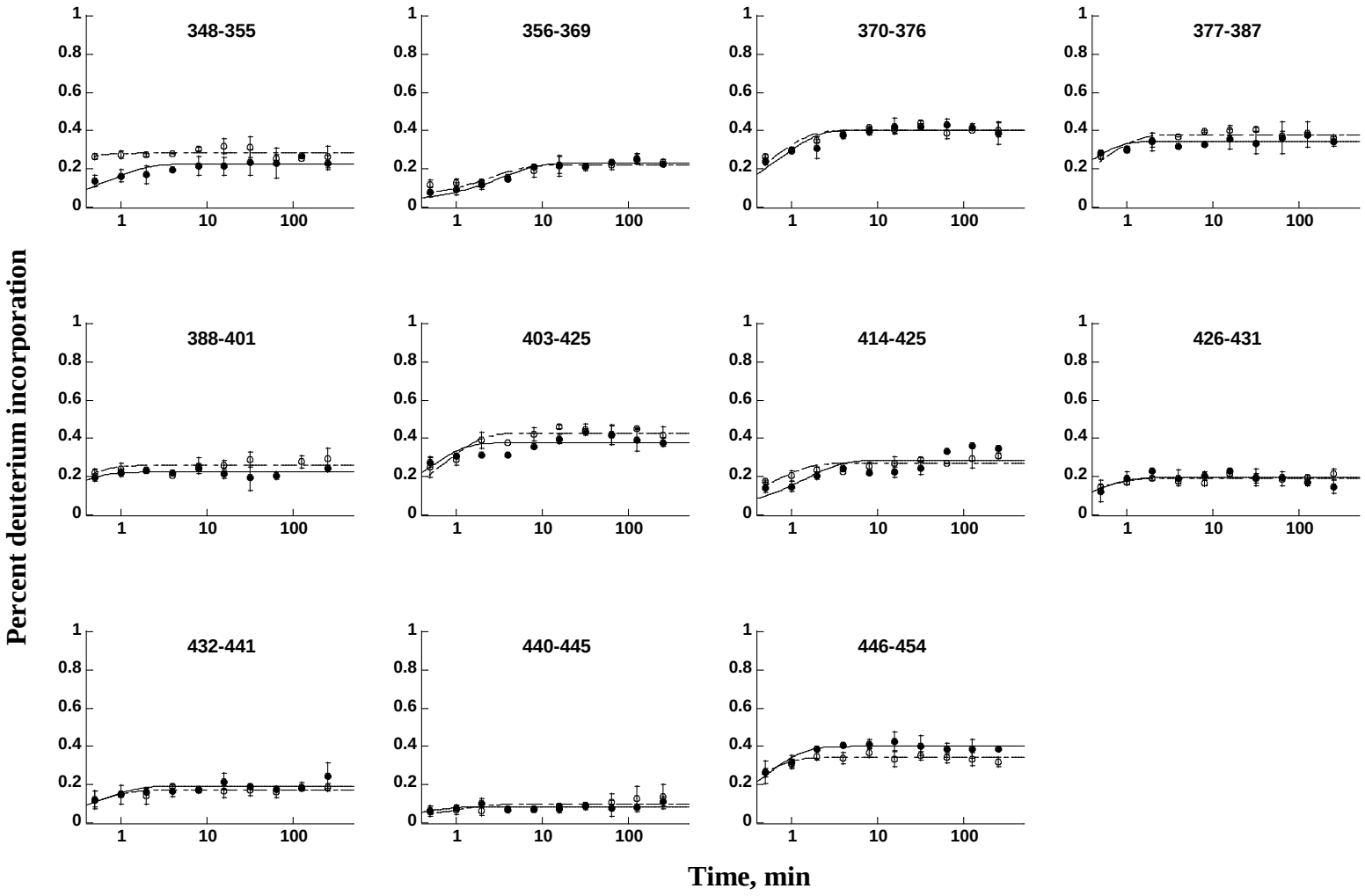

Figure 3.8 Continued.

Figure 3.9 compares the H/D exchange curves of the peptides sensitive to phenylalanine in wild-type PheH to the same peptides in Δ117PheH. Peptide 164-174 was not detected in Δ117PheH, so peptide 167-178 was analyzed instead. The other five peptides were detected. Only the deuterium incorporation curve in the absence of phenylalanine is shown in Figure 3.9 for clarity. The exchange patterns of peptides 241-248, 249-259 and 370-376 in Δ117PheH are similar to those in the wild-type enzyme in the absence of phenylalanine. However, the deuterium incorporation level of peptide 306-317 in Δ117PheH is 10% higher than in wild-type enzyme in the absence of phenylalanine after 1 min, close to the deuterium incorporation level after 16 min in the wild-type enzyme in the presence of phenylalanine. The deuterium incorporation curve of peptide 220-227 for Δ117PheH is between the curves for the wild-type enzyme in the absence and presence of phenylalanine.

Similar HXMS experiments were done for Δ117PheH in the presence of 400 μM BH_4. A total of 23 peptides were identified covering 68% of protein sequence. Four peptides of the eight showing dramatic difference in deuterium incorporation in the presence of phenylalanine were identified in Δ117PheH, 220-227, 241-249, 249-259 and 306-317. Peptides 164-174 and 370-376 were not detected. No dramatic difference in the deuterium incorporation pattern of most of the peptides of Δ117PheH was observed in the presence of BH_4 (Figure 3.10). Peptides 192-213 and 220-227 displayed small decreases in deuterium incorporation in the presence of BH_4, whereas peptides 180-191 and 249-259 displayed small increases.

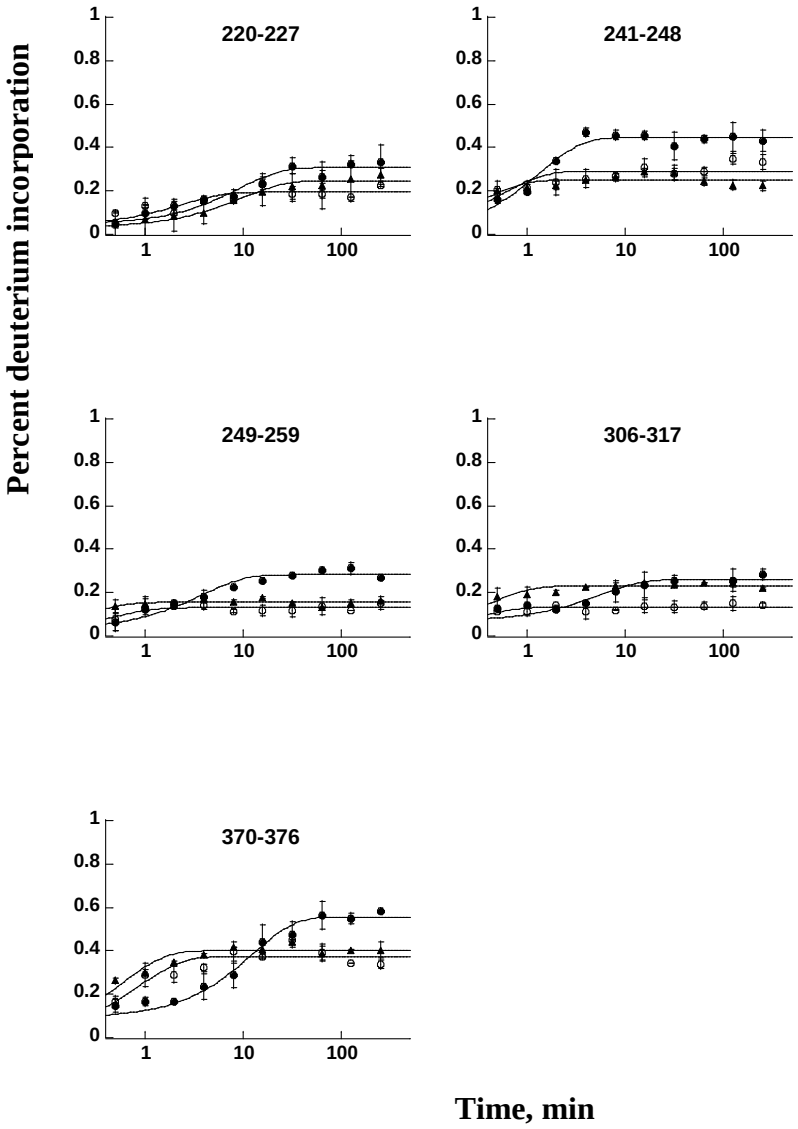

Figure 3.9. Comparison of the deuterium incorporation of the peptides sensitive to phenylalanine in wild-type PheH and Δ117PheH. The curves with symbol "○" and "●" represent the data of wild-type PheH in absence and presence of phenylalanine, respectively. The curve with symbol "▲" represents the data of Δ117PheH in absence of phenylalanine.

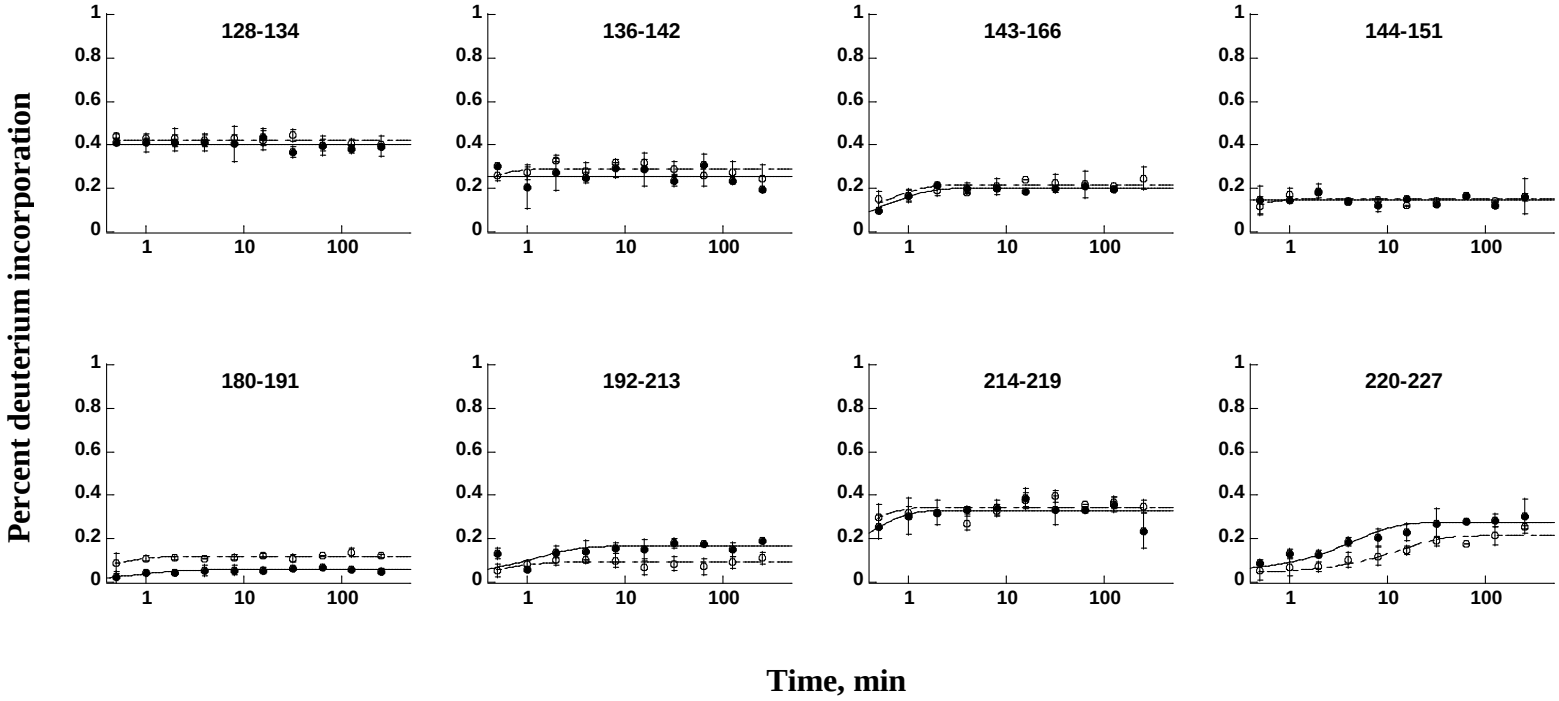

Figure 3.10. Deuterium incorporation into peptides of Δ117PheH in the absence (○, dashed line) and presence (●, solid line) of BH_4. Percent deuterium incorporation was calculated by dividing the observed deuterium incorporation by the number of exchangeable peptides bonds in a peptide. There is no adjustment for back-exchange.

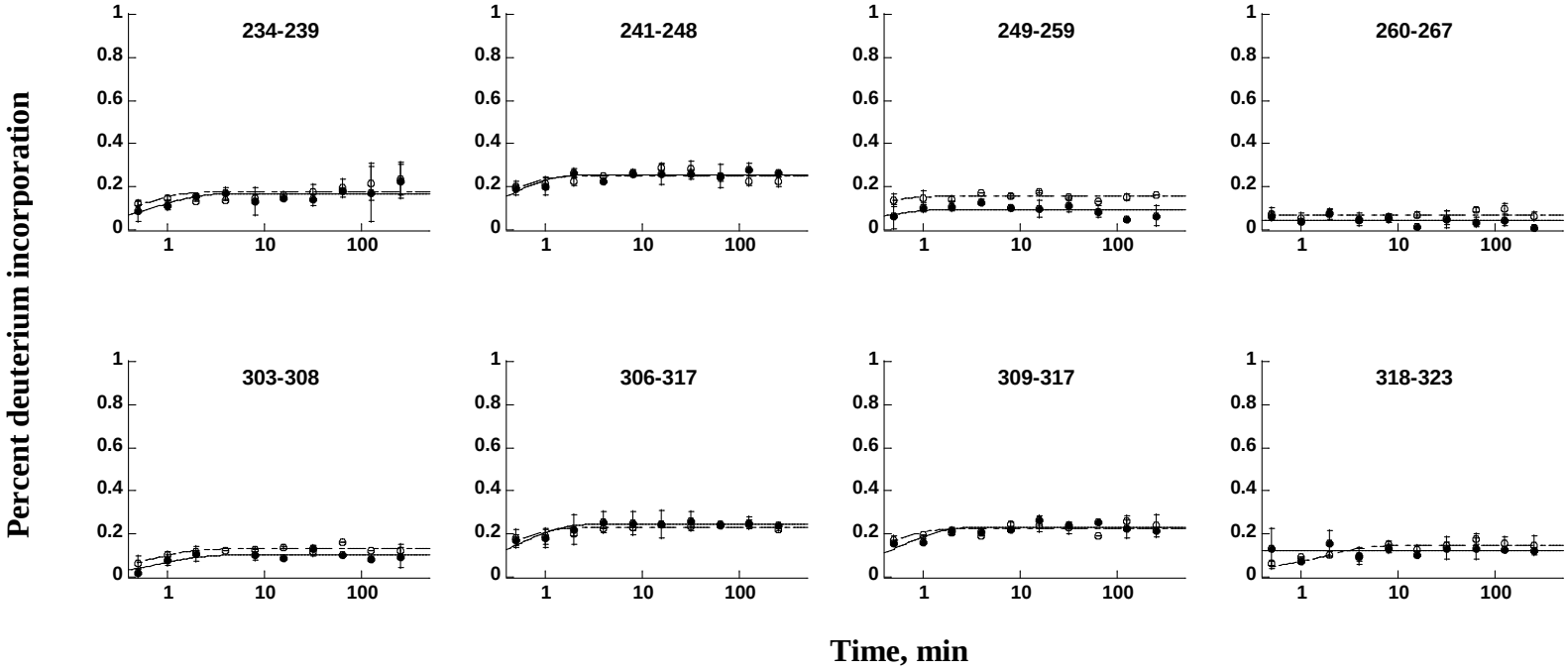

Figure 3.10 Continued.

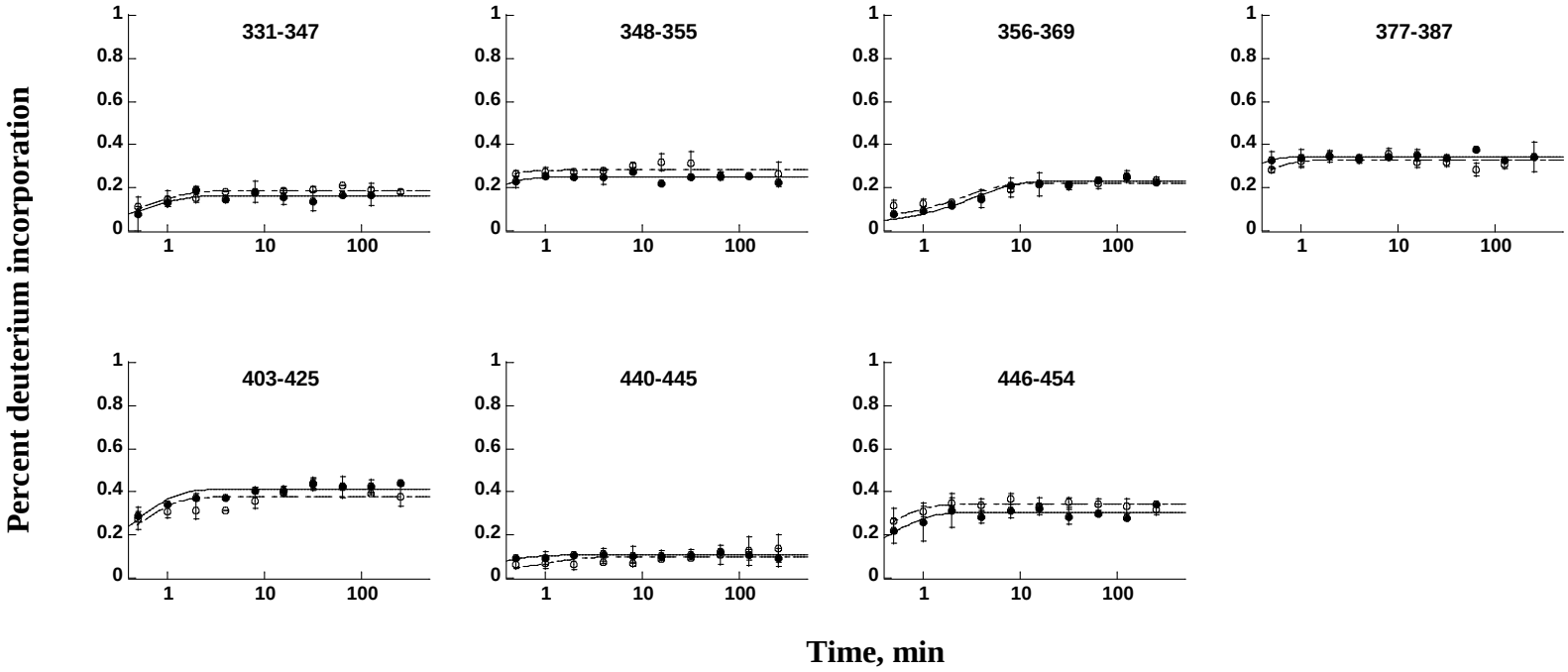

Figure 3.10 Continued.

H/D exchange of phosphorylated PheH

HXMS experiments were also conducted with phosphorylated PheH. A total of 28 peptides were indentified for phosphorylated PheH, covering 79% of the sequence. The deuterium incorporation patterns of most peptides in phosphorylated PheH in the presence of phenylalanine were not significantly affected by phenylalanine (Figure 3.11), suggesting that phenylalanine binding triggers no global conformational changes in phosphorylated PheH. Peptide 438-453 is the only one showing a significant difference in deuterium incorporation pattern in the presence of phenylalanine. Peptides 27-43, 82-91, 164-174 and 205-213 displayed slight differences after 30 min in the presence of phenylalanine. Five of the eight peptides showing dramatic changes in the wild type enzyme in the presence of phenylalanine were analyzed, whereas peptides 220-227, 241-248 and 370-376 were not detected.

Figure 3.12 compares the deuterium incorporation patterns of those peptides whose exchange kinetics in the unphosphorylated enzyme were altered by phenylalanine with the results for the phosphorylated PheH. Only the curves for the phosphorylated PheH in the absence of phenylalanine are shown for clarity. Peptides 241-248 and 370-376 were not detected in phosphorylated PheH. Peptides 249-259 and 306-317, similar to most other peptides in phosphorylated PheH, display similar exchange patterns to those in unphosphorylated PheH in the absence of phenylalanine. However, peptides 39-59, 82-91 and 164-174 show patterns that are more similar to those in unphosphorylated PheH in the presence of phenylalanine. This result suggests that the conformational changes induced by phosphorylation are similar but not identical to those associated with

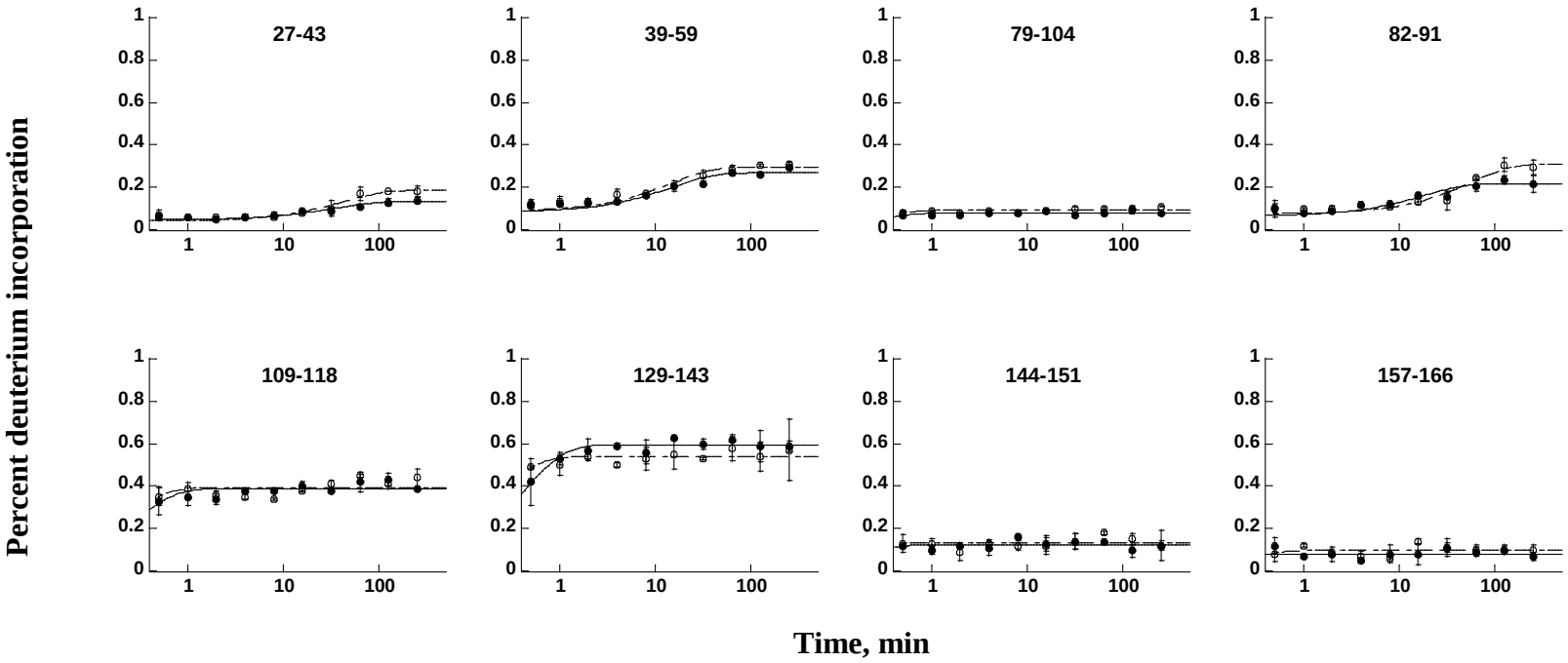

Figure 3.11. Deuterium incorporation into peptides of phosphorylated PheH in the presence (●, solid line) of phenylalanine. Deuterium incorporation in the absence of phenylalanine is also indicated (○, dashed line). Percent deuterium incorporation was calculated by dividing the observed deuterium incorporation by the number of exchangeable peptides bonds in a peptide. There is no adjustment for back-exchange.

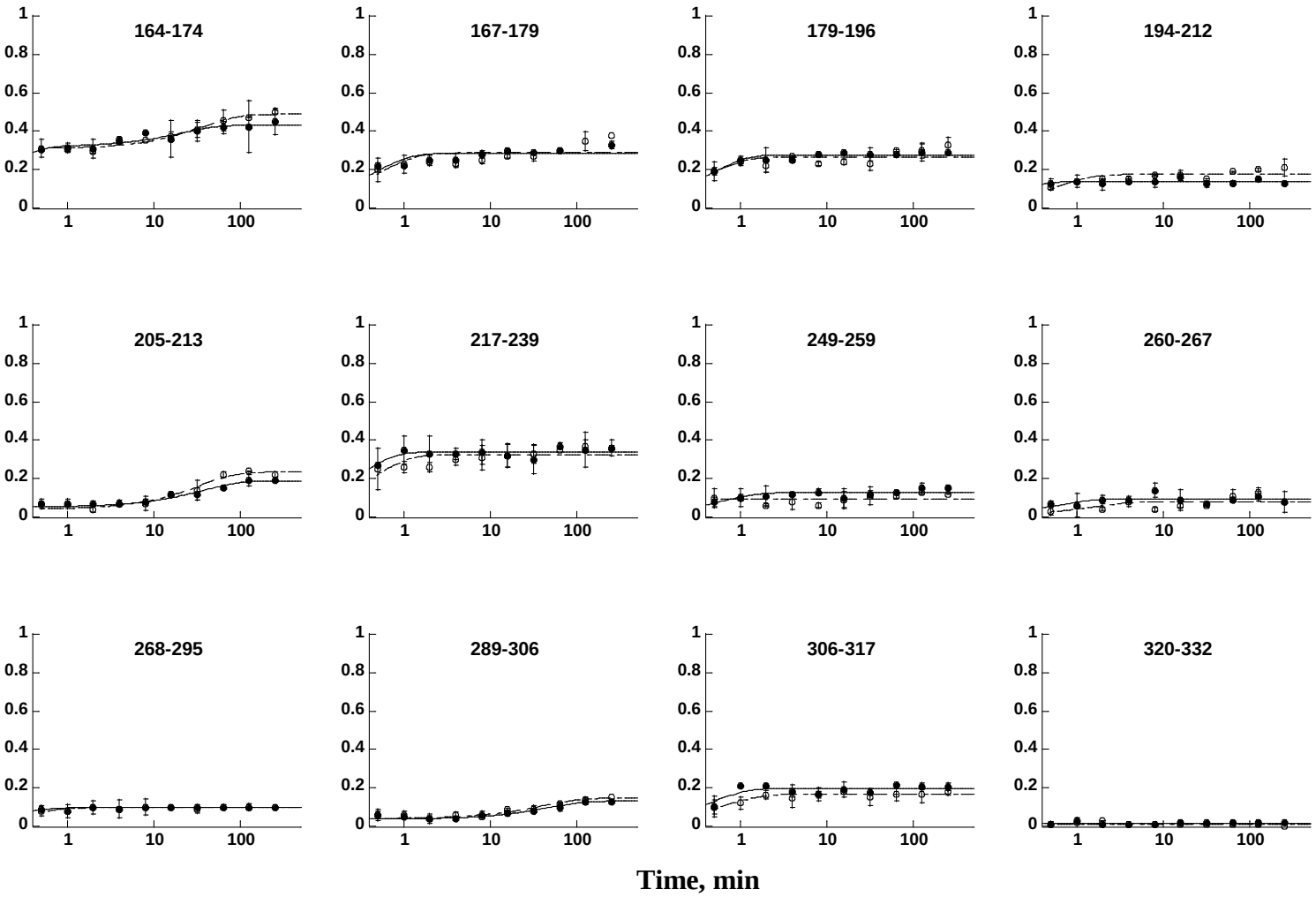

Figure 3.11 Continued.

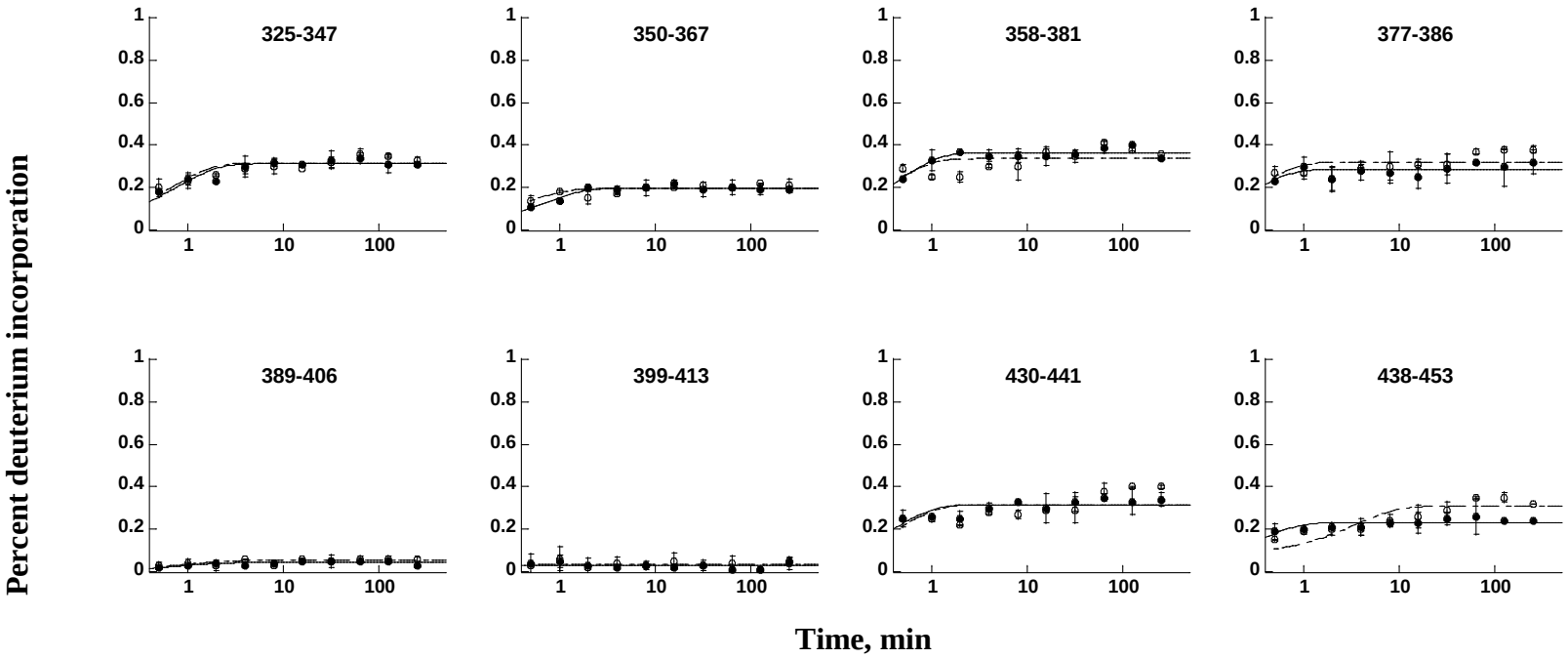

Figure 3.11 Continued.

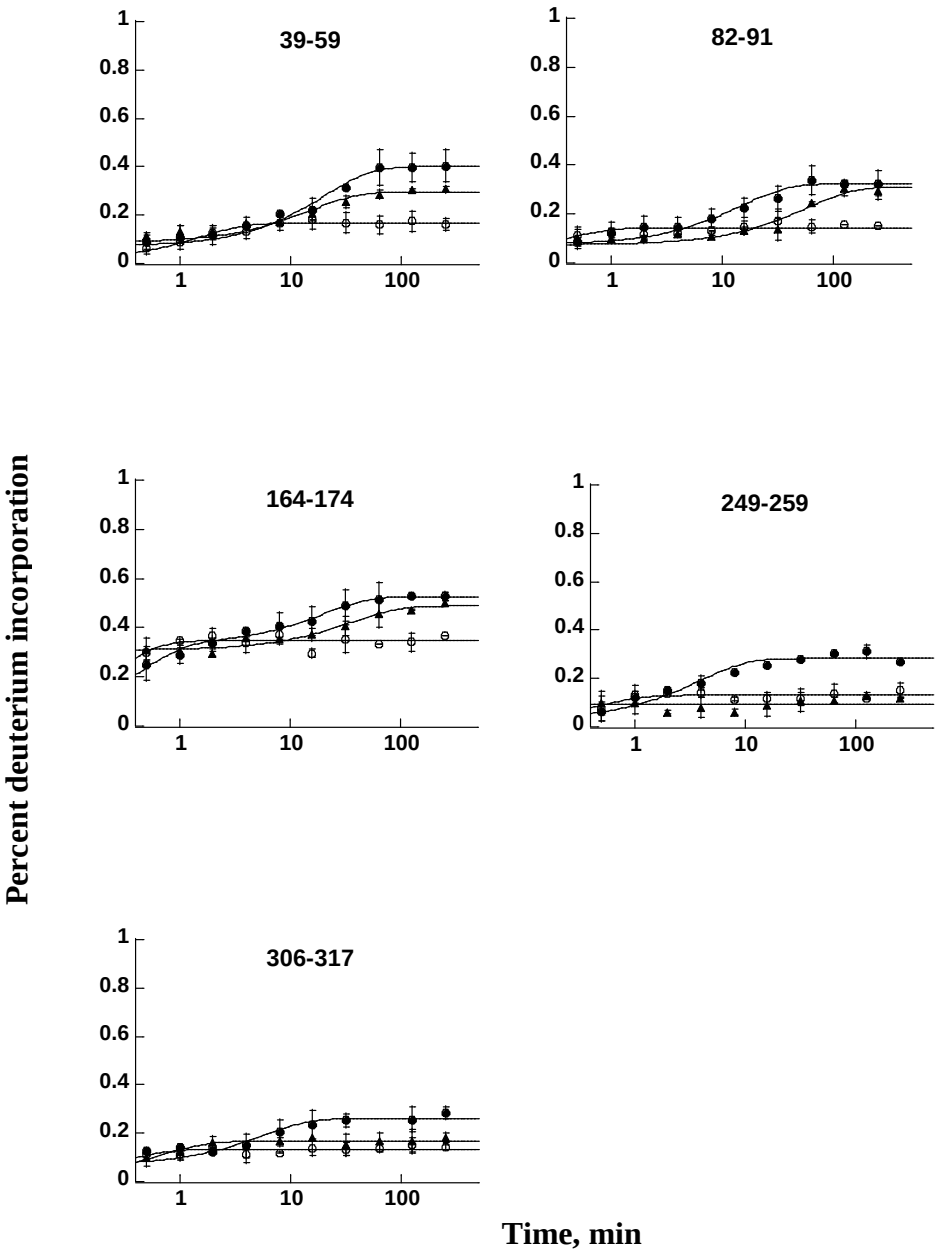

Figure 3.12. Comparison of the deuterium incorporation of the peptides sensitive to phenylalanine in unphosphorylated PheH and phosphorylated PheH. The H/D exchange curves for unphosphorylated PheH in the absence (○) and presence (●) of phenylalanine are also shown for comparison.

phenylalanine activation.

Similar HXMS experiments were done for phosphorylated PheH in the presence of 400 μM BH_4. A total of 28 peptides were identified covering 78% of the protein sequence. Of the eight peptides showing differences in wild type PheH in the presence of phenylalnine, only peptide 249-259 was detected, while peptides 241-248 and 370-376 were not identified. For the remaining five peptides, although the identical peptides were not identified, similar peptides could be analyzed. Most peptides displayed no significant difference in the deuterium incorporation pattern in the presence of BH_4. Peptides 129-143 and 217-239 displayed slight decreases (Figure 3.13).

Discussion

The available crystal structures of PheH with analogs of phenylalanine lack the regulatory domain (*72, 166*). Although the comparison of these structures with the substrate-free structure shows significant structural changes in the catalytic domain, there is no direct evidence showing how the regulatory domain itself changes. In this report, we demonstrate that both the regulatory and catalytic domains undergo significant conformational changes in the presence of phenylalanine. Eight peptides are more accessible to the solvent. These results support Shiman's model that phenylalanine binding converts PheH into an active form that is more open than the substrate-free PheH (*41, 42, 150*).

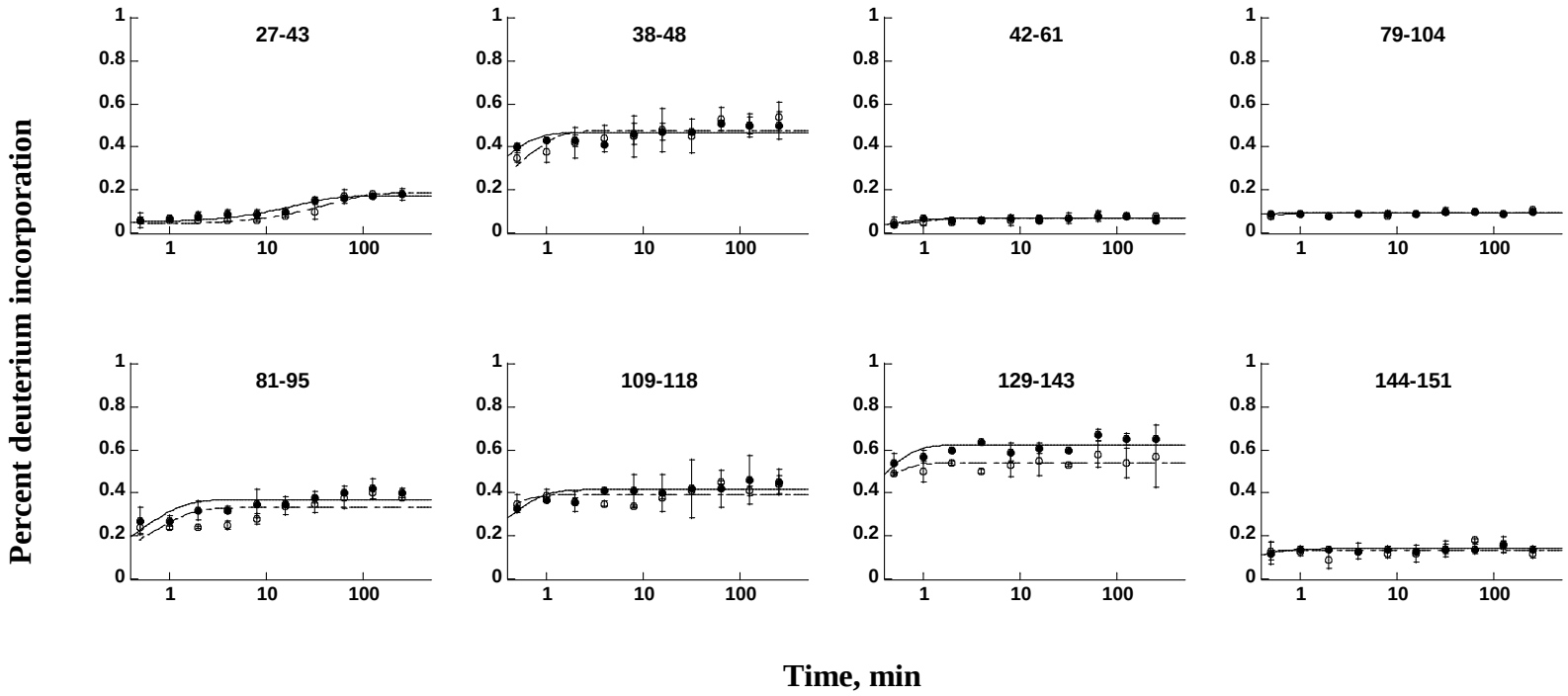

Figure 3.13. Deuterium incorporation into peptides of phosphorylated PheH in the absence (○, dashed line) and presence (●, solid line) of BH_4. Percent deuterium incorporation was calculated by dividing the observed deuterium incorporation by the number of exchangeable peptides bonds in a peptide. There is no adjustment for back-exchange.

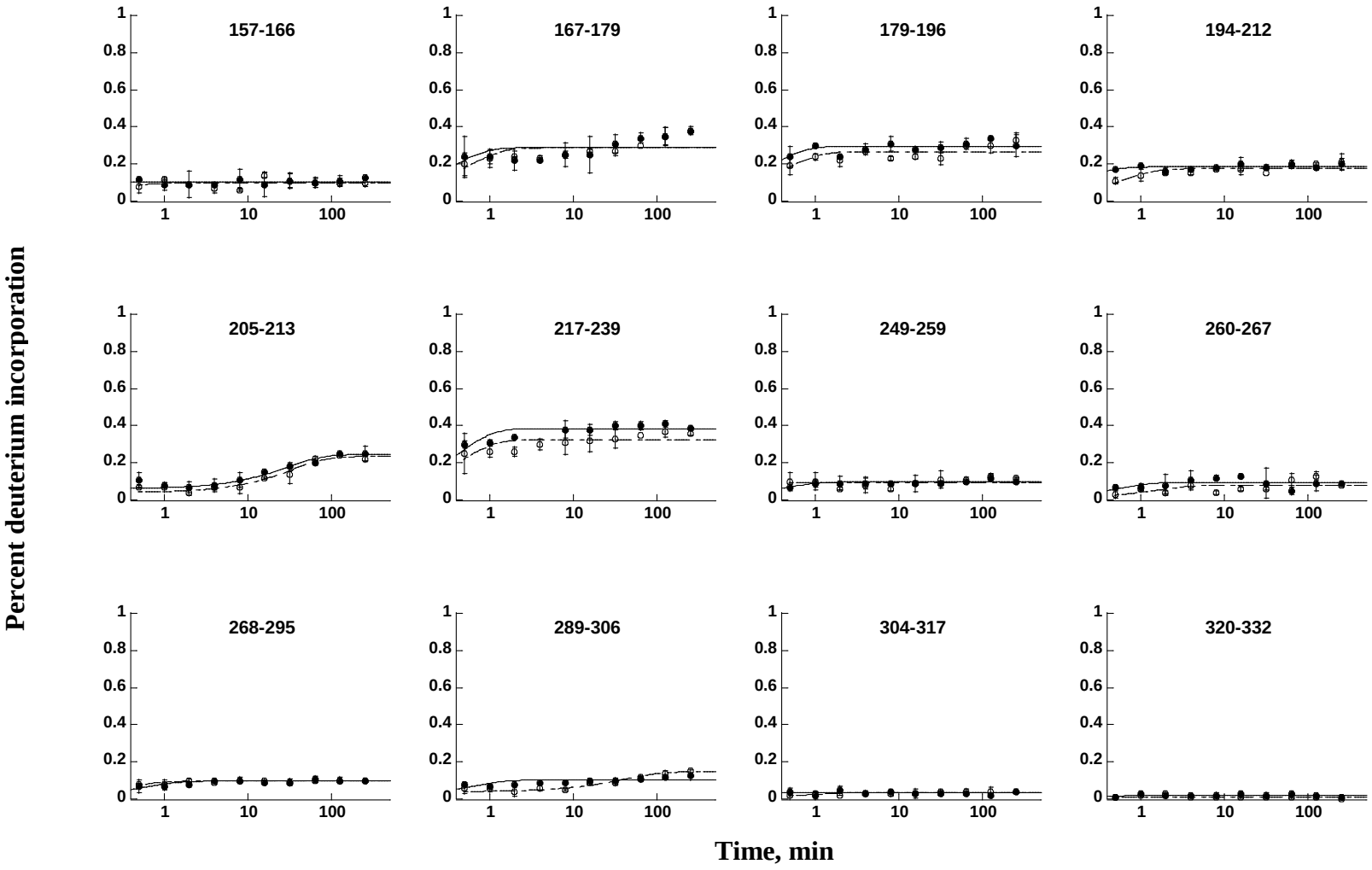

Figure 3.13 Continued.

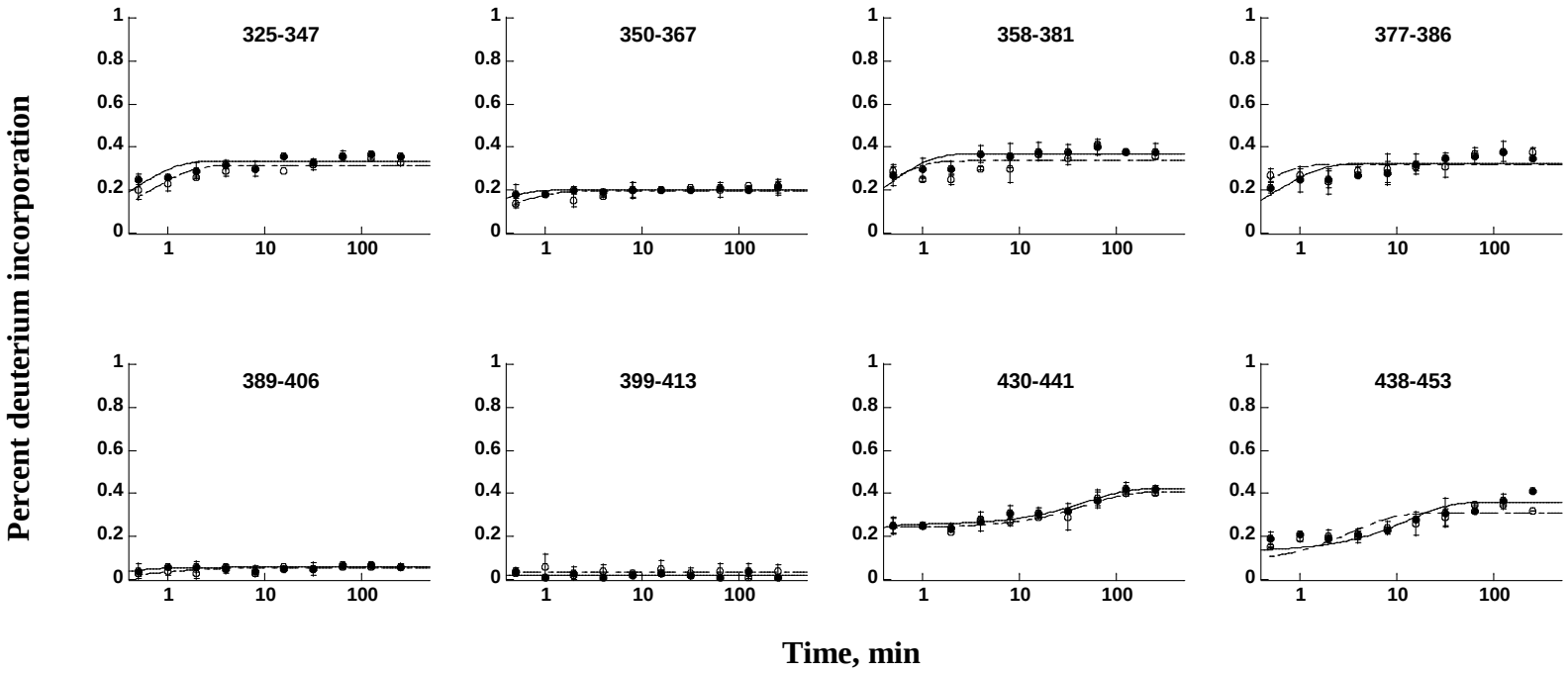

Figure 3.13 Continued.

An interesting finding in this research is that the interdomain regions of the regulatory and catalytic domains are converted into more open structures in the presence of phenylalanine, consistent with the previous proposal by Kobe et al. (*8*) that phenylalanine binding alters the relative orientation of the two domains. A thermal stability study using infrared spectroscopy also suggested that the conformational changes associated with the activation of PheH by phenylalanine are mainly associated with the changes in the tertiary/quaternary structure instead of the secondary structure (*170*). Of the eight peptides showing altered deuterium incorporation in the wild-type enzyme by phenylalanine, peptides 241-248, 249-259, 306-317 and 370-376 are in the interdomain regions between the regulatory and catalytic domains. The altered conformations of these regions may change the accessibility of the active site, allowing substrate to bind more easily.

Peptides 241-248 and 249-259 include residues 247-251 that form hydrogen bonds to BH_4 (*171*). The altered conformation of these two peptides in the wild type enzyme in the presence of phenylalanine may help binding of BH_4. Compared to BH_4, the binding site for phenylalanine is deeper in the active site. Peptide 268-295 includes the three main residues, Arg270, Thr278 and His285, directly interacting with phenylalanine. The deuterium exchange of this peptide was low (about 10% at maximum) and unaffected by phenylalanine. The reason for the unchanged deuterium exchange of this peptide could be that the decreased deuterium incorporation resulted from phenylalanine binding may be masked by the increase in deuterium incorporation caused by the opening of the active site upon phenylalanine activation.

A modeling experiment predicted molecular motions between the two hinge-bending regions of 183-201 and 219-226 upon phenylalanine binding (*11*), consistent with the effect of phenylalanine on the exchange kinetics of peptide 220-227. Peptide 220-227 is a short loop adjacent to the helix 227-237. In the model-derived structure Cys237 is involved in contacts of the catalytic domain with the tetramerization and regulatory domains of an adjacent subunit (*40)*. These contacts may be responsible for the transmission of the activating conformational change to the other subunit, explaining the positive cooperativity observed in phenylalanine activation (*8, 172*). In our results, the peptide containing Cys237 (peptide 234-239) does not show changed deuterium incorporation in the presence of phenylalanine. This peptide is in a helix that may be too rigid to exchange. However, loop 220-227, adjacent to the helix 227-237, does show increased exchange in the presence of phenylalanine.

The N-terminal residues 19-30 of PheH extend over the active site, contacting with residues in peptides 130-136, 249-252, 315-326 and 376-386 (*8*). This N-terminal sequence is proposed to play an autoinhibitory role, partially covering the active site; phenylalanine binding would displace this sequence from the active site (*8*). Our results found increased deuterium incorporation into peptides 241-248, 249-259, 306-317, and 370-376 in the presence of phenylalanine. These peptides are either in or adjacent to the regions contacting the autoregulatory sequence. Peptide 164-174 is close in space to peptide 130-136. The increased deuterium incorporation into these peptides, suggesting exposure of these regions to solvent in the presence of phenylalanine, is consistent with the proposed function of the N-terminal autoregulatory sequence. Two peptides in the N-

terminal autoregulatory sequence show no difference in the presence of phenylalanine. Peptide 3-11 reached maximum exchange (over 90% if adjusted for back-exchange) after 1 min in the absence of phenylalanine, suggesting a mobile conformation, consistent with this peptide being absent in the crystal structure. Peptide 21-38, a long flexible loop plus a small part of β-strand, reached maximum exchange after 2 min. Given the fact that both peptides are highly mobile, the displacement of them would not be reflected in increased deuterium exchange.

Of all the eight peptides, peptide 370-376 displayed the largest difference in the presence of phenylalanine, with not only higher maximum deuterium incorporation but also a dramatically slower exchange rate. Figure 3.5 shows that this peptide is close to both the N-terminus and to the catalytic domain of another subunit. The dramatically different deuterium incorporation pattern of peptide 370-376 in the presence of phenylalanine suggests that this peptide interacts with the N-terminal 18 residues that are missing in the structure of PheH. Alternatively, peptide 370-376 may transmit the conformational change initiated by the displacement of the N-terminal sequence to the other subunit. Peptide 370-376 is close to the loop 356-390 in the other subunit; the latter sequence contacts with the N-terminus of that subunit. This provides another possible mechanism for the conformational changes to be transmitted between the catalytic domains of adjacent subunits, besides the possible contacts between the regulatory and catalytic domains of different subunits through Cys237. The present results suggest that the N-terminus forms a network of interactions with the active site,

the regulatory domain and the adjacent subunit, initiating and transmitting the conformational changes caused by phenylalanine.

Three peptides, 85-112, 129-143 and 205-213 displayed small increases in deuterium incorporation in the presence of phenylalanine (Figure 3.3). Peptide 85-112 includes peptide 82-91, one of the peptides showing dramatically increased deuterium incorporation in the presence of phenylalanine. The relatively small increase of this peptide compared to peptide 82-91 suggests that the residues 92-112 are not affected by phenylalanine. The increased exchange of peptides 129-143 and 205-213 is small enough that we are reluctant to conclude that it reflects a significant conformational change.

The coverage of wild type PheH in the presence of BH_4 (Figure 3.7) is less than in the presence of phenylalanine. Three of the eight peptides sensitive to phenylalanine, 82-91, 249-259 and 306-317, were detected but did not show any significant difference. The other five peptides were not detected reliably. Peptides 241-248 and 249-259 include residues 247-251 which form hydrogen bonds to BH_4 (*171*). Peptide 241-248 was not detected in the wild type enzyme in the presence of BH_4. The reason for the absence of this peptide could be that binding of BH_4 changes the local conformation and shields the pepsin cleavage site. The deuterium incorporation into peptide 249-259 is also low in the absence of BH_4, suggesting that most amide hydrogens of this peptide are involved in interactions that do not exchange. BH_4 binding may form interactions with these amide hydrogens instead of the free ones; therefore there was no decreased deuterium incorporation observed in the presence of BH_4 in peptide 249-259. None of the 22

peptides displayed a dramatic difference in the presence of BH_4, except that peptides 21-38 and 85-112 showed slightly more exchange in the first min. These results show that about 60% of residues in PheH have no significant conformational change in the presence of BH_4, consistent with the basically unchanged crystal structures of PheH upon binding BH_4 (*10*). However, since about 40% of the residues are absent from the analysis, the possibility of some regions exhibiting conformational changes can not be excluded.

Δ117PheH has the same V_{max} value as the wild-type enzyme and a lower K_m for phenylalanine. In addition, there is no lag in tyrosine production if the assay is started by adding phenylalanine (*150*). These kinetics suggest that this truncated mutant behaves similarly to the phenylalanine-activated wild-type enzyme. Δ117PheH lacks the N-terminal sequence. If the increased deuterium incorporation found in the wild-type PheH in the presence of phenylalanine is due only to the displacement of the N-terminal sequence, then similar deuterium incorporation should be seen in Δ117PheH as in the wild-type enzyme in the presence of phenylalanine. Figure 3.9 shows that only peptide 306-317 in Δ117PheH has the same maximum deuterium incorporation as in the wild-type enzyme in the presence of phenylalanine, while peptides 241-248, 249-259 and 370-376 have exchange patterns indistinguishable from those in wild-type enzyme in the absence of phenylalanine. The exchange pattern of peptide 220-227 in Δ117PheH is intermediate between the patterns in wild-type enzyme in the absence and presence of phenylalanine. These results suggest that simple displacement of the N-terminal sequence is not the only reason for the altered exchange of the eight peptides in wild-

type enzyme. There must be some other changes that make these regions more open, and these changes require the regulatory domain. It could be the simple reorientation of the regulatory and catalytic domains, since all these exposed regions are interdomain areas. It also could be a series of complex conformational changes that start as a local change caused by phenylalanine binding and are then transmitted to other parts or domains through the net of interactions formed by N-terminal sequence. In general, our results with Δ117PheH demonstrate that the increased deuterium incorporation of the eight peptides in wild-type enzyme upon binding phenylalanine can not be attributed simply to the displacement of the N-terminal sequence.

The results in Figure 3.8 suggest that although phenylalanine does not have a global effect on the conformation of Δ117PheH, it still may cause some small local changes. For example, the peptides 192-213, 269-284 and 348-355 become slightly less accessible to solvent in the presence of phenylalanine. The reason for the small changes in peptide 192-213 is unclear. Peptides 269-284 and 348-355 include residues interacting with phenylalanine, i.e., Arg270, Thr278, Ser349, Gly346, Ser350 and Glu353 (*13*). Therefore, the small decreased deuterium incorporation could be regarded as local changes due to binding of phenylalanine. The reason for the absence of the small decreased deuterium incorporation of these two peptides in the wild type enzyme in the presence of phenylalanine may be that the large scale conformational changes toward an open structure counteract the small decreases caused by phenylalanine binding.

Some small differences in deuterium incorporation into Δ117PheH were also seen in the presence of BH_4 (Figure 3.10). Peptides 180-191 and 249-259 show slightly

decreased deuterium incorporation, while peptides 192-213 and 220-227 show slightly increased deuterium incorporation. Peptide 249-259 includes the residues Ser251, Phe254 and Leu255 that form contacts with BH_4 (*171*), which explain the protection from exchange. Similar to the result that no difference in exchange is seen in the phenylalanine binding site in the intact enzyme in the presence of phenylalanine, there is also no decreased exchange in peptide 249-259 in the intact enzyme in the presence of BH_4. These results suggest that the regulatory changes have a dominant effect on the conformations of PheH over the local effects caused by substrate binding. Decreased deuterium incorporation into peptide 180-191 of Δ117PheH was also seen in peptide 183-191 of the wild type PheH in the presence of BH_4. The reason is unclear. Peptides 192-213 and 220-227 are far from the binding site of BH_4 in space, and they were not identified in the wild type PheH in the presence of BH_4. Therefore it is hard to know their roles in the regulation by BH_4.

Phosphorylation and phenylalanine activation have been reported to work in concert to activate the enzyme. Phenylalanine-treated PheH is easier to phosphorylate and phosphorylated PheH needs less phenylalanine to be activated (*28, 146*). Phosphorylation does not result in a large-scale conformational change, based on the crystal structures of the phosphorylated and unphosphorylated PheH. Instead, it has been proposed that phosphorylation induces a limited conformational change around the phosphoserine (*8, 161*). A hypothesis explaining the synergy of phenylalanine activation and phosphorylation is that phosphorylation could stabilize the phenylalanine-activated enzyme through electrostatic interaction of phosphoserine with the catalytic core (*8,*

157). The absence of the N-terminal 18 residues in the crystal structures of the phosphorylated and unphosphorylated PheH makes it hard to know how the local structure changes around Ser16. Comparison of the deuterium exchange of these two forms of PheH in Figure 3.12 provides the opportunity to explore the structural effect of phosphorylation. The kinetics of deuterium exchange into peptides 39-59, 82-91 and 164-174 are intermediate between the kinetics of the unphosphorylated enzyme in the absence of phenylalanine and in the presence of phenylalanine. However, the exchange kinetics of peptides 249-259 and 306-317 are not affected by phosphorylation. Based on these results, it seems that phosphorylation mainly affects the conformation of the regulatory domain. Peptides 39-59 and 82-91 are not adjacent to Ser16 in the sequence, which suggests the conformational changes induced by phosphorylation are not restrained to the regions around the phosphoserine. The intermediate kinetics of deuterium incorporation into peptides 39-59, 82-91 and 164-174 in the phosphorylated PheH in the absence of phenylalanine implies that phosphorylation shifts the regulatory domain and part of catalytic domain into an intermediate conformation close to that of the phenylalanine-activated enzyme, consistent with the decreased amount of phenylalanine required for activation. These results suggest the mechanism of activation by phosphorylation is similar to but not identical to that of phenylalanine activation.

Our results provide evidence for the proposal that PheH is converted into an open form upon binding phenylalanine. The results support the model that phenylalanine activation displaces the N-terminal autoinhibitory sequence from the active site and that a reorientation of the regulatory and catalytic domain takes place upon phenylalanine

activation. Phosphorylation at Ser16 changes the regulatory domain of PheH into a similar but not identical conformation as in the phenylalanine-activated form. Although the details of regulation mechanisms of PheH remain unclear, these results provide a better understanding of the structural basis of regulation.

CHAPTER IV

PURIFICATION AND CHARACTERIZATION OF THE REGULATORY DOMAIN OF PHENYLALANINE HYDROXYLASE

Phenylalanine hydroxylase (PheH) catalyzes the hydroxylation of phenylalanine into tyrosine, the initial and rate-limiting step of the catabolic pathway of phenylalanine, using enzyme-bound iron, molecular oxygen and tetrahydropterin (*173*, *174*). Dysfunctions of PheH due to mutations in the human PheH gene cause the serious disease phenylketonuria (PKU), a common disorder in amino acid metabolism. PheH belongs to the aromatic amino acid hydroxylase family that has two other members, tyrosine hydroxylase (TyrH) and tryptophan hydroxylase (TrpH). TyrH and TrpH catalyze the hydroxylation of tyrosine and tryptophan in the biosynthesis of catecholamines and serotonin, respectively (*81*). PheH, TyrH and TrpH, are homotetramers with each subunit consisting of an N-terminal regulatory domain, a catalytic domain and a C-terminal tetramerization domain. The catalytic domain of PheH contains the iron atom responsible for catalysis and determines the substrate specificity (*99*). The three amino acid hydroxylases are 52% identical in the catalytic domains.

The regulatory domain of PheH, the N-terminal 117 residues, is involved in regulation. The major mechanisms of regulation of PheH are activation by phenylalanine, inhibition by BH_4, and additional activation by phosphorylation (*18*). PheH can also be activated by proteolysis, lysolecithin and thiol-modification agents (*175*). The phosphorylation site in PheH is Ser16 in the regulatory domain. The activation by phosphorylation of PheH is believed to work in concert with activation by phenylalanine

(*28*). It is reported that phosphorylation does not affect the V_{max} but instead decreases the amount of phenylalanine required to activate PheH (*27, 28*). The bacterial form of PheH from *Chromabacterium violaceum* that lacks the regulatory domain cannot be activated by phenylalanine. This suggests that all three regulatory processes require the regulatory domain. Both PheH and TyrH are activated by phosphorylation. However, TyrH is not activated by its amino acid substrate or lysolecithin treatment. In contrast, it can be activated by heparin (*176*). The dramatically different regulatory properties of TyrH and PheH are consistent with the low identity of their regulatory domains (*60*).

Only one crystal structure of PheH includes the regulatory domain, that of dimeric rat PheH lacking the C-terminal 24 residues (*8*). The regulatory domain of PheH is an α-β sandwich, forming an interlocking double βαβ motif (βαββαβ) motif. This domain is composed of a four-stranded antiparallel β-sheet flanked on one side by two short α-helices and on the other side by segments 118-131 and 409-422 of the catalytic domain. This structure shows that the N-terminus (residues 19-33) extends over the entrance of the active site of the catalytic domain, contacting residues 130-136, 249-252, 315-326 and 376-379. This sequence is proposed to exert an autoinhibitory function by partly covering the active site in the absence of phenylalanine (*8*). This proposed function is supported by the observation that truncated PheH lacking the N-terminal sequence does not require activation by phenylalanine and is not inhibited by BH_4 (*23, 150*).

It has been postulated that there exist two phenylalanine binding sites in PheH (*20*). Native PheH has been reported to bind 1.5 mol of phenylalanine/mol of subunit. After treatment with N-ethylmaleimide, PheH binds about 1 mol of phenylalanine/mol of

subunit. This modification activates PheH in a way that resembles the activation by proteolysis, for example, shifting the binding curve of phenylalanine from sigmoid to hyperbolic (*20*). The activating phenylalanine remains at the allosteric regulatory site during catalytic turnover and, while there, cannot be hydroxylated (*146*). These results provide evidences for two separate phenylalanine binding sites, a regulatory site and a catalytic site (*18*). The thiol-modification site of PheH was later identified as Cys237 (*34*), which is positioned in the dimer interface, near to the interface of the catalytic and regulatory domains (*8*). In a modeled structure of full-length hPheH, Cys237 is close to residues in the oligomerization and regulatory domains of an adjacent subunit in the dimer, especially Arg68 (*172*). This raises the possibility that the regulatory binding site of phenylalanine may be located near to the interface of the catalytic and regulatory domains. The conformational changes upon phenylalanine binding may modify the relative orientation of the regulatory and catalytic domains, which could be stabilized by phosphorylation, displacing the N-terminal inhibitory sequence away from the active site (*8*).

The only structure with the regulatory domain is rat PheH including the regulatory and catalytic domains (ΔCOOH430) in the phosphorylated and dephosphorylated states with ferric iron (PDB 1PHZ and 2PHM) (*8*). The only structures of PheH with phenylalanine analogues bound are those of the catalytic domain (PDB 1KW0, 1MMT) (*11*). Therefore the present PheH structures cannot establish the existence of a regulatory site of phenylalanine in the regulatory domain. There is no crystal structure of TyrH including the regulatory domain. Little is known about the structure of the regulatory

domain of TyrH, although it has been purified (*69*). In order to test the proposal of a regulatory binding site of PheH, we expressed and purified the regulatory domain of PheH. This research describes the design, expression, purification and some structural studies on the regulatory domain of PheH.

Materials and Experimental Procedures

Materials

Leupeptin and pepstatin A were from Peptides Institute, Inc. (Osaka, Japan). Restriction and DNA modification enzymes were purchased from New England Biolabs (Ipswich, MA). $^{15}NH_4Cl$ was purchased from Cambridge isotope Laboratories, Inc (Andover, MA). Thiamine hydrochloride, imidazole, carbonic anhydrase (from bovine erythrocytes), cytochrome c (from horse heart) and thrombin (from bovine plasma) were from Sigma-Aldrich (St. Louis, MO). Biotin and hemoglobin (from bovine blood) were from USB (Cleveland, Ohio). The FPLC system used was an ÄKTA purifier (GE Healthcare life science, Piscataway, NJ). The pET21b and pET28a were purchased from Novagen (Madison, WI).

Construction for the expression of the regulatory domain of rat PheH

To construct a plasmid coding for the regulatory domain of rat PheH, a unique *NcoI* site was introduced to the wild-type rat phenylalanine hydroxylase cDNA-containing plasmid pERPH5 (*99*) to stop translation before residue 118. Plasmid pERPH5 was subjected to mutagenesis using the oligonucleotide 5'-aag gaa aag aac aca tga CCATGG ttc ccg cgg acc-3'. Site-directed mutagenesis was carried out with the Stratagene QuikChange Kit using *Pfu* DNA polymerase. QIAfilter plasmid midi prep kits and

QIAprep Spin miniprep kits were used for purifying plasmids, which were used to transfect OmniMax competent cells (Invitrogen, Carlsbad, California). Oligonucleotide synthesis and mutant DNA sequencing were conducted by Nucleic Acids Core Facility, The University of Texas Health Science Center.

In order to get better expression, the gene coding for the regulatory domain of rat PheH was moved to pET21b from the pET23d vector of pERPH5 containing the above mutation. A fragment including the gene for the regulatory domain was generated by PCR using the mutant as the template. The oligonucleotide 5'- gg gaa ttc CATATG gca gct gtt gtc ctg gag aat gga -3' was used as the 5' primer to cover the start codon for the regulatory domain gene and create a new NdeI cut site. Another oligonucleotide, 5'- ccg CTCGAG tca tgt gtt ctt ttc ctt gtc tcg -3', was used as the 3' primer that includes a stop codon and also creates a new XhoI cut site. After purification from agarose gels, the PCR fragment encoding the regulatory domain gene was ligated to the empty vector generated by digestion of pET21b by NdeI and XhoI using T4 DNA ligase. Possible recombinants were screened by restriction enzyme analysis to rule out vector self ligation. One positive clone was sequenced to confirm that the cDNA for the regulatory domain of phenylalanine hydroxylase was inserted between the NdeI and XhoI sites of pET21b. This plasmid was named pETRD, encoding the protein $PheH_{1\text{-}117.}$

Similar procedures were conducted using the PCR fragment encoding for the regulatory domain gene and the empty vector generated by digestion of pET28a by NdeI and XhoI to generate a recombinant protein of the regulatory domain of PheH with a 6-histidine tag at the N-terminus. The histidine-tag can be removed by thrombin digestion,

leaving three extra residues (Gly-Ser-His) at the N-termini. This was pEThisRD, encoding the protein hisPheH$_{1-117}$.

Expression and purification of PheH$_{1-117}$

E. coli strain C41(DE3) transformed with the plasmid pETRD was grown overnight at 37 °C in Luria-Bertani medium plus 100 μg/mL ampicillin. Expression was induced by addition of 0.25 mM isopropyl β-D-thioglucanopyranoside (IPTG) when the A_{600} reached 0.8-1.0. After 12-15 h, cells were harvested by centrifugation at 6000 × g for 30 min. Cell pellets were suspended in 50 mM Hepes, 0.2 M NaCl, 1 μM leupeptin, 1 μM pepstatin A, 100 μg/ml lysozyme, and 100 μg/ml phenylmethylsulfonyl fluoride (PMSF), pH 7.5. The cell suspension was sonicated using four bursts of 30 s at 45 W with 30 s intervals, and then centrifuged at 30,000 × g for 30 min. The supernatant was treated with ammonium sulfate. The protein precipitating between 60 and 80% saturation was collected and dissolved in 50 mM Hepes, 0.5 mM EDTA, 10% glycerol, 1 μM leupeptin, and 1 μM pepstatin A, pH 7.5. After dialysis in the same buffer with three buffer-changes at 4 h intervals, the protein was applied to a 2.5 × 14-cm column of Q-Sepharose equilibrated with the same buffer. The column was washed with 150 ml of the same buffer, and the protein was eluted with a 500 ml gradient of the same buffer containing 0-0.2 M NaCl. The fractions were assayed by SDS-polyacrylamide gel electrophoresis. Those fractions showing a band with an apparent molecular weight of 13,000 were pooled and concentrated using an Amicon Ultra centrifugal filter (10,000 MWCO, Millipore). The concentrated sample was then applied to a HiPrep 16/60 Sephacryl S-100 HR (GE Healthcare Life Science, Piscataway, NJ) gel filtration column

in 50 mM Hepes, 0.2 M NaCl, 0.5 mM EDTA, 1 μM leupeptin and 1 μM pepstatin A, pH 7.5. The fractions were assayed by SDS-polyacrylamide gel electrophoresis. Those exhibiting a single band with an apparent molecular weight of 13,000 were pooled and stored at -80°C.

Expression and purification of ^{15}N-labeled hisPheH$_{1-117}$

To prepare ^{15}N labeled protein for NMR, the plasmid pEThisRD was transformed into BL21(DE3). One liter of autoinducing minimal medium used for expression was made from 1 g $^{15}NH_4Cl$, 50 mg kanamycin, 50 mM Na_2HPO_4, 50 mM KH_2PO_4, 5 mM Na_2SO_4, 2 mM $MgSO_4$, 0.5% glycerol, 0.05% glucose, 0.2% lactose and 0.5 × trace metals, pH7.5 (*177*). Yeast extract (0.02%, w/v), 1 μg/ml thiamine hydrochloride and 1 μg/ml biotin were added to improve expression. All the components were autoclaved for sterilization, except that thiamine hydrochloride, biotin, trace metals and kanamycin were sterilized using a 0.22 μm syringe filter (Millipore, Bedford, MA). A freshly transformed single colony was inoculated into 100 ml autoinducing minimal medium; the culture was left shaking at 300 rpm overnight at 37°C. This culture was then diluted into 900 ml of the same medium and kept shaking at 37°C for 5-8 h until the A_{600} reached saturation (about 2.6-2.8). Then the temperature was adjusted to 25°C to express the target protein. After 18-24 h, the cells were harvested by centrifugation at 6000 × g for 30 min. Cell pellets were suspended in 20 mM sodium phosphate buffer, 0.5 M NaCl, 5 mM imidazole, 1 μM leupeptin, 1 μM pepstatin A, 100 μg/ml lysozyme, and 100 μg/ml PMSF, pH 7.5. The cell suspension was sonicated using four bursts of 30 s at 45 W with 30 s intervals, then centrifuged at 30,000 × g for 30 min. The supernatant was

applied to a Histrap FF column (5 ml, GE Healthcare Life Science). A linear gradient of 50-300 mM imidazole in 10 column volumes of 20 mM sodium phosphate buffer, 0.5 M NaCl, pH 7.5, was used to elute the target protein after washing the column with 5 column volumes of 50 mM imidazole in the same buffer. The absorbance of the eluted fractions was monitored continuously at 280 nm. The peak fractions, hisPheH$_{1\text{-}117}$, were pooled and concentrated using an Amicon Ultra centrifugal filter (10,000 MWCO, Millipore, Bedford, MA). The concentrated hisPheH$_{1\text{-}117}$ protein was dialyzed in 20 mM sodium phosphate buffer, 5% glycerol, 1 μM leupeptin, 1 μM pepstatin A, pH 7.5, with 3 buffer-changes at 2 h intervals.

Thrombin digestion

For the NMR analysis, the hisPheH$_{1\text{-}117}$, was cleaved by thrombin. Thrombin (0.2 unit/μl) was added to a protein solution, approximate 1 mg/ml, to reach a ratio of 4 unit thrombin per mg recombinant protein. The mixture was gently shaken overnight at 4°C, followed by purification on a HiPrep 16/60 Sephacryl S-100 HR gel filtration column as described above for the regulatory domain without the histidine tag.

Analytic gel filtration

The molecular weight of PheH$_{1\text{-}117}$ was determined using a HiPrep 16/60 Sephacryl S-100 HR gel filtration column in 50 mM Hepes, 0.2 M NaCl, 0.5 mM EDTA, 1 μM leupeptin and 1 μM pepstatin A, pH 7.5, at room temperature. The flow rate was 0.8 ml/min and the absorbance of the eluate was monitored continuously at 280 nm. The standards used were hemoglobin (66,000), carbonic anhydrase (29,000) and cytochrome c (12,500).

NMR spectroscopy and data processing

Samples for NMR containing 0.69 mM ^{15}N-labelled regulatory domain were prepared in 20 mM sodium phosphate buffer, 5% glycerol, pH 7, in 95% H_2O/5% D_2O. All NMR data were collected at 308 K on a Bruker 700 MHz spectrometer. The ^{1}H-^{15}N HSQC (heteronuclear single-quantum coherence) spectrum was recorded without any ligands and with 5 mM phenylalanine or 5 mM proline. NMR data was processed using NMRpipe and visualized using NMRDraw (*178*).

Results

Expression and purification of PheH$_{1-117}$ and hisPheH$_{1-117}$

To obtain the regulatory domain of PheH, a mutation replacing Val118 with a stop codon was introduced into the plasmid pERPH5 encoding the wild type rat PheH. However, the mutant protein expressed poorly in C41(DE3) cell. Consequently, a DNA fragment including the gene encoding PheH$_{1-117}$ with NdeI and XhoI cut sites at the 5' and 3' ends, respectively, was generated by PCR using this construct as the template. This was ligated into pET21b to yield pETRD. PheH$_{1-117}$ expressed well in C41(DE3) cells, reaching approximately 5% of the total protein, and the protein was soluble. Most proteins under 25 kD, including about one tenth of PheH$_{1-117}$, were precipitated after treatment with 60% saturated ammonium sulfate (data not shown). The majority of PheH$_{1-117}$ was precipitated when the ammonium sulfate concentration was increased to 80%. PheH$_{1-117}$ eluted from the Q-Sepharose column between 40 and 100 mM NaCl. The Q-Sepharose column removed most contaminating proteins, leaving four that have higher molecular weights than PheH$_{1-117}$ (Figure 4.1).

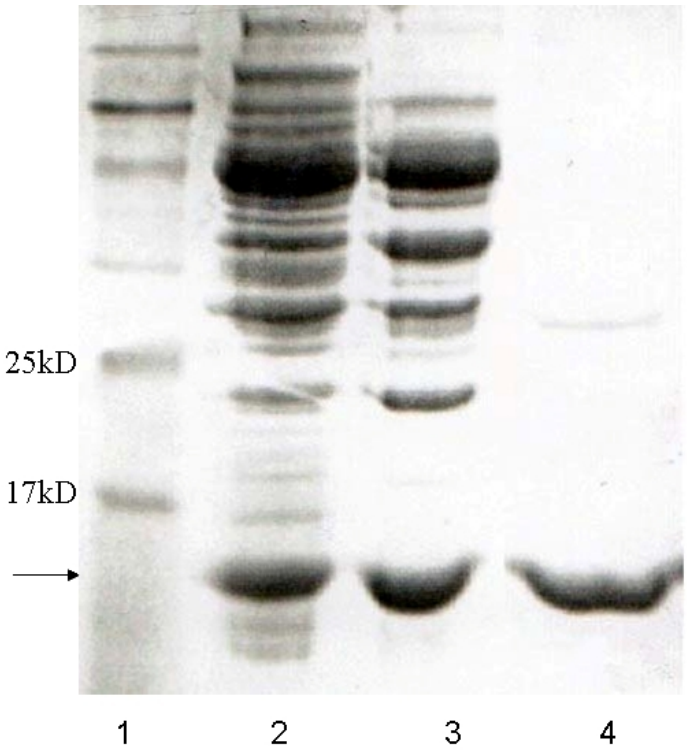

Figure 4.1. SDS-polyacrylamide gel electrophoresis of samples obtained during purification of the regulatory domain of PheH. The gel contained 15% (w/v) polyacrylamide. Lane 1, molecular mass standards in kDa; lane 2, concentrated sample after precipitating between 60 and 80% saturated ammonium sulfate (dialyzed); lane 3, concentrated sample after the Q-Sepharose column; lane 4, eluate from the gel filtration column.

A subsequent gel filtration column yielded $PheH_{1-117}$ of over 95% purity. The yield from 1 liter of cell culture was 3-5 mg. The single band on SDS-polyacrylamide gel corresponding to $PheH_{1-117}$ was sent to the Institutional Mass Spectrometry Laboratory of The University of Texas Health Science Center for identification. Twelve unique peptides generated by trypsin digestion covered 114 of the 117 residues, confirming the protein as $PheH_{1-117}$.

The pure $PheH_{1-117}$ protein is not very stable. It is usually stored at pH 7.0-7.5, 4 °C. At pH 6.5, the concentrated protein will precipitate. Multiple freeze-and-thaw cycles also precipitate this protein. Therefore the protein used in this study was freshly purified or thawed only once to avoid precipitation. The presence of phenylalanine seemed to stabilize the protein, but this property was not characterized further.

The supernatant of the cell lysate including $PheH_{1-117}$ was applied to a Phenyl-Sepharose column in the presence of phenylalanine followed by elution with buffer without phenylalanine. Subsequent SDS-polyacrylamide gel electrophoresis showed that $PheH_{1-117}$ protein did not bind to the column (data not shown).

The $hisPheH_{1-117}$ did not express well in regular M9 minimal medium. However, it was efficiently expressed in the autoinducing minimal medium at 37 °C. Unfortunately, the $hisPheH_{1-117}$ expressed at 37 °C was completely insoluble. If cells were grown at 25 °C, about 40% of the recombinant protein was soluble. When the growth temperature decreased to 16 °C, the protein expressed poorly. The $hisPheH_{1-117}$ grown at 25 °C was over 95% pure after purification on a Histrap FF column. The yield of $hisPheH_{1-117}$ was 5-8 mg from 1 liter of cell culture. An SDS-polyacrylamide gel showed that thrombin

efficiently removed the histidine tag (data not shown). A subsequent purification using a gel filtration column separated the target protein from the thrombin.

Analytical gel filtration

The retention time of the regulatory domain of PheH on a gel filtration column was between carbon anhydrase (29 kD) and cytochrome c (12.5 kD) and close to the former (Figure 4.2). The molecular weight for the monomer of $PheH_{1-117}$ based on its sequence is 13.2 kD. The molecular weight of $PheH_{1-117}$ was determined as about 26 kD based on the result of analytical gel filtration. This suggests that the regulatory domain of PheH is a dimer in solution.

The retention time of the regulatory domain of PheH on gel filtration column in the presence of phenylalanine (5 mM) was significantly earlier than that for protein alone (Figure 4.3). This suggests that phenylalanine binds to and changes the conformation of the regulatory domain of PheH. As a control, a similar experiment was done in the presence of 5 mM proline. Proline has been reported not able to activate PheH (*179*). The retention time was not changed from that for the protein alone.

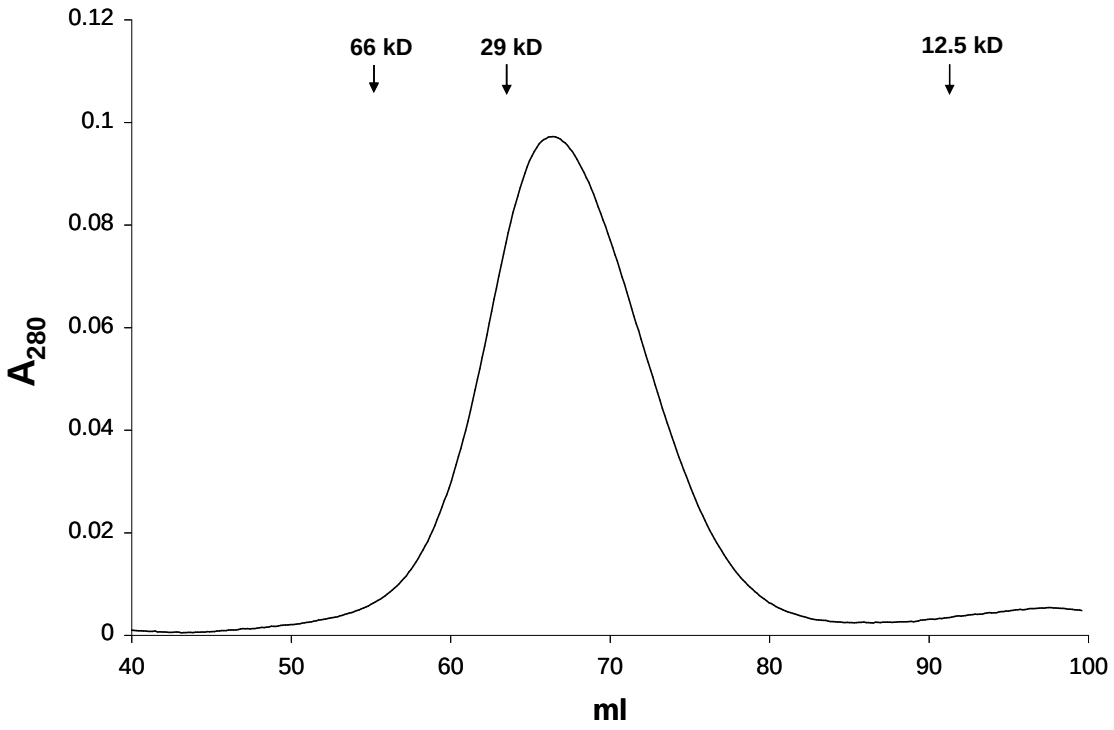

Figure 4.2. Gel filtration chromatography of the regulatory domain of PheH ($PheH_{1-117}$). The protein standards were hemoglobin (66 kD), carbonic anhydrase (29 kD) and cytochrome c (12.5 kD).

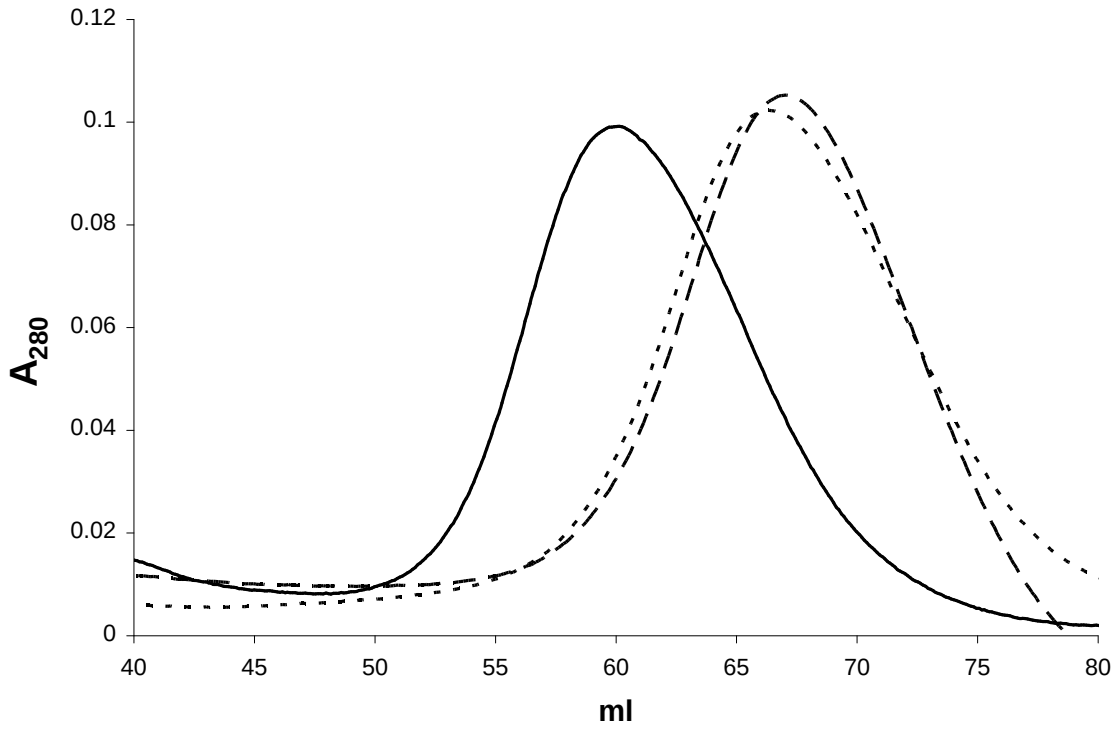

Figure 4.3. Gel filtration chromatography of the regulatory domain of PheH alone (dotted line) or with 5 mM phenylalanine (solid line) or 5 mM proline (dashed line).

NMR spectroscopy

The ^{1}H-^{15}N HSQC spectrum of $PheH_{1-117}$ at pH 7.0 and 308 K is shown in Figure 4.4. Chemical shift perturbation was used to monitor the effect of phenylalanine on $PheH_{1-117}$. In the absence of phenylalanine, about 120 peaks could be seen in the spectrum. Most cross peaks are broad and weak, and some peaks with ^{1}H chemical shift between 7.8 and 8.5 ppm overlap. After the addition of 5 mM phenylalanine, fewer peaks are seen in the spectrum and most of the remaining peaks are stronger and sharper (Figure 4.4A). Some peaks are lost, with others shown at new positions, as indicated with black and green arrows in Figure 4.4B, respectively. Meanwhile, the peaks that do not shift and become more intense and clear are indicated with red arrows. The NMR spectrum of $PheH_{1-117}$ in the presence of 5 mM proline is the same as that of the protein alone (Figure 4.4A). These results suggest that phenylalanine interacts with $PheH_{1-117}$ and causes a significant conformational change.

Discussion

In this study, the regulatory domain of PheH, $PheH_{1-117}$ was successfully expressed and purified. In solution $PheH_{1-117}$ is a dimer. One possible explanation for this observation is that the interface between the regulatory and catalytic domains is large and hydrophobic; the hydrophobic surfaces of two regulatory domains are prone to interact with each other in the absence of the catalytic domain. Figures 4.3 and 4.4 show that $PheH_{1-117}$ changes conformation in the presence of phenylalanine. These results

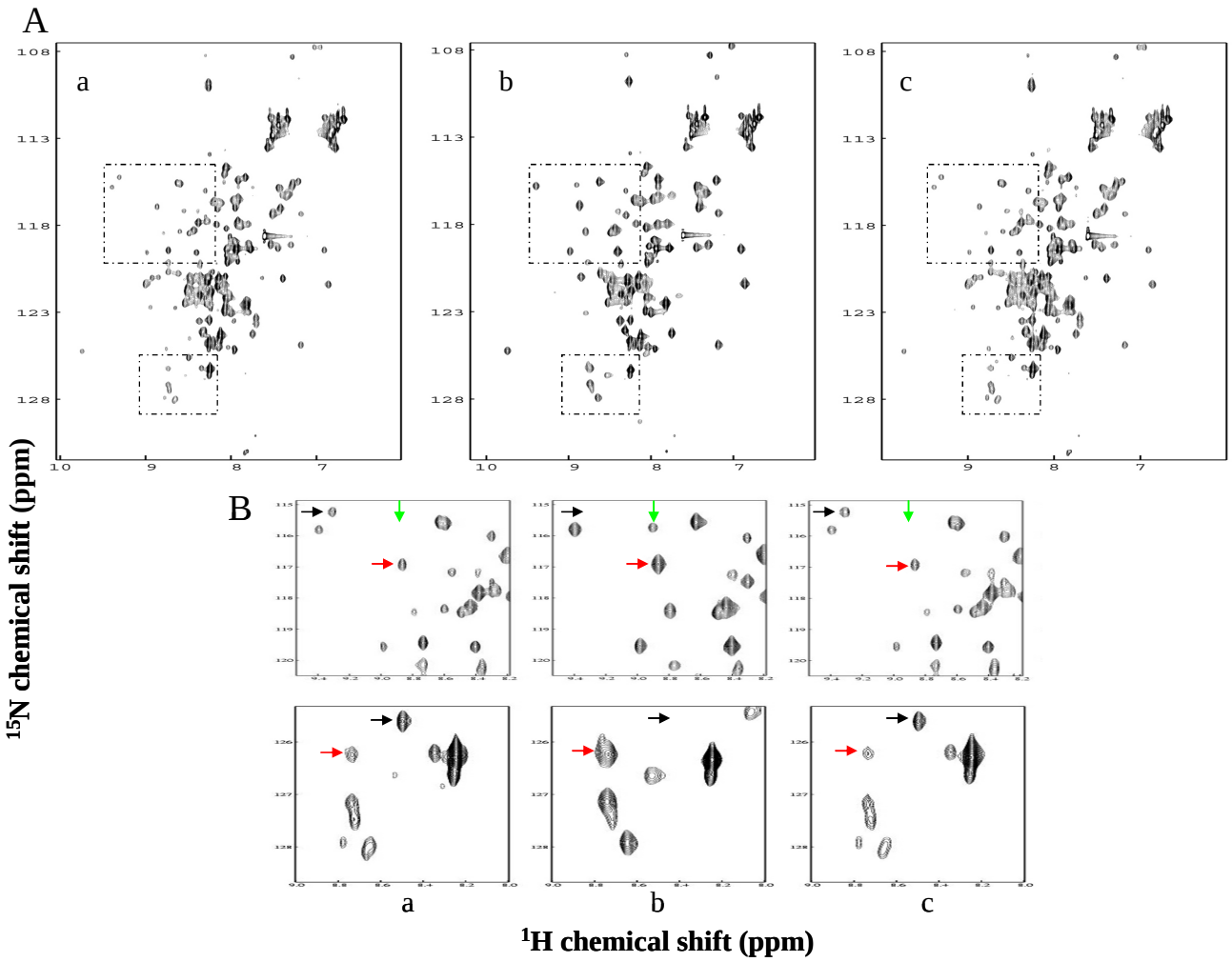

Figure 4.4. NMR spectra of $PheH_{1-117}$. ^{15}N HSQC NMR spectra of the ^{15}N-labeled $PheH_{1-117}$ alone (a), in the presence of 5 mM phenylalanine (b) or 5 mM proline (c) are shown in panel A. The boxed regions in panel A are shown in a larger view in panel B. The black, red and green arrows indicate examples of peaks getting lost, stronger or showing up at new places, respectively in the presence of phenylalanine.

strongly support the proposal that there is a binding site for phenylalanine in the regulatory domain of PheH. The full-length PheH can be purified using a Phenyl-Sepharose column (*22*). This method is based on the observation that PheH undergoes large-scale conformational changes, exposing a hydrophobic site that binds very tightly to the hydrophobic chromatography support if the enzyme is activated by phenylalanine. When phenylalanine is removed from the buffer, the enzyme desorbs from the support. Our results show that $PheH_{1-117}$ cannot be purified using the same method. Although there are several hydrophobic residues in the regulatory domain interface with the catalytic domain, they might be shielded in the dimer.

The regulatory domain of PheH is structurally similar to the regulatory domain of phosphoglycerate dehydrogenase (PGDH). PGDH is allosterically inhibited by serine. In the structure of the PGDH regulatory domain the binding site for the allosteric serine coincides with the residues 65-69 in PheH. These residues are near the interface between the regulatory and catalytic domains.This raises the possibility that phenylalanine could bind to the interface of the regulatory and catalytic domains.

The study of H/D exchange in Chapter III indicated that the addition of phenylalanine to the full-length PheH resulted in the increased solvent accessibility of the interface region between the regulatory and catalytic domains. There is no peptide identified in our study exactly covering residues 65-69. Two peptides near the two ends of 65-69, 39-59 (covering part of β strand Rβ1 and the whole helix Rα1) and 82-91 (covering part of helix Rα2), showed increased exchange in the presence of phenylalanine, suggesting a more open conformation. Peptide 54-61 displayed slightly

increased deuterium incorporation, while 67-81 showed no change. These results are consistent with the finding here that there exists a binding site for phenylalanine in the regulatory domain. It implies that the binding site of phenylalanine in the regulatory domain has a larger effect on residues 39-59 and 54-61. Because residues 82-91 are spacially close to helix Rα1, binding of phenylalanine could directly disrupt the interaction of Rα1 and Rα2 and change the conformation of the regulatory domain.

CHAPTER V

SUMMARY

This study provides structural information to better understand the structure and function of PheH. The active site of PheH contains a five/six-coordinated iron Fe(III) with two/three labile water molecules, forming a 2-His-1-carboxylate facial triad. The results in Chapter II revealed that this arrangement provides plasticity to the iron ligands to optimize the active site for iron binding and amino acid hydroxylation. The results in Chapter III suggest that PheH undergoes global conformational changes, including the displacement of the N-terminus and reorientation of the regulatory and catalytic domains upon activation by phenylalanine. Phosphorylation at Ser16 results in similar conformational changes to those upon phenylalanine activation, but these changes are localized in the vicinity of phosphorylation site. The binding of BH_4 does not significantly change the structure of PheH. The results in Chapter IV introduce the method of purifying the regulatory domain of PheH, $PheH_{1-117}$. The experiments of analytical gel filtration and ^{1}H-^{15}N NMR spectroscopy suggest that $PheH_{1-117}$ is a dimer in solution and there is a phenylalanine binding site in the regulatory domain of PheH.

The overall information provided by this research expands the understanding of the mechanism of activation of PheH by phenylalanine. Future work to determine where the binding site is in the regulatory domain will help further elucidate this regulatory mechanism.

REFERENCES

1. Woo, S. L., Güttler. F., Ledley, F. D., Lidsky, A. S., Kwok, S. C., DiLella, A. G., and Robson, K. J. (1985) The human phenylalanine hydroxylase gene, *Prog. Clin. Biol. Res. 177*, 123-135.

2. Scriver, C. R., Hurtubise, M., Konecki, D., Phommarinh, M., Prevost, L., Erlandsen, H., Stevens, R., Waters, P. J., Ryan, S., McDonald, D., and Sarkissian, C. (2003) PAHdb 2003: What a locus-specific knowledgebase can do, *Hum. Mutat. 21*, 333-344.

3. Wallick, D. E., Bloom, L. M., Gaffney, B. J., and Benkovic, S. J. (1984) Reductive activation of phenylalanine hydroxylase and its effect on the redox state of the non-heme iron, *Biochemistry 23*, 1295-1302.

4. Kaufman, S. (1957) The enzymatic conversion of phenylalanine to tyrosine, *J. Biol. Chem. 226*, 511-524.

5. Erlandsen, H., Fusetti, F., Martinez, A., Hough, E., Flatmark, T., and Stevens, R. C. (1997) Crystal structure of the catalytic domain of human phenylalanine hydroxylase reveals the structural basis for phenylketonuria, *Nat. Struct. Biol. 4*, 995-1000.

6. Fusetti, F., Erlandsen, H., Flatmark, T., and Stevens, R. C. (1998) Structure of tetrameric human phenylalanine hydroxylase and its implications for phenylketonuria, *J. Biol. Chem. 273*, 16962-16967.

7. Erlandsen, H., Flatmark, T., Stevens, R. C., and Hough, E. (1998) Crystallographic analysis of the human phenylalanine hydroxylase catalytic

domain with bound catechol inhibitors at 2.0 Å resolution, *Biochemistry 37*, 15638-15646.

8. Kobe, B., Jennings, I. G., House, C. M., Michell, B. J., Goodwill, K. E., Santarsiero, B. D., Stevens, R. C., Cotton, R. G. H., and Kemp, B. E. (1999) Structural basis of autoregulation of phenylalanine hydroxylase, *Nat. Struct. Biol. 6*, 442-448.
9. Erlandsen, H., Bjorgo, E., Flatmark, T., and Stevens, R. C. (2000) Crystal structure and site-specific mutagenesis of pterin-bound human phenylalanine hydroxylase, *Biochemistry 39*, 2208-2217.
10. Andersen, O. A., Flatmark, T., and Hough, E. (2001) High resolution crystal structures of the catalytic domain of human phenylalanine hydroxylase in its catalytically active Fe(II) form and binary complex with tetrahydrobiopterin, *J. Mol. Biol. 314*, 279-291.
11. Andersen, O. A., Stokka, A. J., Flatmark, T., and Hough, E. (2003) 2.0 Å Resolution crystal structures of the ternary complexes of human phenylalanine hydroxylase catalytic domain with tetrahydrobiopterin and 3-(2-thienyl)-L-alanine or L-norleucine: Substrate specificity and molecular motions related to substrate binding, *J. Mol. Biol. 333*, 747-757.
12. Erlandsen, H., and Stevens, R. C. (1999) The structural basis of phenylketonuria, *Mol. Genet. Metab. 68*, 103-125.
13. Andersen, O. A., Flatmark, T., and Hough, E. (2002) Crystal structure of the ternary complex of the catalytic domain of human phenylalanine hydroxylase

with tetrahydrobiopterin and 3-(2-thienyl)-L-alanine, and its implications for the mechanism of catalysis and substrate activation, *J. Mol. Biol. 320*, 1095-1108.

14. Kaufman, S. (1987) Phenylalanine 4-monooxygenase from rat liver, *Methods Enzymol. 142*, 3-17.
15. Andersson, K. K., Cox, D. D., Que, L., Jr., Flatmark, T., and Haavik, J. (1988) Resonance Raman studies on the blue-green-colored bovine adrenal tyrosine 3-monooxygenase (tyrosine hydroxylase). Evidence that the feedback inhibitors adrenaline and noradrenaline are coordinated to iron, *J. Biol. Chem. 263*, 18621-18626.
16. Kappock, T. J., Harkins, P. C., Friedenberg, S., and Caradonna, J. P. (1995) Spectroscopic and kinetic properties of unphosphorylated rat hepatic phenylalanine hydroxylase expressed in *Escherichia coli*. Comparison of resting and activated states, *J. Biol. Chem. 270*, 30532-30544.
17. Martinez, A., Knappskog, P. M., Olafsdottir, S., Doskeland, A. P., Eiken, H. G., Svebak, R. M., Bozzini, M., Apold, J., and Flatmark, T. (1995) Expression of recombinant human phenylalanine hydroxylase as fusion protein in *Escherichia coli* circumvents proteolytic degradation by host cell proteases, *Biochem. J. 306*, 589-597.
18. Hufton, S. E., Jennings, I. G., and Cotton, R. G. H. (1995) Structure and function of the aromatic amino acid hydroxylases, *Biochem. J. 311*, 353-366.
19. Shiman, R., and Gray, D. W. (1980) Substrate activation of phenylalanine hydroxylase. A kinetic characterizaion, *J. Biol. Chem. 255*, 4793-4800.

20. Parniak, M. A., and Kaufman, S. (1981) Rat liver phenylalanine hydroxylase. Activation by sulfhydryl modification, *J. Biol. Chem. 256*, 6876-6882.

21. Phillips, R. S., Parniak, M. A., and Kaufman, S. (1984) Spectroscopic investigation of ligand interaction with hepatic phenylalanine hydroxylase: Evidence for conformational change associated with activation, *Biochemistry 23*, 3836-3842.

22. Shiman, R., Gray, D. W., and Pater, A. (1979) A simple purification of phenylalanine hydroxylase by substrate-induced hydrophobic chromatography, *J. Biol. Chem. 254*, 11300-11306.

23. Jennings, I. G., Teh, T., and Kobe, B. (2001) Essential role of the N-terminal autoregulatory sequence in the regulation of phenylalanine hydroxylase, *FEBS Letters 488*, 196-200.

24. Wretborn, M., Humble, E., Ragnarsson, U., and Engstrom, L. (1980) Amino acid sequence at the phosphorylated site of rat liver phenylalanine hydroxylase and phosphorylation of a corresponding synthetic peptide, *Biochem. Biophys. Res. Commun. 93*, 403-408.

25. Abita, J. P., Milstien, S., Chang, N., and Kaufman, S. (1976) In vitro activation of rat liver phenylalanine hydroxylase by phosphorylation, *J. Biol. Chem. 251*, 5310-5314.

26. Doskeland, A. P., Schworer, C. M., Doskeland, S. O., Chrisman, T. D., Soderling, T. R., Corbin, J. D., and Flatmark, T. (1984) Some aspects of the

phosphorylation of phenylalanine 4-monooxygenase by a calcium-dependent and calmodulin-dependent protein kinase, *Eur. J. Biochem. 145*, 31-37.

27. Shiman, R., and Jefferson, L. S. (1982) Iron-dependent regulation of rat liver phenylalanine hydroxylase activity in vivo, in vitro, and in perfused liver, *J. Biol. Chem. 257*, 839-844.

28. Doskeland, A. P., Doskeland, S. O., Ogreid, D., and Flatmark, T. (1984) The effect of ligands of phenylalanine 4-monooxygenase on the cAMP-dependent phosphorylation of the enzyme, *J. Biol. Chem. 259*, 11242-11248.

29. Kowlessur, D., Yang, X.-J., and Kaufman, S. (1995) Further studies of the role of Ser-16 in the regulation of the activity of phenylalanine hydroxylase, *Proc. Natl. Acad. Sci. 92*, 4743-4747.

30. Citron, B. A., Davis, M. D., and Kaufman, S. (1994) Electrostatic activation of rat phenylalanine hydroxylase, *Biochem. Biophys. Res. Commun. 198*, 174-180.

31. Shiman, R. (1980) Relationship between the substrate activation site and catalytic site of phenylalanine hydroxylase, *J. Biol. Chem. 255*, 10029-10032.

32. Iwaki, M., Phillips, R. S., and Kaufman, S. (1986) Proteolytic modification of the amino-terminal and carboxyl-terminal regions of rat hepatic phenylalanine hydroxylase, *J. Biol. Chem. 261*, 2051-2056.

33. Fisher, D. B., and Kaufman, S. (1973) The stimulation of rat liver phenylalanine hydroxylase by lysolecithin and α-chymotrypsin, *J. Biol. Chem. 248*, 4345-4353.

34. Gibbs, B. S., and Benkovic, S. J. (1991) Affinity labeling of the active site and the reactive sulfhydryl associated with activation of rat liver phenylalanine hydroxylase, *Biochemistry 30*, 6795-6802.

35. Knappskog, P. M., and Martinez, A. (1997) Effect of mutations at Cys237 on the activation state and activity of human phenylalanine hydroxylase, *FEBS Lett 409*, 7-11.

36. Thorolfsson, M., Teigen, K., and Martinez, A. (2003) Activation of phenylalanine hydroxylase: Effect of substitutions at Arg68 and Cys237, *Biochemistry 42*, 3419-3428.

37. Chiappelli, F., Haggerty, D. F., Lynch, M., and Popjak, G. (1981) Translation of phenylalanine hydroxylase-specific mRNA in vitro: Evidence for pretranslational control by glucocorticoids, *Proc. Natl. Acad. Sci. USA. 78*, 2105-2109.

38. Shiman, R., Gray, D. W., and Hill, M. A. (1994) Regulation of rat liver phenylalanine hydroxylase. I. Kinetic properties of the enzyme's iron and enzyme reduction site, *J. Biol. Chem. 269*, 24637-24646.

39. Xia, T., Gray, D. W., and Shiman, R. (1994) Regulation of rat liver phenylalanine hydroxylase. III. Control of catalysis by (6R)-tetrahydrobiopterin and phenylalanine, *J. Biol. Chem. 269*, 24657-24665.

40. Rose, G. A., Lumb, F. H., and Dent, C. E. (1957) Discussion on generalized aches and pains from metabolic bone disease, *Proc. R. Soc. Med. 50*, 371-380.

41. Folling, A. (1967) [Phenylketonuria], *Tidsskr Nor Laegeforen 87*, Suppl: 451-454.

42. Paine, R. S. (1957) The variability in manifestations of untreated patients with phenylketonuria (phenylpyruvic aciduria), *Pediatrics 20*, 290-302.

43. Ledley, F. D., Koch, R., Jew, K., Beaudet, A., O'Brien, W. E., Bartos, D. P., and Woo, S. L. (1988) Phenylalanine hydroxylase expression in liver of a fetus with phenylketonuria, *J. Pediatr. 113*, 463-468.

44. Scriver, C. R., and Kaufman, S. (2001) Hyperphenylalanemia: Phenylalanine hydroxylase deficiency, in The metabolic and molecular bases of inherited disease (Scriver, C. R., Beaudet, A. L., Sly, D. S., and Valle, D., Eds.), pp 1667-1724, McGraw-Hill, New York.

45. Sarkissian, C. N., and Gamez, A. (2005) Phenylalanine ammonia lyase, enzyme substitution therapy for phenylketonuria, where are we now?, *Mol Genet Metab 86 Suppl 1*, S22-26.

46. Kure, S., Hou, D. C., Ohura, T., Iwamoto, H., Suzuki, S., Sugiyama, N., Sakamoto, O., Fujii, K., Matsubara, Y., and Narisawa, K. (1999) Tetrahydrobiopterin-responsive phenylalanine hydroxylase deficiency, *J Pediatr 135*, 375-378.

47. Wang, L., Surendran, S., Michals-Matalon, K., Bhatia, G., Tanskley, S., Koch, R., Grady, J., Tyring, S. K., Stevens, R. C., Guttler, F., and Matalon, R. (2007) Mutations in the regulatory domain of phenylalanine hydroxylase and response to tetrahydrobiopterin, *Genet Test 11*, 174-178.

48. Fang, B., Eisensmith, R. C., Li, X. H., Finegold, M. J., Shedlovsky, A., Dove, W., and Woo, S. L. (1994) Gene therapy for phenylketonuria: Phenotypic correction

in a genetically deficient mouse model by adenovirus-mediated hepatic gene transfer, *Gene Ther 1*, 247-254.

49. Mochizuki, S., Mizukami, H., Ogura, T., Kure, S., Ichinohe, A., Kojima, K., Matsubara, Y., Kobayahi, E., Okada, T., Hoshika, A., Ozawa, K., and Kume, A. (2004) Long-term correction of hyperphenylalaninemia by AAV-mediated gene transfer leads to behavioral recovery in phenylketonuria mice, *Gene Ther 11*, 1081-1086.

50. Onishi, A., Liotta, L. J., and Benkovic, S. J. (1991) Cloning and expression of *Chromobacterium violaceum* phenylalanine hydroxylase in *Escherichia coli* and comparison of amino acid sequence with mammalian aromatic amino acid hydroxylases, *J. Biol. Chem. 266*, 18454-18459.

51. Pember, S. O., Villafranca, J. J., and Benkovic, S. J. (1986) Phenylalanine hydroxylase from *Chromobacterium violaceum* is a copper-containing monooxygenase. Kinetics of the reductive activation of the enzyme, *Biochemistry 25*, 6611-6619.

52. Carr, R. T., Balasubramanian, S., Hawkins, P. C. D., and Benkovic, S. J. (1995) Mechanism of metal-independent hydroxylation by *Chromobacterium violaceum* phenylalanine hydroxylase, *Biochemistry 34*, 7525-7532.

53. Chen, D., and Frey, P. (1998) Phenylalanine hydroxylase from *Chromobacterium violaceum*. Uncoupled oxidation of tetrahydropterin and the role of iron in hydroxylation, *J. Biol. Chem. 273*, 25594-25601.

54. Volner, A., Zoidakis, J., and Abu-Omar, M. M. (2003) Order of substrate binding in bacterial phenylalanine hydroxylase and its mechanistic implication for pterin-dependent oxygenases, *J. Biol. Inorg. Chem. 8*, 121-128.

55. Hagedoorn, P. L., Schmidt, P. P., Andersson, K. K., Hagen, W. R., Flatmark, T., and Martinez, A. (2001) The effect of the substrate, dihydrobiopterin and dopamine on the EPR spectroscopic properties and the midpoint potential of the catalytic iron in recombinant human phenylalanine hydroxylase, *J. Biol. Chem. 276*, 22850-22856.

56. Fitzpatrick, P. F. (1991) The steady state kinetic mechanism of rat tyrosine hydroxylase, *Biochemistry 30*, 3658-3662.

57. Knappskog, P. M., Flatmark, T., Aarden, J. M., Haavik, J., and Martinez, A. (1996) Structure/function relationships in human phenylalanine hydroxylase. Effect of terminal deletions on the oligomerization, activation and cooperativity of substrate binding to the enzyme, *Eur. J. Biochem. 242*, 813-821.

58. Panay, A. J., and Fitzpatrick, P. F. (2008) Kinetic isotope effects on aromatic and benzylic hydroxylation by *Chromobacterium violaceum* phenylalanine hydroxylase as probes of chemical mechanism and reactivity, *Biochemistry 47*, 11118-11124.

59. Erlandsen, H., Kim, J. Y., Patch, M. G., Han, A., Volner, A., Abu-Omar, M. M., and Stevens, R. C. (2002) Structural comparison of bacterial and human iron-dependent phenylalanine hydroxylases: Similar fold, different stability and reaction rates, *J. Mol. Biol. 320*, 645-661.

60. Fitzpatrick, P. F. (2003) Mechanism of aromatic amino acid hydroxylation, *Biochemistry 42*, 14083-14091.

61. Siltberg-Liberles, J., Steen, I. H., Svebak, R. M., and Martinez, A. (2008) The phylogeny of the aromatic amino acid hydroxylases revisited by characterizing phenylalanine hydroxylase from *Dictyostelium discoideum*, *Gene 427*, 86-92.

62. Daubner, S. C., Melendez, J., and Fitzpatrick, P. F. (2000) Reversing the substrate specificities of phenylalanine and tyrosine hydroxylase: Aspartate 425 of tyrosine hydroxylase is essential for L-DOPA formation, *Biochemistry 39*, 9652-9661.

63. Nagatsu, T., Levitt, M., and Udenfriend, S. (1964) Tyrosine hydroxylase: The initial step in norepinephrine biosynthesis, *J. Biol. Chem. 239*, 2910-2917.

64. Haycock, J. W., Meligeni, J. A., Bennett, W. F., and Waymire, J. C. (1982) Phosphorylation and activation of tyrosine hydroxylase mediate the acetylcholine-induced increase in catecholamine biosynthesis in adrenal chromaffin cells, *J. Biol. Chem. 257*, 12641-12648.

65. Haycock, J. W. (2002) Peptide substrates for ERK1/2: Structure function studies of serine 31 in tyrosine hydroxylase, *J. Neurosci. Methods 116*, 29-34.

66. Kumer, S. C., and Vrana, K. E. (1996) Intricate regulation of tyrosine hydroxylase activity and gene expression, *J. Neurochem. 67*, 443-462.

67. Grima, B., Lamouroux, A., Boni, C., Julien, J.-F., Javoy-Agid, F., and Mallet, J. (1987) A single human gene encoding multiple tyrosine hydroxylases with different predicted functional characteristics, *Nature 326*, 707-711.

68. Kaneda, N., Kobayashi, K., Ichinose, H., Kishi, F., Nakazawa, A., Kurosawa, Y., Fujita, K., and Nagatsu, T. (1987) Isolation of a novel cDNA clone for human tyrosine hydroxylase: Alternative RNA splicing produces four kinds of mRNA from a single gene, *Biochem. Biophys. Res. Commun. 147*, 971-975.

69. Daubner, S. C., Lohse, D. L., and Fitzpatrick, P. F. (1993) Expression and characterization of catalytic and regulatory domains of rat tyrosine hydroxylase, *Protein Sci. 2*, 1452-1460.

70. Goodwill, K. E., Sabatier, C., Marks, C., Raag, R., Fitzpatrick, P. F., and Stevens, R. C. (1997) Crystal structure of tyrosine hydroxylase at 2.3 Å and its implications for inherited diseases, *Nat. Struc. Biol. 4*, 578-585.

71. Hegg, E. L., and Que, L. (1997) The 2-His-1-carboxylate facial triad - An emerging structural motif in mononuclear non-heme iron (II) enxymes, *Eur. J. Biochem. 250*, 625-629.

72. Quinsey, N. S., Lenaghan, C. M., and Dickson, P. W. (1996) Identification of Gln313 and Pro327 as residues critical for substrate inhibition in tyrosine hydroxylase, *J. Neurochem. 66*, 908-914.

73. Daubner, S. C., McGinnis, J. T., Gardner, M., Kroboth, S. L., Morris, A. R., and Fitzpatrick, P. F. (2006) A flexible loop in tyrosine hydroxylase controls coupling of amino acid hydroxylation to tetrahydropterin oxidation, *J. Mol. Biol. 359*, 299-307.

74. Daubner, S. C., and Fitzpatrick, P. F. (1998) Mutation to phenylalanine of tyrosine 371 in tyrosine hydroxylase increases the affinity for phenylalanine, *Biochemistry 37*, 16440-16444.

75. Ellis, H. R., Daubner, S. C., McCulloch, R. I., and Fitzpatrick, P. F. (1999) Phenylalanine residues in the active site of tyrosine hydroxylase: Mutagenesis of Phe300 and Phe309 to alanine and metal ion-catalyzed hydroxylation of Phe300, *Biochemistry 38*, 10909-10914.

76. Ellis, H. R., Daubner, S. C., and Fitzpatrick, P. F. (2000) Mutation of serine 395 of tyrosine hydroxylase decouples oxygen-oxygen bond cleavage and tyrosine hydroxylation, *Biochemistry 39*, 4174-4181.

77. Almas, B., Le Bourdelles, B., Flatmark, T., Mallet, J., and Haavik, J. (1992) Regulation of recombinant human tyrosine hydroxylase isozymes by catecholamine binding and phosphorylation structure/activity studies and mechanistic implications, *Eur. J. Biochem. 209*, 249-255.

78. Daubner, S. C., Lauriano, C., Haycock, J. W., and Fitzpatrick, P. F. (1992) Site-directed mutagenesis of serine 40 of rat tyrosine hydroxylase. Effects of dopamine and cAMP-dependent phosphorylation on enzyme activity, *J. Biol. Chem. 267*, 12639-12646.

79. Fitzpatrick, P. F. (1989) The metal requirement of rat tyrosine hydroxylase, *Biochem. Biophys. Res. Commun. 161*, 211-215.

80. Ramsey, A. J., Hillas, P. J., and Fitzpatrick, P. F. (1996) Characterization of the active site iron in tyrosine hydroxylase: Redox states of the iron, *J. Biol. Chem. 271*, 24395-24400.

81. Fitzpatrick, P. F. (1999) The tetrahydropterin-dependent amino acid hydroxylases, *Ann. Rev. Biochem. 68*, 355-381.

82. Sutherland, C., Alterio, J., Campbell, D. G., Le Bourdelles, B., Mallet, J., Haavik, J., and Cohen, P. (1993) Phosphorylation and activation of human tyrosine hydroxylase in vitro by mitogen-activated protein (MAP) kinase and MAP-kinase-activated kinases 1 and 2, *Eur. J. Biochem. 217*, 715-722.

83. Vulliet, P. R., Hall, F. L., Mitchell, J. P., and Hardie, D. G. (1989) Identification of a novel proline-directed serine/threonine protein kinase in rat pheochromocytoma, *J. Biol. Chem. 264*, 16292-16298.

84. Dunkley, P. R., Bobrovskaya, L., Graham, M. E., von Nagy-Felsobuki, E. I., and Dickson, P. W. (2004) Tyrosine hydroxylase phosphorylation: Regulation and consequences, *J Neurochem 91*, 1025-1043.

85. Campbell, D. G., Hardie, D. G., and Vulliet, P. R. (1986) Identification of four phosphorylation sites in the N-terminal region of tyrosine hydroxylase, *J. Biol. Chem. 261*, 10489-10492.

86. Bevilaqua, L. R. M., Graham, M. E., Dunkley, P. R., von Nagy-Felsobuki, E. I., and Dickson, P. W. (2001) Phosphorylation of Ser19 alters the conformation of tyrosine hydroxylase to increase the rate of phosphorylation of Ser40, *J. Biol. Chem. 276*, 40411-40416.

87. McCulloch, R. I., and Fitzpatrick, P. F. (1999) Limited proteolysis of tyrosine hydroxylase identifies residues 33-50 as conformationally sensitive to phosphorylation state and dopamine binding, *Arch. Biochem. Biophys. 367*, 143-145.

88. Ramsey, A. J., and Fitzpatrick, P. F. (1998) Effects of phosphorylation of serine 40 of tyrosine hydroxylase on binding of catecholamines: Evidence for a novel regulatory mechanism, *Biochemistry 37*, 8980-8986.

89. Abate, C., and Joh, T. H. (1991) Limited proteolysis of rat brain tyrosine hydroxylase defines an N-terminal region required for regulation of cofactor binding and directing substrate specificity, *J. Mol. Neurosci. 2*, 203-215.

90. Ramsey, A. J., and Fitzpatrick, P. F. (2000) Effects of phosphorylation on binding of catecholamines to tyrosine hydroxylase: Specificity and thermodynamics, *Biochemistry 39*, 773-778.

91. Kuczenski, R., Segal, D. S., and Mandell, A. J. (1975) Regional and subcellular distribution and kinetic properties of rat brain choline acetyltransferase--some functional considerations, *J Neurochem 24*, 39-45.

92. Lloyd, T., and Kaufman, S. (1974) The stimulation of partially purified bovine caudate tyrosine hydroxylase by phosphatidyl-L-serine, *Biochem.Biophys.Res.Commun. 59*, 1262-1269.

93. Katz, I. R., Lloyd, T., and Kaufman, S. (1976) Studies on phenylalanine and tyrosine hydroxylation by rat brain tyrosine hydroxylase, *Biochim. Biophys. Acta. 445*, 567-578.

94. Daubner, S. C., and Piper, M. M. (1995) Deletion mutants of tyrosine hydroxylase identify a region critical for heparin binding, *Protein Sci. 4*, 538-541.

95. Neckameyer, W. S., and White, K. (1992) A single locus encodes both phenylalanine hydroxylase and tryptophan hydroxylase activities in *Drosophila*, *J. Biol. Chem. 267*, 4199-4206.

96. Gahn, L. G., and Roskoski, R., Jr. (1993) Tyrosine hydroxylase activity and entrinsic fluorescence changes produced by polyanions, *Biochem. J. 295*, 189-194.

97. Frantom, P. A., Seravalli, J., Ragsdale, S. W., and Fitzpatrick, P. F. (2006) Reduction and oxidation of the active site iron in tyrosine hydroxylase: Kinetics and specificity, *Biochemistry 45*, 2372-2379.

98. Fitzpatrick, P. F. (1991) Studies of the rate-limiting step in the tyrosine hydroxylase reaction: Alternate substrates, solvent isotope effects, and transition state analogs, *Biochemistry 30*, 6386-6391.

99. Daubner, S. C., Hillas, P. J., and Fitzpatrick, P. F. (1997) Characterization of chimeric pterin dependent hydroxylases: Contributions of the regulatory domains of tyrosine and phenylalanine hydroxylase to substrate specificity, *Biochemistry 36*, 11574-11582.

100. Davis, M. D., and Kaufman, S. (1989) Evidence for the formation of the 4a-carbinolamine during the tyrosine-dependent oxidation of tetrahydrobiopterin by rat liver phenylalanine hydroxylase, *J. Biol. Chem. 264*, 8585-8596.

101. Moran, G. R., Derecskei-Kovacs, A., Hillas, P. J., and Fitzpatrick, P. F. (2000) On the catalytic mechanism of tryptophan hydroxylase, *J. Am. Chem. Soc. 122*, 4535-4541.

102. Eser, B. E., Barr, E. W., Frantom, P. A., Saleh, L., Bollinger, J. M., Jr., Krebs, C., and Fitzpatrick, P. F. (2007) Direct spectroscopic evidence for a high-spin Fe(IV) intermediate in tyrosine hydroxylase, *J. Am. Chem. Soc. 129*, 11334-11335.

103. Hillas, P. J., and Fitzpatrick, P. F. (1996) A mechanism for hydroxylation by tyrosine hydroxylase based on partitioning of substituted phenylalanines, *Biochemistry 35*, 6969-6975.

104. Eser, B. E., and Fitzpatrick, P. F. (2010) Measurement of intrinsic rate constants in the tyrosine hydroxylase reaction, *Biochemistry 49*, 645-652.

105. Hirsch, E., Graybiel, A. M., and Agid, Y. A. (1988) Melanized dopaminergic neurons are differentially susceptible to degeneration in Parkinson's disease, *Nature 334*, 345-348.

106. Haavik, J., and Toska, K. (1998) Tyrosine hydroxylase and Parkinson's disease, *Mol. Neurobiol. 16*, 285-309.

107. Haavik, J. (1997) L-DOPA is a substrate for tyrosine hydroxylase, *J. Neurochem. 69*, 1720-1728.

108. Mockus, S. M., and Vrana, K. E. (1998) Advances in the molecular characterization of tryptophan hydroxylase, *J. Mol. Neurosci. 10*, 163-179.

109. Miguez, J. M., Simonneaux, V., and Pevet, P. (1997) The role of the intracellular and extracellular serotonin in the regulation of melatonin production in rat pinealocytes, *J. Pineal. Res. 23*, 63-71.

110. Walther, D. J., Peter, J., Bashammakh, S., Hörtnagl, H., Voits, M., Fink, H., and Bader, M. (2003) Synthesis of serotonin by a second tryptophan hydroxylase isoform, *Science 299*, 76.

111. Walther, D. J., and Bader, M. (2003) A unique central tryptophan hydroxylase isoform, *Biochemical Pharmacology 66*, 1673-1680.

112. Patel, P. D., Pontrello, C., and Burke, S. (2004) Robust and tissue-specific expression of TPH2 versus TPH1 in rat raphe and pineal gland, *Biol. Psychiatry 55*, 428-433.

113. Lovenberg, W., Jequier, E., and Sjoerdsma, A. (1968) Tryptophan hydroxylation in mammalian systems, *Adv. Pharmacol. 6*, 21-36.

114. Hasegawa, H., Yanagisawa, M., Inoue, F., Yanaihara, N., and Ichiyama, A. (1987) Demonstration of non-neural tryptophan 5-mono-oxygenase in mouse intestinal mucosa, *Biochem J 248*, 501-509.

115. Zhang, X., Beaulieu, J. M., Sotnikova, T. D., Gainetdinov, R. R., and Caron, M. G. (2004) Tryptophan hydroxylase-2 controls brain serotonin synthesis, *Science 305*, 217.

116. Darmon, M. C., Guibert, B., Leviel, V., Ehret, M., Maitre, M., and Mallet, J. (1988) Sequence of two mRNAs encoding active rat tryptophan hydroxylase, *J. Neurochem. 51*, 312-316.

117. Grenett, H. E., Ledley, F. D., Reed, L. L., and Woo, S. L. C. (1987) Full-length cDNA for rabbit tryptophan hydroxylase: Functional domains and evolution of aromatic amino acid hydroxylases, *Proc. Natl. Acad. Sci. 84*, 5530-5534.

118. Daubner, S. C., and Fitzpatrick, P. F. (1993) Lysine241 of tyrosine hydroxylase is not required for binding of tetrahydrobiopterin substrate, *Arch. Biochem. Biophys. 302*, 455-460.

119. Windahl, M. S., Petersen, C. R., Christensen, H. E., and Harris, P. (2008) Crystal structure of tryptophan hydroxylase with bound amino acid substrate, *Biochemistry 47*, 12087-12094.

120. Ehret, M., Cash, C. D., Hamon, M., and Maitre, M. (1989) Formal demonstration of the phosphorylation of rat brain tryptophan hydroxylase by Ca2+/calmodulin-dependent protein kinase, *J. Neurochem. 52*, 1886-1891.

121. Makita, Y., Okuno, S., and Fujisawa, H. (1990) Involvement of activator protein in the activation of tryptophan hydroxylase by cAMP-dependent protein kinase, *FEBS Letts. 268*, 185-188.

122. Kuhn, D. M., Arthur, R., Jr., and States, J. C. (1997) Phosphorylation and activation of brain tryptophan hydroxylase: Identification of serine-58 as a substrate site for protein kinase A, *J. Neurochem. 68*, 2220-2223.

123. Banik, U., Wang, G. A., Wagner, P. D., and Kaufman, S. (1997) Interaction of phosphorylated tryptophan hydroxylase with 14-3-3 proteins, *J. Biol. Chem. 272*, 26219-26225.

124. Furukawa, Y., Ikuta, N., Omata, S., Yamauchi, T., Isobe, T., and Ichimura, T. (1993) Demonstration of the phosphorylation-dependent interaction of tryptophan hydroxylase with the 14-3-3 protein, *Biochem. Biophys. Res. Commun. 194*, 144-149.

125. Moran, G. R., Daubner, S. C., and Fitzpatrick, P. F. (1998) Expression and characterization of the catalytic core of tryptophan hydroxylase, *J. Biol. Chem. 273*, 12259-12266.

126. Joh T. H., H. O., and Abate C. (1986) Phenylalanine hydroxylase, tyrosine hydroxylase and tryptophan hydroxylase, in Neuromethods Series 1: Neurochemistry, Neurotransmitter Enzymes (Boulton A. A., Baker G. B., and Yu P. H., Eds.), pp.1-32, Humana, Clifton NJ.

127. Johansen, P. A., Wolf, W. A., and Kuhn, D. M. (1991) Inhibition of tryptophan hydroxylase by benserazide and other catechols, *Biochem. Pharmacol. 41*, 625-628.

128. Kuhn, D. M., and Geddes, T. J. (1999) Peroxynitrite inactivates tryptophan hydroxylase via sulfhydryl oxidation. Coincident nitration of enzyme tyrosyl residues has minimal impact on catalytic activity, *J. Biol. Chem. 274*, 29726-29732.

129. Fitzpatrick, P. F. (2000) The aromatic amino acid hydroxylases, in Advances in Enzymology and Related Areas of Molecular Biology (Purich, D. L., Ed.), pp 235-294, John Wiley & Sons, Inc., New York.

130. Moran, G. R., Phillips, R. S., and Fitzpatrick, P. F. (1999) The influence of steric bulk and electrostatics on the hydroxylation regiospecificity of tryptophan hydroxylase: Characterization of methyltryptophans and azatryptophans as substrates, *Biochemistry 38*, 16283-16289.

131. McKinney, J., Teigen, K., Frøystein, N. A., Salaün, C., Knappskog, P. M., Haavik, J., and Martínez, A. (2001) Conformation of the substrate and pterin cofactor bound to human tryptophan hydroxylase. Important role of Phe313 in substrate specificity, *Biochemistry 40*, 15591-15601.

132. Daubner, S. C., Moran, G. R., and Fitzpatrick, P. F. (2002) Role of tryptophan hydroxylase Phe313 in determining substrate specificity, *Biochem. Biophys. Res. Commun. 292*, 639-641.

133. McCulloch, R. I., Daubner, S. C., and Fitzpatrick, P. F. (2001) Effects of substitution at serine 40 of tyrosine hydroxylase on catecholamine binding, *Biochemistry 40*, 7273-7278.

134. Eisensmith, R. C., and Woo, S. L. C. (1991) Phenylketonuria and the phenylalanine hydroxylase gene, *Mol. Biol. Med. 8*, 3-18.

135. Nakata, H., and Fujisawa, H. (1982) Tryptophan 5-monooxygenase from mouse mastocytoma P815 a simple purification and general properties, *Eur. J. Biochem. 124*, 595-601.

136. Okuno, S., and Fujisawa, H. (1982) Purification and some properties of tyrosine 3-monooxygenase from rat adrenal, *Eur. J. Biochem. 122*, 49-55.

137. Fitzpatrick, P. F., Chlumsky, L. J., Daubner, S. C., and O'Malley, K. L. (1990) Expression of rat tyrosine hydroxylase in insect tissue culture cells and purification and characterization of the cloned enzyme, *J. Biol. Chem. 265*, 2042-2047.

138. Wang, L., Erlandsen, H., Haavik, J., Knappskog, P. M., and Stevens, R. C. (2002) Three-dimensional structure of human tryptophan hydroxylase and its implications for the biosynthesis of the neurotransmitters serotonin and melatonin, *Biochemistry 41*, 12569-12574.

139. Pavon, J. A., and Fitzpatrick, P. F. (2006) Insights into the catalytic mechanisms of phenylalanine and tryptophan hydroxylase from kinetic isotope effects on aromatic hydroxylation, *Biochemistry 45*, 11030-11037.

140. Pavon, J. A., and Fitzpatrick, P. F. (2005) Intrinsic isotope effects on benzylic hydroxylation by the aromatic amino acid hydroxylases: Evidence for hydrogen tunneling, coupled motion, and similar reactivities, *J. Am. Chem. Soc. 127*, 16414-16415.

141. Kaufman, S., and Mason, K. (1982) Specificity of amino acids as activators and substrates for phenylalanine hydroxylase, *J. Biol. Chem. 257*, 14667-14678.

142. Koehntop, K. D., Emerson, J. P., and Que, L., Jr. (2005) The 2-His-1-carboxylate facial triad: A versatile platform for dioxygen activation by mononuclear non-heme iron(II) enzymes, *J. Biol. Inorg. Chem. 10*, 87-93.

143. Ramsey, A. J., Daubner, S. C., Ehrlich, J. I., and Fitzpatrick, P. F. (1995) Identification of iron ligands in tyrosine hydroxylase by mutagenesis of conserved histidinyl residues, *Protein Sci 4*, 2082-2086.

144. Gibbs, B. S., Wojchowski, D., and Benkovic, S. J. (1993) Expression of rat liver phenylalanine hydroxylase in insect cells and site-directed mutagenesis of putative non-heme iron-binding sites, *J. Biol. Chem. 268*, 8046-8052.

145. Fitzpatrick, P. F., Ralph, E. C., Ellis, H. R., Willmon, O. J., and Daubner, S. C. (2003) Characterization of metal ligand mutants of tyrosine hydroxylase: Insights into the plasticity of a 2-histidine-1-carboxylate triad, *Biochemistry 42*, 2081-2088.

146. Shiman, R., Jones, S. H., and Gray, D. W. (1990) Mechanism of phenylalanine regulation of phenylalanine hydroxylase, *J. Biol. Chem. 265*, 11633-11642.

147. Fitzpatrick, P. F. (1994) Kinetic isotope effects on hydroxylation of ring-deuterated phenylalanines by tyrosine hydroxylase provide evidence against partitioning of an arene oxide intermediate, *J. Am. Chem. Soc. 116*, 1133-1134.

148. Frantom, P. A., Pongdee, R., Sulikowski, G. A., and Fitzpatrick, P. F. (2002) Intrinsic deuterium isotope effects on benzylic hydroxylation by tyrosine hydroxylase, *J. Am. Chem. Soc. 124*, 4202-4203.

149. Martinez, A., Abeygunawardana, C., Haavik, J., Flatmark, T., and Mildvan, A. S. (1993) Conformation and interaction of phenylalanine with divalent cation at the active site of human recombinant tyrosine hydroxylase as determined by proton NMR, *Biochemistry 32*, 6381-6390.

150. Daubner, S. C., Hillas, P. J., and Fitzpatrick, P. F. (1997) Expression and characterization of the catalytic domain of human phenylalanine hydroxylase, *Arch. Biochem. Biophys. 348*, 295-302.

151. Kemsley, J. N., Mitic, N., Zaleski, K. L., Caradonna, J. P., and Solomon, E. I. (1999) Circular dichroism and magnetic circular dichroism spectroscopy of the catalytically competent ferrous active site of phenylalanine hydroxylase and its interaction with pterin cofactor, *J. Am. Chem. Soc. 121*, 1528-1536.

152. Grzyska, P. T., Müller, T. A., Campbell, M. G., and Hausinger, R. P. (2007) Metal ligand substitution and evidence for quinone formation in taurine α-ketoglutarate dioxygenase, *J. Inorg. Biochem. 101*, 797-808.

153. Kaufman, S. (1983) Phenylketonuria and its variants, *Adv. Hum. Genet. 13: 217-297*.

154. Phillips, R. S., and Kaufman, S. (1984) Ligand effects on the phosphorylation state of hepatic phenylalanine hydroxylase, *J. Biol. Chem. 259*, 2474-2479.

155. Phillips, R. S., Iwaki, M., and Kaufman, S. (1983) Ligand effects on the limited proteolysis of phenylalanine hydroxylase: Evidence for multiple conformational states, *Biochem. Biophys. Res. Commun. 110*, 919-925.

156. Flatmark, T., Stokka, A.J., and Berge, S.V. (2001) Use of surface plasmon resonance for real-time measurements of the global conformational transition in human phenylalanine hydroxylase in response to substrate binding and catalytic activation, *Anal. Biochem. 294*, 95-101.

157. Horne, J., Jennings, I. G., Teh, T., Gooley, P. R., and Kobe, B. (2002) Structural characterization of the N-terminal autoregulatory sequence of phenylalanine hydroxylase, *Protein Sci. 11*, 2041-2047.

158. Flatmark, T., and Stevens, R. C. (1999) Structural insight into the aromatic amino acid hydroxylases and their disease-related mutant forms, *Chem. Rev. 99*, 2137-2160.

159. Døskeland, A. P., Døskeland, S. O., Ogreid, D., and Flatmark, T. (1984) The effect of ligands of phenylalanine 4-monooxygenase on the cAMP-dependent phosphorylation of the enzyme, *J. Biol. Chem. 259*, 11242-11248.

160. Miranda, F. F., Teigen, K., Thórólfsson, M., Svebak, R. M., Knappskog, P. M., Flatmark, T., and Martínez, A. (2002) Phosphorylation and mutations of Ser16 in human phenylalanine hydroxylase, *J. Biol. Chem. 277*, 40937-40943.

161. Miranda, F. F., Thórólfsson, M., Teigen, K., Sanchez-Ruiz, J. M., and Martínez, A. (2004) Structural and stability effects of phosphorylation: Localized structural changes in phenylalanine hydroxylase, *Protein Sci. 13*, 1219-1226.

162. Yan, X., Watson, J., Ho, P. S., and Deinzer, M. L. (2004) Mass spectrometric approaches using electrospray ionization charge states and hydrogen-deuterium exchange for determining protein structures and their conformational changes, *Mol. Cell. Proteomics 3*, 10-23.

163. Maier, C. S., and Deinzer, M. L. (2005) Protein conformations, interactions, and H/D exchange, *Methods Enzymol. 402*, 312-360.

164. Li, J., and Fitzpatrick, P. F. (2008) Characterization of metal ligand mutants of phenylalanine hydroxylase: Insights into the plasticity of a 2-histidine-1-carboxylate triad, *Arch. Biochem. Biophys. 475*, 164-168.

165. Pavon, J. A., and Fitzpatrick, P. F. (2009) Demonstration of a peroxide shunt in the tetrahydropterin-dependent aromatic amino acid monooxygenases, *J. Am. Chem. Soc. 131*, 4582–4583.

166. Daubner, S. C., and Fitzpatrick, P. F. (1999) Site-directed mutants of charged residues in the active site of tyrosine hydroxylase, *Biochemistry 38*, 4448-4454.

167. Flockhart, D. A., and Corbin, J. D. (1984) Preparation of the catalytic subunit of cAMP-dependent protein kinase, in Brain Receptor Methodologies, Part A (Maranos, P. J., Campbell, I. C., and Cohen, R. M., Eds.), pp 209-215, Academic Press, New York.

168. Royo, M., and Daubner, S. C. (2006) Kinetics of regulatory serine variants of tyrosine hydroxylase with cyclic AMP-dependent protein kinase and extracellular signal-regulated protein kinase 2, *Biochim. Biophys. Acta. 1764*, 786-792.

169. Weis, D. D., Engen, J. R., and Kass, I. J. (2006) Semi-automated data processing of hydrogen exchange mass spectra using HX-Express, *J. Am. Soc. Mass Spectrom. 17*, 1700-1703.

170. Chehin, R., Thorolfsson, M., Knappskog, P. M., Martinez, A., Flatmark, T., Arrondo, J. L., and Muga, A. (1998) Domain structure and stability of human

phenylalanine hydroxylase inferred from infrared spectroscopy, *FEBS Lett. 422*, 225-230.

171. Andersen, O. A., Flatmark, T., and Hough, E. (2002) Crystal structure of the ternary complex of the catalytic domain of human phenylalanine hydroxylase with tetrahydrobiopterin and 3-(2-thienyl)-L-alanine, and its implications for the mechanism of catalysis and substrate activation., *J. Mol. Biol. 320*, 1095-1108.

172. Thórólfsson, M., Teigen, K., and Martínez, A. (2003) Activation of phenylalanine hydroxylase: Effect of substitutions at Arg68 and Cys237, *Biochemistry 42*, 3419-3428.

173. Kaufman, S. (1971) The phenylalanine hydroxylating system from mammalian liver, in Advances in Enzymology (Alton Meister, Ed.), pp 245-316, Interscience Publishers, New York.

174. Kaufman, S. (1993) The phenylalanine hydroxylating system, *Adv. Enzymol. Relat. Areas. Mol. Biol. 67*, 77-264.

175. Kappock, T. J., and Caradonna, J. P. (1996) Pterin-dependent amino acid hydroxylases, *Chem. Rev. 96*, 2659-2756.

176. Stone, A. L. (1980) Studies on a molecular basis for the heparin-induced regulation of enzymatic activity of mouse striatal tyrosine hydroxylase in vitro. Inhibition of heparin activation and of the enzyme by poly-L-lysyltyrosine and poly-L-lysylphenylalanine and their constituent peptides, *J. Neurochem. 35*, 1137-1150.

177. Studier, F. W. (2005) Protein production by auto-induction in high-density shaking cultures, *Protein Expr. Purif. 41*, 207-234.

178. Cornilescu, G., Delaglio, F., and Bax, A. (1999) Protein backbone angle restraints from searching a database for chemical shift and sequence homology, *J. Biomol. NMR 13*, 289-302.

179. Kaufman, S., and Mason, K. (1982) Specificity of amino acids as activators and substrates for phenylalanine hydroxylase, *J. Biol. Chem. 257*, 14667-14678.

VITA

Jun Li received her Bachelor of Science degree in basic medical sciences from Peking University Health Science Center in 2003. She entered the biochemistry and biophysics program at Texas A&M University in September, 2004. In May of 2005, she joined the laboratory of Dr. Paul Fitzpatrick to investigate the structural basis of catalytis and regulation of phenylalanine hydroxylase. Dr. Li may be reached at Department of Biochemistry and Biophysics, Texas A&M University, 2128 TAMU, College Station, TX 77843. Her email is sherrylijcn@hotmail.com.